Title
Neuronal activity suppression of Kv1.1 channelmRNA translation in dendrites

Author
Haddick, Patrick C. G

Publication Date
2006

Peer reviewed|Thesis/dissertation

Neuronal Activity Suppression of Kv1.1 Channel mRNA Translation in Dendrites

by

Patrick C.G. Haddick

DISSERTATION

Submitted in partial satisfaction of the requirements for the degree of

DOCTOR OF PHILOSOPHY

in

Neuroscience

in the

GRADUATE DIVISION

of the

UNIVERSITY OF CALIFORNIA, SAN FRANCISCO

Date University Librarian

Degree Conferred:.....

Acknowledgments

There are many family, friends, and colleagues I want to thank who have supported and inspired me in graduate school. Foremost, I want to thank Lily Y. Jan for the opportunity to join her lab and provide the resources and tools that have led me to a successful thesis. Her patience, support, and trust in my abilities that at times exceeded my own opinion has provided me the confidence and perseverance needed to overcome many technical and intellectual challenges of research.

Yuh Nung Jan has also been an invaluable guide. His prescient questions about the motivation behind experiments and the interpretation of results have helped me become a better experimentalist. Together, Lily and Yuh Nung have created a lab environment that encourages its members to be diligent scientists, realize their potential, and take the risks in science that make research a stimulating and rewarding experience.

I collaborated closely with Kimberly Raab-Graham throughout graduate school and I am tremendously grateful to be able to share the joys and frustrations of research and scientific discovery with her. I have learned a tremendous amount from Kim – from the trivial details of an experimental protocol to how an experimental finding fits into the larger context of a scientific field. She has the keen ability to see the unexpected and help me overcome my innate pessimism.

I want to thank the 88 or so Jan lab members who have overlapped with me during my time as a graduate student in the lab, as well as the predecessors who were instrumental in generating the high degree of respect that the Jan lab has earned over the years.

I want to thank Cindy Huang, Toral Surti, and Yang Xiang for their electrophysiology experiments on rapamycin's effect on Kv1.1. These experiments unfortunately did not lead to publishable results. We had many engaging discussions that highlighted the technical limitations of electrophysiological recordings to answer our questions and I have a new found respect for those who incorporate neuronal recordings into their research.

I had the great fortune to be in the lab at a time when a number of other graduate students were also in the lab. Alex Fay was very deserving of that milkshake after we finished writing the book chapter about voltage-gated ion channels. We have become great friends and I am excited to hear his experiences and accomplishments as he begins medical school this year. I will always have fond memories of conversations with Helen Lai during the late nights in lab and Toral Surti is one of the kindest people I know. She always makes me smile and wish there was more time to talk to her. At first, Cindy Huang and I seemed to have little in common but we realized we had more in common than imagined and am glad to consider her a friend. Finally, Friederike Haass is a very thorough scientist and I am impressed by her varied interests and passions. I would also like to thank the technicians for their support and the postdocs in the lab who generously offered useful suggestions and advice.

I have no regrets choosing the Neuroscience program at UCSF for graduate school. I am inspired by the many talents of my classmates. In particular, Stephanie Albin and Jeremy Kay have been invaluable lifelong friends and confidantes. The organization and advocacy on behalf of its students would not be possible without Pat Veitch as administrator and Louis Reichardt as director. I am deeply thankful for the members of

my thesis committee, Mark von Zastrow, Steven Finkbeiner, and Liqun Luo for their comments and encouragement to make me proud of my thesis and view it as an opportunity to reflect upon the past seven years of graduate school and realize how much I have learned and grown as a scientist.

Outside of UCSF, I have had countless friends and family to enjoy those times away from lab and provide a healthy life balance. I am fortunate to maintain friendships that began as far back as kindergarten and forge new ones today. I want to particularly thank Kenneth Martin for challenging me to be a better person and I look forward to sharing our future together. Finally, I want to thank my brother and sister-in-law, Erik and Lillian, my sister and niece, Kristina and Gina, and my parents.

Lily Y. Jan directed and supervised the research that forms the basis for this thesis. She is a co-author for Chapters 1 and 2. Yuh Nung Jan is a co-author for Chapter 2 and provided advice for this chapter and the appendix. Alex Fay is a co-author for Chapter 1 and helped in the writing and editing of this chapter. Kimberly Raab-Graham is a co-author for Chapter 2 and collaborated in the experimental design, procedures, and analysis for this chapter and the appendix. This work is comparable to work for a standard thesis awarded by the University of California, San Francisco.

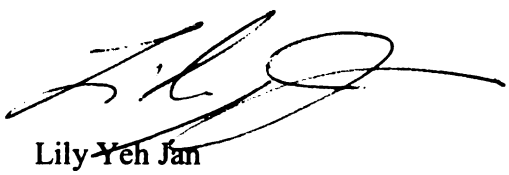

Lily Yeh Jan

Abstract

Ion channels play crucial roles in a variety of cellular activities. A superfamily of ion channels known as voltage-gated ion channels is responsive to changes in the electrical potential across the cell membrane in which they reside. This property of voltage sensitivity allows voltage-gated ion channels to be major contributors to the electrical communication utilized by cells. The prominence of these channels in many biological processes has made them a popular drug target in hopes of treating a variety of pathologies. Chapter I is a broad overview of these voltage-gated ion channels with a particular emphasis on the pharmacology developed and discovered for these channels.

Voltage-gated ion channels play an integral role in neuronal signaling. A challenge for a neuron is managing the proper number and type of signaling proteins required for up to thousands of synaptic connections with other neurons. One strategy for neurons to deal with this problem is to translate the necessary proteins locally, near the required site for the protein to function optimally. Transcripts isolated from synaptosomes were quantified and the most abundant transcripts were considered to be candidate transcripts that are locally translated.

Chapter II explores how the local translation of one of the candidate transcripts, the voltage-gated potassium channel Kv1.1 is regulated in neurons. Kv1.1 mRNA was detected in neuronal dendrites and we developed a novel method to visualize the local translation of Kv1.1 using Kaede, a photo-convertible fluorescent protein. Inhibiting NMDA glutamate receptors, PI3 kinase, or mTOR increased the local translation of Kaede-Kv1.1 in dendrites. These findings suggest neuronal activity suppresses the local translation of Kv1.1.

The appendix details other candidate transcripts that were further characaterized. A particular focus is on 14-3-3 eta as a candidate transcript that is locally translated as well as the functional significance of the interaction between 14-3-3 and GABA-B receptors.

Table of Contents

List of Tables

Chapter I.

No Tables

Chapter II.

Chapter III.

No Tables

Appendix

No Tables

List of Figures

Chapter I.

No Figures

Chapter II.

Chapter III.

No Figures

Appendix

CHAPTER I

Introduction to Voltage-Gated Ion Channels

Introduction

Cells create differences in voltage and ion concentration across membranes through the action of ATP-dependent ion pumps, and the ions flow down the electrochemical gradients through ion channels underlies the generation and propagation of action potentials, release of hormones and neurotransmitters, and many other functions essential for cellular signaling and homeostasis. Mammalian cell membranes typically maintain a resting membrane potential of –50 to –90 mV, a range that is close to the equilibrium potential for potassium (K^+) and far from the equilibrium potentials for sodium (Na^+) and calcium (Ca^{2+}). Relatively voltage-insensitive background K^+ channels maintain hyperpolarized membrane potentials at rest, resisting the depolarizing shifts in membrane potential that open voltage-dependent Na^+, K^+, and Ca^{2+} channels.

A sufficiently strong depolarizing stimulus, such as a sodium current through an ionotropic glutamate receptor, can precipitate an action potential by initiating the sequential opening and closing of voltage-gated ion channels. Voltage-gated Na^+ channels open earliest and further depolarize the membrane before they inactivate and become non-conductive. More slowly activating voltage-gated K^+ channels then open and return the membrane towards its resting potential before they inactivate. Voltage-gated Ca^{2+} channels also open upon depolarization, stimulating neurotransmitter release as well as longer term (e.g., transcriptional) effects that depend on calcium as a second messenger.

It is clear from the roles of voltage-gated ion channels in the neuronal action potential that channels must be selective for a specific ion, and must open and inactivate within the proper voltage range. The conformational changes that lead to opening and

closing of channels are known as "gating," and occur in response to stimuli such as ligands or voltage. Selectivity and gating depend on structural elements of the channel proteins, and X-ray crystallographic studies in the last few years have provided the first high-resolution insights into the 3-dimensional organization and functional properties of channels. However, before the channels can affect cellular physiology, they must fold properly, co-assemble with homologous or auxiliary subunits, and reach the plasma membrane through the secretory pathway. While gating and selectivity have been tractable properties to study with electrophysiological techniques for decades, only recently have genetic, molecular biological, biochemical, and immunological approaches enabled channel biologists to understand the pre- and post-translational modification, assembly, and trafficking of ion channels.

With so many levels of regulation of ion channel activity, one can imagine that mutations of ion channels at critical amino acid residues could lead to various defects in channel folding, trafficking, or conduction. Indeed, a number of ion channel-related diseases, or channelopathies, have been described, including epilepsy, arrhythmia, myotonia, diabetes, and even cancer, in humans. In addition, animal models, particularly mouse and the fruit fly *Drosophila melanogaster*, have helped to reveal the physiological roles of both wild-type and mutant channels.

As the roles that channels play in pathophysiology become clearer, the importance of developing pharmacological tools to manipulate channel function grows. Nature has provided many highly specific channel blockers in the form of peptide toxins from venomous snakes, spiders, sea snails, scorpions, and other species. While useful for laboratory studies, these toxins have poor bioavailability, so the identification and

development of organic small molecule blockers and openers has become an important goal of pharmacological research.

This review will give an overview of the current state of knowledge about the structures of ion channels; the mechanisms of selectivity and gating; the cell biology of ion channels, including co-assembly of channel subunits with other proteins and trafficking of ion channels; the physiological functions of ion channels and their roles in disease; and pharmacological tools available for the manipulation of ion channels *in vitro* and *in vivo*. While a vast array of ion channels exists with different selectivities and mechanisms of activation, I will focus on voltage-gated K^+, Na^+, and Ca^{2+} channels.

Cloning and Evolutionary Relationships

Cloning of the first voltage-gated ion channel, from the eel *Electrophorus electricus*, revealed four repeats of a six transmembrane segment (TMS) topology, with a highly charged fourth TMS in each repeat [1]. Further cloning of other voltage-gated channels indicated that an amphipathic α-helix, with an arginine residue at approximately every third position, is a conserved motif among voltage-gated ion channels. This charged helix appeared to be a region of the channel that is sensitive to changes in transmembrane potential.

Identification of the genes for voltage-gated K^+ channels, beginning with the *Shaker* mutant of *Drosophila* [2, 3], revealed an evolutionary relationship among voltage-gated ion channels. Whereas the Na^+ and Ca^{2+} channels contain four pseudorepeating domains (DI-IV), each containing six TMS, the voltage-gated K^+ channels are made up of only one domain of six TMS and assemble as tetramers. Thus, it appears that voltage-

gated sodium and Ca^{2+} channels emerged evolutionarily by successive gene duplications from a K^+ channel precursor. With the sequencing of genomes of organisms from all kingdoms of life, it is clear that voltage-gated ion channel genes are both ancient and ubiquitous. Na^+ channels of 24TMS topology have been found in some lower organisms, such as cnidarians and ctenophores [4], and one 24TMS voltage-gated Ca^{2+} channel is present in the yeast *Saccharomyces cerevisiae* [5]. Among the voltage-gated cation channels, only K^+ channels are present in prokaryotes, though a Na^+ channel of 6TM topology from *Bacillus halodurans* has been cloned and characterized [6]. Bacterial K^+ channels that can be over-expressed and purified in large quantities provided the raw materials for the X-ray crystallographic studies that show the details of ion selectivity and voltage-sensing at an atomic level.

Nomenclature

The naming of ion channels has been an idiosyncratic process over the years, as researchers named channels for mutant or knockout phenotypes, or with acronyms derived from channel functional properties. For example, K^+ channels related to the *Shaker* channel from *Drosophila* have alternately been called Shaker, Kv1.x, or KCNA channels. In the interest of consistency, we will follow IUPHAR nomenclature for voltage-gated sodium (Nav) [7] and Ca^{2+} channels (Cav) [8]. For voltage-gated K^+ channels, we use Kv names for the A-type and delayed rectifier channels Kv1.x, Kv2.x, Kv3.x, Kv4.x, Kv5.1, Kv6.x, Kv8.1, and Kv9.x. We use the more common literature names for the KCNQ1-5 channels and for the calcium-activated K^+ channels of large (BK), intermediate (IK), and small (SK) conductance. The more widely used,

Drosophila-derived names EAG, ERG, and ELK are employed instead of KCNH1-8 or Kv10.x/Kv11.x/Kv12.x [9].

Potassium Channels

K^+ channels are essential in both excitable and non excitable cells for the control of membrane potential, regulation of cell volume, and the secretion of salt, neurotransmitters and hormones. They allow the selective, diffusional passage of potassium ions across biological membranes, and are capable of up to 10,000-fold selectivity of potassium over sodium. Voltage-gated K^+ channels, unlike the related voltage-gated Na^+ and Ca^{2+} channels, are expressed not only in heart, neurons, and muscle cells, but also in many non-excitable cells.

While best known for their role in repolarizing the membrane of neurons and cardiomyocytes during an action potential, K^+ channels are, in fact, expressed in most mammalian cell types. They play a critical role in such diverse processes as epithelial salt balance across epithelial cells, particularly in the kidney and colon, T cell signaling, and insulin release by pancreatic beta cells. Accordingly, a growing number of K^+ channels are potential targets for treatment of diseases, and K^+ channel mutations have been linked to a number of diseases. For example, missense mutations in KCNQ2 or KCNQ3 that reduce M-channel current cause an autosomal dominant form of seizure disorder, benign neonatal familial convulsions. And a number of voltage-gated K^+ channel mutations can cause arrhythmias by delaying the repolarization phase of the cardiac action potential.

With the sequencing of the human genome, over 80 K^+ channels genes have now been identified, and can be grouped into several classes based on their transmembrane

topologies. The inwardly-rectifying K^+ channels have two TMS flanking the highly conserved pore region including the P loop, which confers potassium selectivity (see "Selectivity," below), and assemble as tetramers. The two-P, or KCNK channels, consist of two inward rectifier-type domains linked together, and function as dimers. The voltage-gated and calcium-activated K^+ channels have a pore domain with an inward rectifier-type topology, containing the conserved P loop, preceded by four transmembrane domains (five, in the case of BK channels). A highly charged fourth TMS functions as the voltage sensor in the voltage-gated channels. The N- and C-terminal domains of K^+ channels are cytoplasmic and can regulate channel electrophysiological properties and trafficking, and can be a platform for phosphorylation, channel-lipid interactions, and co-assembly with other proteins. In addition to these pore-forming, or α-subunits, a number of cytosolic and transmembrane proteins co-assemble with K^+ channels and alter channel sensitivity to various ligands or to voltage, or regulate subcellular localization of the channel complex.

The last six years have brought high-resolution structures of several bacterial K^+ channels, as well as cytoplasmic domains and beta subunits of several mammalian channels. The structure of KcsA in 1998 [10] showed the atomic details of potassium coordination by the selectivity filter. While the KcsA structure shows a channel in the closed state, the structure of the calcium-activated MthK [11] reveals the conformation of an open channel. A structure of the voltage-gated K^+ channel, KvAP, was published in 2003 [12], but there is still much debate regarding the organization of transmembrane helices of this class of channels and the conformational changes involved in voltage gating [13]. The increasing use of structural biology as a tool for studying ion channels

will allow for more detailed understanding of gating, selectivity, disease-causing mutations, as well as the interactions between channels and the drugs that modulate them.

A vast pharmacology exists for K^+ channels, including many peptide toxins isolated from microbes and venomous animals, and therapeutically more useful small organic compounds. Many of these agents act on multiple K^+ channels subtypes, on account of the conserved structural elements among K^+ channels, while others show potent specificity for a single channel subtype.

Voltage-Gated K^+ channels

Voltage-gated K^+ channels are generally divided into subgroups depending on sequence homology and the ability to heteromultimerize. The three Shal K^+ channels (Kv4.1-4.3 or KCND1-3), for example, can co-assemble with each other but not with Shaker (Kv1.1-1.8 or KCNA1-8) K^+ channels. The Kv channels activate upon depolarization and inactivate either through fast or slow inactivation, and are also known as delayed rectifiers, since upon depolarization they repolarize the membrane after a delay. Other voltage-gated K^+ channels, the KCNQ channels and KCNH (HERG, EAG, ELK) channels, activate more slowly and are known as slow delayed rectifiers. While electrophysiological studies have demonstrated the diverse activation and inactivation properties of voltage–gated K^+ channels, high resolution structural studies and spectroscopy are beginning to provide detailed molecular models for the voltage-dependent properties of these channels.

Selectivity

The region of K^+ channels responsible for selectivity, the P-loop, was identified more than a decade ago by sequence alignment and mutagenesis studies, and a tripeptide motif Gly-Tyr-Gly, was found to be crucial for distinguishing potassium from other monovalent cations [14]. It was not until MacKinnon and colleagues solved the crystal structure of the KcsA channel from *Streptomyces lividans* [10] that the geometry of potassium coordination by the channel pore became clear. The four subunits of the K^+ channel symmetrically surround the permeating potassium ions of the structure, with the channel reaching its narrowest point at the GYG region of the P-loop. In this region, known as the selectivity filter, rings of four carbonyl oxygens coordinate potassium ions as they move through the constriction in single-file. The oxygens, in effect, mimic the hydration sphere of a potassium ion in solution, and therefore lower the dehydration energy required to move the ion from bulk solvent into the protein channel. The geometry of the pore provides a more favorable coordination sphere for potassium than for sodium, which has a smaller atomic radius and a higher dehydration energy. Some have argued recently, though, that the channel pore may not be rigid, and that the nature of carbonyl dipole moments themselves favor potassium over sodium [15].

Conduction occurs in the direction of the electrochemical gradient for potassium at rates approaching the diffusion limit. Repulsion between closely-spaced potassium ions in the selectivity filter facilitates such rapid conduction [10]. The narrow selectivity filter makes up less than a third of the distance of the conduction pathway, and the rest of the channel pore is wide enough to contain water molecules that hydrate ions as they pass through the inner cavity. Thus, each ion is only briefly dehydrated. Ions in the water-

filled cavity below the selectivity filter are further stabilized by the orientation of negative dipoles of the four pore helices towards the cavity.

Voltage-Activation

With the cloning and sequencing of the first voltage-gated K^+ channels, *Shaker* from *Drosophila melanogaster* in 1987 [3], and the previously cloned voltage-gated sodium and Ca^{2+} channels, it became clear that the charged S4 TMS was likely to be important for voltage sensing. Electrophysiological studies had already shown that a "gating current" of 12-13 charges precedes the conduction of ions through the channel, indicating that a charged part of the channel protein moves across the transmembrane electric field in a voltage-dependent manner [16]. Site-directed mutagenesis of basic residues in S4 confirmed the importance of S4 in voltage gating [17]. Later experiments showed that acidic residues in the S2 and S3 segments are important for stabilizing S4 basic residues within the membrane [18]. Based on the presumed topology of the channel and the magnitude of gating currents, several models for voltage sensor movement were proposed [4]. The S4 helix might undergo a simple translation, altering the register of S2-S4 and S3-S4 interactions, and exposing some S4 residues to the extracellular solution. Alternatively, voltage sensing could be a combination of helical translation and rotation of S4. Resonance energy transfer experiments measured relatively small changes in the distance of S4 segments relative to one another, results not consistent with dramatic conformational changes [19, 20]. A way to reconcile the measured distances with the necessity of moving 12-13 charges through the transmembrane electric field is a thinning of the membrane around S4, such that four basic residues could move from the

cytoplasmic side of the membrane to the extracellular side with only a modest translation and rotation.

The structure of the bacterial voltage-gated K^+ channels KvAP showed an unexpected orientation of S1-S4, with an S3-S4 voltage-sensing "paddle" on the outer edge of each subunit and touching lipid [12]. The data led MacKinnon and colleagues to propose that the voltage paddle is flexible and can swing across the bilayer upon voltage activation [21]. A caveat of the crystallization procedure, however, was the use of an antibody against the S3-S4 region to co-crystallize with the channel. The antibody likely distorted the voltage-sensing portion of channel so that it may not be resting in its normal position for the depolarized state (assuming that crystallization in detergent mimics the zero mV state of the channel). In addition, parts of the structure that appear to be on the cytoplasmic side of the membrane in the structure are glycosylated in homologous mammalian channels, suggesting that they are unlikely to move through the membrane [13]. Thus, the mechanics of voltage-sensing are still an open question that will require more high resolution structural and computational studies before it can be answered definitively.

Gating

Diverse stimuli can cause channel opening and closing, a process known as "gating," and their effects must ultimately affect potassium movement through the permeation pathway of the channel. Structural and spectroscopic studies, coupled with measurements of the solvent accessibility of residues in open versus closed states have identified two "gates" that restrict ion permeation. One is at the cytoplasmic face of the

channel, where the inner pore-lining helices constrict and can block ion passage through the narrow opening. This region was mapped through the differential accessibility of cysteine-modifying reagents to cytseine mutations in S6 in the open and closed states [22]. Structures of the KcsA channel, which is presumably in the closed state [10], and MthK, a calcium-sensitive channel in the open state [11], confirmed this result. The KcsA structure has straight pore-lining helices that constrict at the cytoplasmic side to limit access to the selectivity filter. MthK, when opened by calcium, swings open its pore helices around a glycine hinge in M2 (S6), such that there is an opening of 12 Angstroms from the cytoplasm to the inner pore. While voltage-gated K^+ channels may make use of this glycine hinge, they also have a Pro-X-Pro motif (though KvAP lacks this element) at the cytoplasmic mouth of the channel that acts as a hinge and may make the opening narrower than that of MthK [23]. Interestingly, this more constricted opening may explain in part the ten-fold lower conductance of Kv channels compared to MthK.

The second gate is at the selectivity filter, which can adopt a conformation that prevents permeation of ions. This kind of gating underlies C-type (slow) inactivation of Kv channels, an inactivation mechanism that persists in the absence of fast inactivation (see below) and is dependent on the extracellular potassium concentration. The structure of KcsA in the presence of low potassium (3 mM) shows a collapsed structure that coordinates fewer potassium ions than the high potassium (200 mM) structure [24]. The structure of a bacterial inwardly-rectifying K^+ channels has a slightly different pore structure, and also appears to be a non-conducting form [25] that may represent a C-type inactivated conformation.

A related question for voltage-gated channels is how voltage sensing is coupled to the channel gates to allow for opening following voltage driven channel conformational changes that give rise to the gating current. During voltage-sensing, the S4 domain's charged residues move outwards, likely exerting tension on the S4-S5 linker. Some studies have suggested that this linker interacts with the C-terminal end of S6 in the HERG K^+ channels [26] and the Kv1.2 channel [27].

Fast Inactivation

A-type, or rapidly inactivating, K^+ channels inactivate on a scale of tens to hundreds of milliseconds after depolarization. This inhibition is mediated by a peptide of about 30 amino acids either at the N-terminus of the channel or at the N-terminus of a β-subunit. The peptide binds to the cytoplasmic side of the K^+ channel pore and prevents ion conduction until it is reversed by repolarization [28]. Although no structure of the inactivation peptide bound to the pore has been solved, the prevailing model has been the "ball-and-chain." The N-terminal "ball" of basic and hydrophobic residues is tethered by a "chain" of linker residues to the T1 domain or β-subunit, and probably snakes through the space between the T1 domain and the membrane in order to reach the pore [29]. The "ball" residues are not well conserved among channels, but hydrophobic residues seem to be of particular importance in binding to the pore [30].

Interacting Proteins

There are many cytoplasmic proteins that have been found to interact with voltage-gated K^+ channels, and to alter the electrophysiological properties or localization

of the pore-forming α-subunits. The β-subunits exist in three forms, β1-3, β1 and β3 having several splice variants, and co-assemble with Kv α-subunits in the endoplasmic reticulum [31]. While β1 and β3 are capable of converting slowly-inactivating delayed rectifiers to transient A-type currents, β2 seems primarily to increase Kv surface expression. These subunits are members of the aldo-keto reductase family and bind NADPH. The function of the co-factor is not clear, and while mutation of catalytic residues seems to have no effect on trafficking of β2 subunits, disruption of the cofactor binding site leads to improper targeting of alpha subunits [32]. Large-conductance calcium-activated K^+ (BK) channels interact with another type of β-subunit, which has two transmembrane segments and modifies the voltage activation and calcium sensitivity of the BK α-subunits.

A second class of proteins that directly affect voltage-gated potassium activity is the KChIPs (K^+ Channel Interacting Proteins), which interact primarily with members of the Kv4 (*Shal*) sub-family. KChIPs are cytoplasmic calcium-binding proteins that have four EF-hand Ca^{2+}-binding motifs, and bind to the N-terminal domain of Kv4.x channels. KChIPs1-3 affect α-subunit activity similarly, by increasing current density, shifting the voltage activation curve to more hyperpolarized potentials, speeding up recovery from inactivation, and slowing the time constant of inactivation [33]. KChIP4 may compete competitively with other KChIPs, fails to increase current density, and can remove rapid inactivation from Kv4.x currents [34].

KCNE (MinK and MiRP) proteins are a class of transmembrane subunits that modulate voltage-gated K^+ channel function. They contain a single transmembrane helix with a glycosylated, extracellular N-terminus and a cytoplasmic C-terminal domain.

KCNE1 assembles with KCNQ1 to form the slow component of the cardiac delayed rectifier K^+ current (IKs), part of the repolarization phase of the cardiac action potential. Its effect on KCNQ1 is to slow voltage activation and increase conductance, and mutations in KCNE1 that reduce KCNQ1/KCNE1 conductance can be arrhythmogenic [35]. KCNE1 can also interact with Kv4.3 and decreases its activation and inactivation rates while increasing current density [36], while KCNE3 has been found to co-immunoprecipitate with and affect the electrophysiological properties of Kv2.1 and Kv3.1 [37].

Cytoskeletal and scaffolding proteins may help to target or maintain voltage-gated K^+ channels at specific sub-cellular locations. Filamin, an actin-binding protein, co-localizes with Kv4.2 and may aid in the synaptic targeting of this channel [38]. Integrins, a type of cell adhesion molecule, may help to maintain Kv4.x channel complexes at the neuromuscular junction [39], and interact with Kv1.3 in T lymphocytes. The scaffolding protein PSD-95 can mediate synaptic clustering of Kv channels with other channels and signaling proteins [40].

Kv Channels: Physiological Functions, Disease Relevance, Pharmacology

Threshold of voltage activation and channel localization play key roles in the physiological function of the various Kv subunits. K^+ channels that activate at subthreshold potentials will tend to resist excitation near the resting potential, while channels that activate at more depolarized potentials will tend to play a more important role in the repolarization phase of an action potential. Axonal or axon terminal K^+ channels shape action potentials and modulate neurotransmitter release, whereas

somatodendritic channels affect synaptic integration and shape backpropagating action potentials.

Kv1 channels are predominantly localized to membranes immediately adjacent to the nodes of Ranvier (the juxtaparanodal region) of myelinated axons, axonal membrane of unmyelinated axons, and nerve terminals [41], though they have also been found in somatodendritic membranes [42]. Their main functions at axonal locations are repolarization during an action potential and spike broadening at the terminal in order to regulate calcium influx, and thereby neurotransmitter release. Kv1 channels form sustained currents, except when they contain a Kv1.4 subunit or β1 subunits that confer fast inactivation. Kv1.5 is expressed in the heart, where it makes up the ultra-rapidly activating K^+ current [43], a part of the repolarization phase of the cardiac action potential, while Kv1.3 modulates T-lymphocyte activation by promoting calcium influx at hyperpolarized potentials [44].

Kv2 channels produce sustained currents that are localized predominantly in the cell body and dendritic membranes. Kv2.1 has a more restricted distribution in the soma and proximal dendrites [45], while Kv2.2 is found along the length of dendrites [46]. The α-subunits Kv5.1, 6.1-6.3, 8.1, and 9.1-9.3 are all non-functional when expressed alone in heterologous systems. However, many of them can co-assemble with Kv2 channels, acting as dominant negatives in some cases and increasing conductance in others [47, 48].

The four Kv3 channels can make up either transient or sustained currents, and have more depolarized thresholds for voltage activation (>-10 mV) than most other Kv channels. Coupled with their rapid deactivation (within milliseconds), this high threshold

makes these channels suited to their role in high-frequency spiking neurons [49]. Accordingly, Kv3 expression has been observed in most types of high-frequency firing neurons, such as neocortical interneurons [50] and auditory principal neurons [51].

The three Kv4 channels all form A-type currents that are expressed predominantly in somatodendritic membrane. This localization implies that Kv4 channels play a role in synaptic integration and backpropagating action potentials, which are of particular importance for informing dendritic membranes of neuronal firing activity. Their coincidence with sub-threshold post-synaptic inputs can lead to synaptic plasticity through long-term potentiation. Immunohistochemistry [52] and electrophysiological studies [53] suggest that Kv4 channels, especially Kv4.2, are likely to mediate the A-type currents in dendrites of hippocampal pyramidal neurons. These currents increase in density with distance from the soma, leading to a dampening of backpropagating action potential amplitude in distal dendrites [54]. The inhibition of A-type potassium currents by neurotransmitter receptor-coupled phosphorylation [55] provides a mechanism for increasing backpropagating action potential amplitude or frequency and NMDA receptor activation. Kv4 channels are also responsible for the transient outward potassium current ($I_{K,to}$) during the repolarization of the cardiac action potential, as Kv4.2 knockout mice lack this $I_{K,to}$ [56]. This current likely consists of Kv4.2/3 subunits and KChIP2, since a gradient in KChIP2 expression across the ventricular wall reflects the increase in $I_{K,to}$ in the epicardium compared to the endocardium [57].

Despite their ubiquitous expression in both excitable and non-excitable cells, Kv channel mutations have been implicated in a relatively small number of diseases. Mutations in Kv1.1 can cause episodic ataxia type-1 (EA-1), an autosomal dominant

disorder characterized by stress- or alcohol-induced attacks of imbalance and loss of coordination. EA-1 and its associated loss of function mutations cause an increase in action potential duration, repetitive firing, and elevated neurotransmitter release. These EA-1 mutations either yield non-functional channels or channels with impaired Kvβ1-mediated N-type inactivation [58]. An intriguing pharmacological mystery with episodic ataxia is the ability of the carbonic anhydrase inhibitor acetazolamide to relieve attacks [59]. In addition to this Kv1.1 disorder, Kv4.3, in accordance with its importance in the cardiac transient outwardly-rectifying K^+ channels, has been found to be down-regulated in paroxysmal atrial fibrillation [60].

The most potent blockers of Kv channels are toxins from a variety of venomous creatures, which can block either a single channel type or a range of voltage-gated channels with high affinity. Since peptide toxins make poor pharmaceutical agents, however, the channel blockers used clinically are smaller, less specific organic compounds. The least specific blockers, Ba^{2+}, Cs^+ and tetraethylammonium (TEA) are simply cationic species that block the conduction pathway, whether they are applied to the inner or outer face of the channel. Another general blocker of K^+ channels is 4-aminopyridine, which blocks voltage-gated channels at micromolar to millimolar concentrations and likely acts at the cytoplasmic opening of the channel [61]. A slightly more potent inhibitor is quinidine, an antiarrhythmic derivative of the antimalarial drug quinine, and a voltage-dependent open channel blocker [62].

Dendrotoxins are potent peptide toxins from the venom of mamba snakes that have nanomolar affinities for Kv channels. Dendrotoxin K is specific for Kv1.1, while α-dendrotoxin targets A-type potassium currents and β- and γ-dendrotoxins block primarily

non-inactivating potassium currents. The scorpion peptide margatoxin and stichodactyla toxin from sea anemone inhibit Kv1.3 at nanomolar concentrations, and can block experimental autoimmune encephalomyelitis [63]. The prospect of Kv1.3 blockers as immunosuppressants has made the development of small molecule inhibitors a promising endeavor [64, 65]. Other selective peptide toxins include BDS-I and BDS-II, from sea anemone, which block Kv3.4, and the spider toxin heteropodatoxin-2 and phrixotoxin-2 from tarantula, which are selective for Kv4 channels.

Large Conductance Calcium-Activated K^+ channels: Physiological Functions, Disease Relevance, Pharmacology

Large-conductance calcium-activated K^+ (BK) channels are voltage-dependent, have an intrinsic calcium sensing ability and a conductance ranging from 100-250 pS, and play diverse roles in neuronal and non-neuronal tissues. In hippocampal neurons, they mediate both the repolarizing phase of an action potential and the fast afterhyperpolarization, and respond directly to calcium influx through N-type Ca^{2+} channels [66]. And in adrenal chromaffin cells, the hypothalamic-pituitary-adrenocortical stress axis modulates epinephrine release by alternative splicing of mRNA of BK channels, which regulate hormone release [67]. In the cochlea, a gradient of BK splice variants/β-subunit complexes with varying kinetics underlies frequency tuning along the cochlear hair cell membrane [68]. The gradient makes those hair cells with more slowly gating BK channels (more β-subunit) tuned to lower frequencies, while hair cells sensitive to higher frequencies have faster-gating BK channels (less β-subunit). Deletion of BK causes hearing loss in knockout mice, and seems to be correlated with down-regulated KCNQ4 expression in outer hair cell membrane that leads to degeneration of

those cells [69]. BK is the most abundant channel in vascular smooth muscle, and channel composition is important in regulating vascular tone, since impaired β-subunit expression leads to increased vasoconstriction and hypertension [70]. More recently, BK channels have been found to be essential for killing of certain microorganisms by neutrophils, and may function by promoting the release of microbicidal serine proteases into the phagosome [71].

There are several peptide toxins that block BK channels specifically, including iberiotoxin, slotoxin, and BmBKTx1, all of which are from scorpion venom. Charybdotoxin, another scorpion toxin, has also been used as a BK blocker, but it inhibits some voltage-gated K^+ channels, as well as the intermediate conductance calcium-activated K^+ channels (IK). Non-peptide inhibitors include the indole diterpenes paxilline, penitrem A, and verruculogen. There are several activators of the benzimidazolone family, such as NS-1619 and NS-004, that have only moderate specificity for BK. The opener BMS-204352 may limit ischemic damage during stroke [72], while NS-8 may be useful as a treatment for incontinence [73]. BK activators may also be useful in the treatment of erectile dysfunction [74], since arousal stimulates increased BK current, causing hyperpolarization and relaxation of the cavernosal smooth muscle cell membranes.

Intermediate Conductance Calcium-Activated K^+ channels: Physiological Functions, Disease Relevance, and Pharmacology

Intermediate conductance (IK) and small conductance (SK) calcium-activated K^+ channels are both voltage-insensitive 6TM K^+ channels, and derive their calcium

sensitivity from calmodulin, which is constitutively bound to the channel C-terminal domain. IK channels have conductances of 20-80 pS, are found mostly in non-neuronal tissues, and are often important for secretion and volume regulation. In red blood cells, increased IK channel activity can lead to cell shrinkage that promotes the concentration and aggregation of hemoglobin S in sickle cell anemia patients [75]. In T lymphocytes, IK channels are up-regulated upon mitogen stimulation [76], and maintain cytoplamic calcium concentrations necessary for activation [77]. The importance of IK in T-cell activation could make it a potentially useful target for auto-immune diseases such as multiple sclerosis and rheumatoid arthritis [78].

The only peptide toxin that inhibits IK channels potently is charybdotoxin, but, as was mentioned above, it is not specific. The antifungal clotrimazole blocks IK at micromolar concentrations, but has the undesirable property of also being a cytochrome P450 inhibitor. An analogue that does not affect cytochrome activity, TRAM-34, has been reported [79], and may be a more promising pharmaceutical candidate. IK blockers have been proposed as possible treatments for sickle cell anemia [80], diarrhea, and rheumatoid arthritis [81]. As is the case with Kv1.3 blockers, IK inhibitors may be useful as immunosuppressants. Activators include 1-ethyl-2-benzimidazolinone (1-EBIO), a more potent analogue NS309, chlorzoxanone, and zoxazolamine, and may be useful in treating cystic fibrosis and vascular disorders [81].

Small Conductance Calcium-Activated K^+ channels: Physiological Functions, Disease Relevance, and Pharmacology

SK channels have conductances of 4-20 pS, and are best known for mediating the neuronal afterhyperpolarization (AHP) of medium duration. This current activates within milliseconds and has a duration on the order of hundreds of milliseconds. Depending on channel localization, the SK AHP can regulate bursting behavior in neuronal firing, set a tonic firing frequency or instantaneous firing rate, modulate rhythmic oscillations in activity, or affect spike frequency adaptation [82]. The three SK genes, SK1-3, have varying sensitivities to the bee venom peptide toxin apamin, a property that has helped in distinguishing these channels eletrophysiologically. Apamin-blocked AHP has been proposed to play a role in learning and memory [83], and hippocampi of Alzheimer's disease patients have been found to have reduced numbers of apamin binding sites [84]. SK activity can also regulate catecholamine release in adrenal chromaffin cells [85]. And genetic studies have suggested SK3 involvement in schizophrenia [86] and anorexia nervosa [87].

Apamin is the most potent blocker of SK channels, and more recently, the scorpion peptide toxins scyllatoxin [88] and BmSKTx [89] have been identified as selective blockers of SK channels. Tubocurarine, a plant-derived, non-peptide inhibitor of the nicotinic acetylcholine receptor, also blocks SK channels at the same site as apamin [90]. Dequalinium and bicuculline are other non-peptide blockers of SK channels, but the former is a mitochondrial poison and the latter blocks GABA-A chloride channels. Synthesis of bisquinolinium cyclophane compounds related to dequalinium has yielded blockers such as UCL-1684, which is at least 100-fold more potent than dequalinium [91]. SK activators, such as 1-EBIO, NS309, and chlorzoxanone, also stimulate IK

channel activity, and are thought to act by increasing the interaction between SK and calmodulin [92].

KCNQ Channels: Physiological Functions, Disease Relevance, and Pharmacology

Channels of the KCNQ family are voltage-gated, activate slowly, and play critical roles in cardiac, neuronal, and auditory function. Mutations in four of the five KCNQ channels (KCNQ1-4) underlie genetic disorders in humans. The first member of the family, KCNQ1, was cloned as a gene associated with long-QT syndrome type 1 [93]. KCNQ1, co-assembled with KCNE1, was subsequently identified as the slow delayed-rectifier current of the cardiac action potential. KCNQ1 was later also found to form a prominent current in colonic crypt cells (with KCNE3) [94] that mediates intestinal chloride homeostasis, and to modulate potassium recycling in the inner ear (with KCNE1) [95].

Long-QT syndrome type 1 is caused by mutations in either KCNQ1 or KCNE1 that lead to non-functional or smaller currents than wild-type. These mutations are located throughout the channel [96]. The reduced channel activity leads to a prolongation of the repolarization phase of the cardiac action potential and lengthening of the QT phase of the electrocardiogram. The result can be *torsade de pointes*, a life-threatening arrhythmia. Autosomal-dominant LQT1, or Romano-Ward syndrome, is the result of dominant negative mutations in KCNQ1 or KCNE1, while the rarer Jervall-Lange-Nielsen syndrome is recessive and causes both LQT1 and congenital bilateral deafness. Deafness results from a failure of mutant channels to maintain high endolymph K^+ concentration. Auditory stimulation leads to potassium influx into hair cells from the

endolymph, followed by K^+ exit from the basal side of hair cells and recycling to the endolymph through the stria vascularis. This last step in recycling occurs through KCNQ1/KCNE1 channels, so reduced channel activity leads to reduced endolymph potassium levels and reduced endolymph potential, which diminishes sensitivity to auditory stimuli. Potassium leaves hair cells through KCNQ4 channels on the basal side of the outer hair cell membrane [97], and a loss of this channel's function can lead to outer hair cell degeneration [98]. KCNQ4 is expressed almost exclusively in the inner ear, and mutations in this channel cause nonsyndromic autosomal dominant deafness-2 (DFNA-2) [99]. Several DFNA-2-associated mutations in KCNQ4 cluster around the pore region [100].

Two other members of the KCNQ family, KCNQ2 and KCNQ3, make up the M-current, a neuronal current that is activated sub-threhold and inhibited by muscarinic acetylcholine receptor activation, and affects neuronal excitability. While KCNQ2 and KCNQ3 expressed alone produce relatively small currents, together they form channels with over ten times the current expected from summing their individual conductances [101]. In addition to M1 muscarinic receptors, other receptors that can mediate M-current inhibition include B2 bradykinin receptors, substance P, and luteinizing hormone-releasing hormone receptors [102]. This coupling is a way for neurotransmitters to excite the post-synaptic membrane, by inhibiting a potassium conductance that resists excitation. While knockout of KCNQ2 is lethal, a mouse with a dominant negative KCNQ2 restricted to neurons has increased hippocampal pyramidal neuron excitability, reduced spike frequency adaptation, spontaneous seizures, and behavioral hyperexcitability [103].

Mutations in KCNQ2 and KCNQ3 are associated with a seizure disorder in neonates, benign neonatal familial convulsions (BNFC), and predispose affected individuals to epilepsy later in life. BFNC caused by KCNQ2/3 mutations can be the result of relatively modest (25%) reductions in current [104]. Mutations that cause loss of channel function in BNFC include pore mutations and frameshift truncations of KCNQ2 and KCNQ3 that yield non-functional channels, and do not act as dominant negatives [96]. KCNQ4 and KCNQ5 can also co-assemble with KCNQ3, and may contribute to the diversity of M-currents found in the nervous system [105].

The cardiac I_{Ks} and the neuronal M-current are the two major pharmaceutical targets in the KCNQ family, and there are specific pharmacologies for each. Several anti-arrhythmic drugs can block KCNQ1/KCNE1 complexes selectively, particularly the chromanols HMR1556 and chromanol 293B, and can prolong the cardiac action potential and block ventricular tachycardia by prolonging I_{Ks} [106]. These blockers are both enantioselective, (-)3R,4S being the potent enantiomer in each case [107], and both more potently inhibit KCNQ1/KCNE1 complexes than KCNQ1 tetramers [108, 109]. Benzodiazapenes such as L-768673 and L-7 also block I_{Ks} [110]. Mefenemic acid and the chloride channel blocker DIDS non-specifically activate KCNQ1.

Linopirdine is a relatively specific M-current inhibitor, and was shown to enhance learning and cognition in a mouse model [111], but failed to show a clear effect in a human Alzheimer's disease trial [112]. The M-current is also blocked by XE991, though this drug inhibits KCNQ1 and KCNQ4, as well. An activator of KCNQ2/3, retigabine, is in clinical trials as an anticonvulsant to treat epilepsy, and may also be useful in treating neuropathic pain [113]. The BK activator BMS-204352 also stimulates M-current.

KCNH K^+ Channels: Physiological Functions, Disease Relevance, Pharmacology

Channels of the KCNH family include EAG (ether-à-go-go), HERG (human ether-à-go-go-related gene), and ELK (ether-à-go-go-like gene). These names derive from the channels' homology to the *Drosophila ether-à-go-go* channel, and are characterized by their slow activation and direct activation by cyclic nucleotides. Another important property of these channels is that they are voltage-dependent and activate at sub-threshold or near-threshold potentials, suggesting that they could play a role in resting membrane potential regulation [114] and spike frequency adaptation[115]. HERG is best known for its role in the fast delayed rectifier current (I_{Kr}) of the cardiac action potential, where it carries a large portion of the outward current during repolarization. The channel has an unusual, bell-shaped current-voltage curve, with increasing currents up to +10 mV, then progressively smaller currents at more depolarized potentials [116]. This behavior is the result of slow voltage activation coupled with unusually fast C-type inactivation at depolarized potentials [117]. Mutations in HERG are associated with long-QT syndrome, type 2, and account for the reduced potassium currents that lead to prolongation of the cardiac QT phase.

In general, the function of KCNH channels in the mammalian nervous system is not well characterized, despite the well-studied role of these channels in *Drosophila* neuromuscular function. ERG mRNA is present throughout the brain [118], and has been suggested to play a role in firing frequency and spike frequency adaptation in cerebellar Purkinje neurons [119]. The three ELK channels have predominantly neuronal expression, and can co-assemble with one another. Although their functional importance

is unknown, their activation at potentials near the resting potential suggests a role in neuronal excitability. EAG channels are expressed predominantly in non-neuronal tissues, and are notably up-regulated in various tumors. Transfection of normal cells with the gene encoding EAG can lead to transformation to tumor cells [120], and EAG expression has been reported to be a marker for cervical cancer [121]. HERG also has oncogenic potential in neoplastic hematopoietic cells [122]. This unexpected role for ion channels in cell proliferation is likely related to cell cycle-dependent changes in channel activity [123].

The rapid delayed rectifier potassium current of the heart, I_{Kr}, is a major drug target for the treatment of arrhythmia, and the class III methanesulfonalide antiarrhythmics block this current carried by HERG/KCNE2. The methanesulfonalides include dofetilide, E-4031, ibutilide, D-solatol, and MK-499. They are open channel blockers that enter the cytoplasmic mouth of channel and bind to residues in the central cavity [124]. Class III antiarrhythmics prolong the ventricular action potential by increasing the QT phase. While these drugs can work by pore block, there are also reports that they can rescue channel mutants with folding defects and increase trafficking to the plasma membrane [125]. Unfortunately, many of these drugs are associated with drug-induced long QT syndrome, an increased risk for torsade de pointes, and sudden cardiac death [126]. Still, the class III antiarrhythmics are useful as a therapy for atrial fibrillation or flutter [127].

Antihistamines (astemizole, terfenadine), antipsychotics (chlorpromazine, haloperidol), some antibiotics, and gastrointestinal prokinetic agents (cisapride) have also been found to cause drug-induced long QT syndrome and ventricular arrhythmia [126].

Peptide toxins that block other voltage-gated K^+ channels are generally not effective against HERG, but recently two scorpion peptides, Ergtoxin and BeKm-1, have been identified, and specifically inhibit HERG, but not ELK or EAG channels [128, 129].

Although relatively little is known about EAG and ELK pharmacology relative to HERG's, EAG is a potential target for anti-tumor therapies, as both the antihistamine astemizole [130] and the tricyclic antidepressant imipramine [131] can inhibit EAG-mediated cell proliferation. The physiological roles of ELK channels are still unknown, and the search for their function would be aided by specific pharmacological tools.

Other Sub-Families of K^+ channels: Inwardly-Rectifying and Two-P K^+ channels

The inward rectifier sub-family contains the basic transmembrane unit of a K^+ channels, two TMS flanking the P-loop. The unique electrophysiological feature of these channels is inward rectification: a larger conductance at membrane potentials favoring inward current than at potentials favoring outward current. This property is the result of blockade of the cytoplasmic side of the pore by magnesium or polyamines at depolarized potentials. These channels are open around the resting potential and resist small depolarizations, but are blocked upon stronger depolarizations, such as those following the opening of voltage-gated Na^+ channels.

Inwardly-rectifying K^+ channels help to set the resting membrane potential of excitable cells, and play more specialized roles in other cells types. The ATP-sensitive K_{ATP}, channel, for example, is an octamer of four Kir 6.1 or 6.2 subunits and four sulfonylurea receptor (SUR) subunits. Inhibition of K_{ATP} in pancreatic beta cells promotes insulin release. Another class of inward rectifier is the GIRK channels, which

are opened by binding to the G-protein $G_{\beta\gamma}$ subunit, and so are linked to the activity of G-protein coupled receptors.

The two-P, or KCNK, channels [132] have only recently been identified, and make up a sub-family of fourteen members in humans. Their topology consists of two inward rectifier channels linked in tandem, so they contain two P loops per subunit and presumably assemble as dimers. Functionally, the two-P channels are thought to carry background, or leak, potassium conductances, which set the resting potential of many cell types and can modulate the excitability of neurons, heart and muscle cells, and endocrine cells. While no high-affinity, specific agents for two-P channels have been identified, a number of physiological stimuli, such as mechanical stretch, acid, and polyunsaturated fatty acids do affect channel open probability. Some neurotransmitters can inhibit two-P channels, further enhancing membrane excitability through second messenger pathways [133]. Two-P channels may also be a target for general anesthetics, as agents such as halothane and chloroform open some KCNK channels at clinically relevant concentrations [134].

Voltage-Gated Na^+ channels

Voltage-gated Na^+ channels and K^+ channels are responsible for action potential generation. In the initial phase of a neuronal action potential, small inward currents through post-synaptic ligand-gated cation channels sum to produce a threshold depolarization. This depolarization activates a large inward sodium current that depolarizes the cell even further and then inactivates within several hundred milliseconds. Voltage-gated Na^+ channels carry this large inward current, spreading the depolarization

from the axon initial segment, to the nodes of Ranvier along the axon, and ultimately to the nerve terminal where neurotransmitter release occurs. By contrast, voltage-gated K^+ channels are responsible for the repolarization of the membrane: they open after voltage-gated Na^+ channels and carry a large, opposing outward current that returns the membrane potential towards its resting value, reverses Na^+ channel inactivation, and allows the neuron to fire another action potential.

For repetitive neuronal firing to be possible, voltage-gated Na^+ channels must be highly selective for sodium over other ions, must open rapidly in the correct range of membrane potential, must inactivate quickly, and then recover upon membrane repolarization. In addition, the channels must be targeted to the correct subcellular locations, such as the axon initial segment and nodes of Ranvier. Voltage-gated Na^+ channels are expressed in excitable cells of the central and peripheral nervous systems, the heart, skeletal muscle, as well as several other excitable cell types. They have been found in many animal species, both vertebrates and invertebrates, though they are absent in the nematode *C. elegans*. Recently, a superfamily of bacterial voltage-gated Na^+ channels has even been identified, though these Na^+ channels resemble voltage-gated K^+ channels in topology rather than their mammalian sodium-selective counterparts [6, 135].

In their groundbreaking electrophysiological studies of the squid giant axon, Hodgkin and Huxley measured sodium- and potassium-selective conductances [136], but did not yet know what cellular components mediated these ionic fluxes, or if they were even separate entities. The discovery of two toxins that could inhibit the axonal sodium current but not the potassium current, tetrodotoxin (TTX) from puffer fish and saxitoxin

from *Gonyaulax* marine dinoflagellates, gave the first strong evidence that sodium and potassium traversed the membrane through distinct pathways [137, 138].

A voltage-gated Na^+ channel from the electric eel *Electrophorus electricus* was the first voltage-gated ion channel to be cloned [1], and its primary structure immediately provided clues to the function of the channel. The channel is made up of four homologous repeats (DI-IV) of six putative TMS, each repeat having a cluster of positively charged residues that were proposed to be part of the voltage-sensing mechanism. The fourth TMS (S4) of each repeat has a positively-charged residue approximately every third residue, while the determinants of ion selectivity are residues in the region between the S5 and S6 TMS (the SS1-SS2 region). The S6 transmembrane domain lines the ion conduction pathway. Inactivation of the channel appears to be mediated by an interaction of the linker between the third and fourth repeats of the Na^+ channel with the cytoplasmic ends of the S5 and S6 TMS [139, 140].

The cytoplasmic N- and C-terminal domains of the Na^+ channel, as well as cytoplasmic linker regions between the repeats, provide sites for post-translational modifications and co-assembly with cytoplasmic domains of other proteins. Mutations in many parts of the channel can interfere with the electrophysiological function or the targeting of voltage-gated Na^+ channels, and lead to a number of cardiac, neurological, and skeletomuscular disorders. In the following sections, we will discuss in more detail the molecular basis for the electrophysiolgical and cell biological properties of voltage-gated Na^+ channels, their physiological significance in both normal and disease states, and the pharmacology of voltage-gated Na^+ channels.

A Single Family of Voltage-Gated Na^+ Channel α-Subunits

The mammalian repertoire of voltage-gated Na^+ channels consists of ten members, which are so closely related that they make up a single family. This is in contrast to voltage-gated K^+ channels, which can be divided into at least twelve sub-families, and the three sub-families of voltage-gated Ca^{2+} channels. Nine of the α-subunits, Nav1.1-1.9, have more than 70 % identity in the transmembrane and extracellular amino acids, while the tenth channel, Nax, is approximately 50 % identical to the other nine Na^+ channels, but has sequence differences in some of the key regions for selectivity, voltage sensing and inactivation.

The brain Na^+ channel was originally isolated as a trimer of the pore-forming α-subunit Nav1.2 with the β-1 and β-2 auxiliary subunits [141], but in other tissues the α-subunits may interact with only one or none of the cloned β-subunits. There are four β-subunits, of which two, β-2 and β-4, form disulfide bonds with the α-subunit; β-1 and β-3 interact non-covalently with the α-subunit. These proteins have a single TMS, a short cytoplasmic domain, and a heavily glycosylated extracellular domain. The extracellular domain has an IgG-type fold that is homologous to several cell adhesion proteins, and is thought to mediate clustering of channels with other proteins at nodes of Ranvier and the axon initial segment, as well as cell-cell contact. In addition to affecting the sub-cellular localization of voltage-gated Na^+ channels, β-subunits can also modulate the electrophysiological properties of α-subunits, such as the rate of fast inactivation and voltage-dependence of activation. β-subunits' effects may help to explain functional differences between heterologously expressed α-subunits and native channels.

All members of the voltage-gated Na^+ channel family share the same topology, with four pseudo-repeats, each containing six putative TMS, and cytoplasmic N- and C-termini. The fourth TMS of the first three repeats have 4-5 lysines or arginines, while the S4 of the fourth repeat has 7-8 positively-charged residues. Current models suggest that all four S4 segments shift towards the extracellular side of the membrane during voltage activation [142]. A number of studies of the gating charge indicate that the positively charged residues may be mostly surrounded by water-filled crevices, such that the entire transmembrane electric field is compressed into a distance of a few Angstroms [143]. Accordingly, relatively modest translations of the S4 segments may be sufficient to carry the entire gating charge.

Selectivity

While K^+ channel selectivity is determined by backbone carbonyl coordination of ions in the selectivity filter, it is charged side chains in the Na^+ channel pore that appear to be crucial for selectivity. Voltage-gated Na^+ channels are approximately ten-fold more selective for sodium over potassium and have a negligible permeability to calcium. The SS1-SS2 region of the four repeats has a conserved set of residues, D (repeat I), E (repeat II), K (repeat III), and A (repeat IV), known as the DEKA region. These four residues are thought to form a ring of side chains that allow for sodium permeation while excluding potassium and calcium. Mutation of the pore lysine residue of the DEKA motif eliminates the channel's selectivity among alkali metal ions and makes the channel permeable to calcium and even to large organic cations such as tetraethylammonium (TEA) [144]. Ca^{2+} channels have four glutamate (E) residues at the equivalent positions,

and in fact, a Na^+ channel can be converted to a Ca^{2+} channel by mutating the D, K, and A of the DEKA region to glutamates [145]. Voltage-gated K^+ channels are presumed to have a four-fold rotationally symmetric pore, since they are composed of four equivalent monomers, and the coordination of potassium resembles the geometry of a hydrated potassium ion [146]. By contrast, the Na^+ channel pore clearly uses the asymmetry afforded by four non-equivalent repeats in order to discriminate among ions.

Inactivation

Na^+ channel inactivation allows for the recovery of the resting membrane potential and for repetitive firing, and many disease mutations of Na^+ channels affect this aspect of channel activity. Voltage-gated Na^+ channel inactivation can be divided into a fast inactivation, which occurs within milliseconds of channel opening, and slow inactivation, which occurs on a timescale of hundreds of milliseconds to minutes. Although inactivation depends on voltage activation of the channel, inactivation itself does not require the voltage-gated migration of any charged residues [147]. Rather, it appears to be a conformational change that leads to blockage of the conduction pore by a cytoplasmic region between the third and fourth repeats of the channel.

Fast inactivation of voltage-gated Na^+ channels is essential for proper firing of action potentials and for preventing backward propagation of action potentials along the axon. It limits the duration of the depolarization mediated by sodium influx, and gives a directionality to the action potential: once the Na^+ channels at a given node of Ranvier have opened and inactivated as part of an action potential, the action potential will propagate only in the direction of open Na^+ channels, towards the axon terminal. Three

residues in the III-IV linker region are critical for inactivation, and have been termed the IFM (Isoleucine-Phenylalanine-Methionine) motif [139, 148]. These residues likely dock to the inner mouth of the channel, since mutations of residues in the cytoplasmic end of the DIV S6 TMS [149] and in the DIV S4-S5 loop [150] can disrupt fast inactivation.

While fast inactivation directly affects action potential duration, slow inactivation plays a role in spike frequency adaptation and may even be important for memory of previous channel activity [151]. Near the resting potential, very few channels undergo fast inactivation, but slow inactivation can be a factor in regulating the duration of openings in this range. Thus, slow inactivation can decrease membrane excitability by keeping voltage-gated Na^+ channels closed in the steady state. The P-region, or SS1-SS2, appears to be important for slow inactivation, since a residue in this part of the hNav1.5 (D II) was found to be a critical determinant of the probability of entry into a slow inactivated state [152]. As is the case with voltage-gated K^+ channels, voltage-gated Na^+ channel slow inactivation may be due to a collapse of the pore in response to other conformational changes within the channel.

Trafficking

A well characterized example of voltage-gated Na^+ channel trafficking is the localization of Nav1.2 at the axon initial segment of neurons. Although the β-subunits are involved in adhesion and channel trafficking, they do not themselves target Na^+ channels to the axon. Rather, the α-subunit contains several motifs that allow for its proper localization. A di-leucine motif in the C-terminal domain is responsible for internalization of the channel in somadendritic membrane, but not axonal membrane

[153]. Axonal channels may be trapped by the ankyrin G β-IV spectrin complex, while the Na^+ channels in non-axonal membrane are untethered and retrieved by endocytosis [154]. While the C-terminus is sufficient for axonal targeting, it cannot localize Nav1.2 at the initial segment of the axon. The channel has an acidic cluster in the cytoplasmic II-III linker that acts as a retention motif for the axon initial segment [155]. This motif binds to the clustering protein ankyrin G, and is conserved in Nav1.1, 1.3, 1.4, 1.5, and 1.6.

Interactions between ankyrin G and β-spectrin help Na^+ channels to cluster at high density in the post-synaptic membrane of neuromuscular junctions [156]. Ankyrin G is also essential for targeting of voltage-gated Na^+ channels to the axon initial segment and nodes of Ranvier, as mice with ankyrin G knocked out fail to properly localize axonal Na^+ channels [157]. Neurofascin and NrCAM are cell adhesion proteins that cluster with ankyrin G at the axon initial segment, and are important for Na^+ channel accumulation at nodes of myelinating cells [158]. Cell adhesion molecules prevent channels from diffusing away from nodes of Ranvier and the axon initial segment.

Physiological Functions

Of the nine members of the Nav1.x family, seven are expressed in the central and/or peripheral nervous system; Nav1.5 is found primarily in heart muscle; and Nav1.4 is localized to skeletal muscle cells. Nax has a wider distribution, and has been identified in heart, uterus, glia, the peripheral nervous system, and in smooth muscle.

Within neurons, Na^+ channels are often localized at the axon initial segment and nodes of Ranvier, where they play an essential role in the propagation of action potentials. These channels generally carry transient, fast-inactivating sodium currents that

allow for rapid recovery and repetitive firing of neurons. Somatic integration of excitatory synaptic inputs causes action potential initiation at the axon initial segment. The insulating properties of myelin allow the action potential to jump rapidly from node to node and ultimately to the synaptic terminal, where the opening of voltage-gated Ca^{2+} channels stimulates neurotransmitter release.

Although some voltage-gated Na^+ channels are selectively retrieved from somatodendritic membrane, Na^+ channels are still present in dendrites. At post-synaptic dendritic sites, Na^+ channels may amplify excitatory post-synaptic potentials as they travel towards the soma. In addition, action potentials can backpropagate from the soma to the dendrites, and the efficiency of backpropagation is dependent on the dendritic Na^+ channel density [159]. In Purkinje neurons, for example, dendritic Na^+ channel density decreases steeply with distance from the soma [160], so backpropagating action potentials dissipate quickly. In mitral cells or hippocampal CA1 neurons [159, 161], however, there is a higher ratio of Na^+ to K^+ channels in the dendrites, allowing for regenerative action potential backpropagation. The coincidence of subtheshold post-synaptic stimulation and backpropagating action potentials is thought to underlie some forms of synaptic plasticity. The calcium influxes mediated by this coincidence could mediate long-term potentiation (LTP) and other transcriptional changes in neuronal activity.

While the best characterized voltage-gated sodium currents are transient and fast-inactivating, sodium currents with different inactivation properties are important for modulating excitability. Persistent sodium currents are present at subthreshold potentials, where channels can open but fast inactivation does not occur. Their activation can

effectively depolarize the cell, such that it is closer to the threshold for action potential firing. More substantial depolarization by a persistent sodium current, however, can lead to resting inactivation of Na^+ channels and decreased excitability. This distinction underlies the ability of some skeletal muscle Na^+ channel mutations that disrupt fast inactivation to cause myotonia (hyperexcitability), while others cause paralysis (hypoexcitability). Inhibiting persistent sodium currents also decreases excitability as K^+ channels that are open at rest push the membrane towards more hyperpolarized potentials. Persistent currents have been found electrophysiologically in central [162] and peripheral neurons [163], and are thought to be mediated by Nav1.6. There are other reports of TTX-resistant persistent sodium currents, as well [164].

In addition to the rapidly inactivating and persistent sodium currents, a resurgent sodium current has also been characterized [165]. It appears after a large depolarization, such as an action potential, followed by a return to a slightly depolarized potential (-40 mV). The resurgent current increases slowly and decays slowly, and might facilitate repetitive firing. The molecular identity of this current is not known, though mice lacking Nav1.6 also lack the resurgent current [166].

Several Na^+ channel family members are expressed predominantly in the peripheral nervous system, particularly in sensory neurons, and are thought to play a role in pain sensation. The Na^+ channel blocking activity of local anesthetics provides further evidence for the role of voltage-gated sodium currents in nociception. Nav1.7 is expressed at the terminal of sensory neurons, while Nav1.8 is exclusively expressed in sensory, especially nociceptive, neurons. Both channels respond to inflammatory factors involved in hyperalgesia, like nerve growth factor (NGF) [167, 168], which increases

expression of these channels in response to tissue damage and and leads to inflammatory pain sensation. Primary erythermalgia, a chronic human inflammatory disorder, which causes intermittent extreme pain and redness in the feet and hands, maps to the Nav1.7 locus [169], and the associated mutations lead to hyperexcitability of nociceptive DRG neurons [170]. Accordingly, mice with Nav1.7 deleted from sensory neurons have increased mechanical and thermal pain thresholds and decreased inflammatory pain responses [171]. Nav1.8 is also likely to play a role in inflammatory pain on account of its up-regulation by NGF and the analgesic effects of Nav1.8 antisense in models of inflammatory pain [172].

Nav1.3 is generally expressed in the adult central nervous system, but upon nerve damage such as axotomy this channel and the β-3 subunit can be upregulated in sensory neurons [173]. This expression of Nav1.3 may be an important cause of hyperexcitability and neuropathic pain following nerve injury. Its upregulation can be suppressed by glial-derived neurotrophic factor (GDNF) [174], a factor associated with analgesia. Nav1.9, by contrast, provides a persistent sodium current that is down-regulated after axotomy [175]. Since Nav1.9 is activated at more hyperpolarized potentials compared to other Na^+ channels and has relatively slow kinetics of activation and inactivation [164], a decrease in its expression could remove resting inactivation of other Na^+ channels and thereby increase excitability. Thus, activation of Nav1.9 might be an effective way to minimize neuropathic pain.

In the central nervous system, changes in the localization of neuronal channels in myelinated neurons may play a role in the degenerative processes of multiple sclerosis (MS). Nav1.6 is usually localized to the nodes of Ranvier, but its distribution throughout

the axon becomes more diffuse during the demyelination characteristic of MS. Nav1.6 is also up-regulated and co-localizes with the sodium-calcium exchanger, as well as with β-amyloid precursor protein, a marker for axonal damage, in MS-damaged neurons. The persistent current mediated by Nav1.6 may cause increased calcium influx into the cell via the sodium-calcium exchanger and thus provide a mechanism for toxicity [176].

The predominant voltage-gated Na^+ channel subunit in heart cells is Nav1.5, which plays a key role in the depolarization and plateau phases of the cardiac action potential. A number of arrhythmias and other cardiac diseases are due to mutations in Nav1.5, and drugs from the class 1 antiarrhythmics are blockers of the heart voltage-gated Na^+ channel. Brain Na^+ channels Nav1.1 and 1.3 have also been identified in the sinoatrial node of the heart, where no Nav1.5 is expressed. The associated currents are TTX-sensitive and their blockade results in greater heart rate variability and lower spontaneous heart rate [177].

The Nax Na^+ channel has only 50 % identity to members of the Nav1.x family, and notably has fewer charges in the S4 segments and low conservation of residues in the III-IV linker region that mediates fast inactivation. A mouse with this gene knocked out has a reduced capacity to regulate NaCl intake under both high- and low-salt conditions [178]. Nax is expressed, among other places, in the circum ventricular organs of the brain, which control salt and water homeostasis, consistent with its role in osmoregulation.

Channelopathies

Na^+ channels expressed in skeletal muscle, heart, and the nervous system have been implicated in a number of genetic disorders, and Na^+ channel activity plays a role in many other disease states. Inherited mutations that affect channel activity most frequently change the inactivation properties of the Na^+ channel, rendering the cells where they are expressed either more or less excitable than they would normally be. Other mutations affect voltage-dependent activation or assembly with other proteins required for proper channel function.

Mutations in the skeletal muscle Na^+ channel, Nav1.4, are associated with several channelopathies, including paramyotonia congenita, potassium-aggravated myotonia, hyperkalemic periodic paralysis, and hypokalemic periodic paralysis. Myotonias are characterized by difficulty with muscle relaxation, triggered by exercise, cold, or a rise in plasma potassium levels, and produce repetitive activity in an electromyogram. The most common mutations are T1313M, in the III-IV linker, and R1448H/C in the S4 of domain IV, both of which slow fast inactivation [179]. Both types of mutation lead to a persistent current that slightly depolarizes muscle cells, enough to decrease the firing threshold, but not sufficient to lead to resting inactivation of the Na^+ channel population. Potassium-aggravated myotonia is frequently found to be associated with the G1306E/V/A mutations in the III-IV linker [180]. These mutations in the fast inactivation loop slow inactivation and lead to a persistent current with more frequent, longer openings.

Periodic paralysis, in contrast to myotonia, is a disorder caused by reduced muscle excitability, and is manifested by a silent electromyogram. Hyperkalemic periodic

paralysis (HyperPP) can be triggered by stress, fasting, potassium-rich foods, or exercise. The episodic muscle weakness associated with the disorder is the result of incomplete channel inactivation, which leads to a persistent sodium current that can depolarize the resting membrane potential from –90 mV to as high as –50 mV [96]. This depolarization causes most of the Na^+ channels to be inactivated at rest and makes them unable to initiate an action potential, explaining the silent electromyogram. Approximately 90 % of families with this disorder have a mutation in S6 (DII), T704M, which causes a 10 mV leftward shift in the voltage-dependent opening of the channel [96]. Thus, channels open at more negative potentials, well outside their inactivation range, creating a persistent current that depolarizes the resting membrane potential. Mutations of Nav1.4 can also lead to hypokalemic periodic paralysis. These mutations lie in DII S4, and enhance both fast and slow inactivation [181].

The cardiac Na^+ channel, Nav1.5, is associated with several inherited arrhythmic disorders, including Long-QT Syndrome Type 3, Brugada Syndrome, and conduction disorder. Long-QT Syndrome is caused by a slowed repolarization of the cardiac action potential, manifested by a lengthening of the QT phase of the electrocardiogram. This arrhythmia can lead to lower ventricular filling, ventricular fibrillation, decreased cardiac output, and death. All Nav1.5 mutations that cause long-QT 3 result in defects in fast inactivation [182]. The most severe of these is the ΔKPQ1505-7 deletion in the III-IV loop [183 1995]. Impaired inactivation prolongs the plateau of the cardiac action potential with a persistent sodium current, resulting in slower repolarization and a QT interval that is 2-5 % longer than normal [96]. Class Ib antiarrhythmics such as mexiletine have been used to reduce the persistent sodium current of the mutant channel.

Brugada syndrome [184] is a cardiac arrhythmia that elevates the ST segment of the electrocardiogram, substantially increasing the risk of idiopathic ventricular fibrillation in affected individuals. The elevated ST segment is the result of a voltage gradient between the epicardium and the endocardium: the loss of sodium current has a greater effect on the epicardium, on account of its counteracting the transient outward potassium current ($I_{K,to}$), than on the endocardium, where this potassium current is less prominent. The epicardium thus repolarizes pre-maturely relative to the endocardium, resulting in an arrhythmogenic transmural voltage gradient. Disease mutations are found at amino acids throughout the channel, and generally render the channel non-functional [185].

In the central nervous system, mutants of both the Na^+ channel α-subunit Nav1.1 and the β-1 subunit have been found to cause generalized epilepsy with febrile seizures. The β-subunit mutation (C121W) maps to a cysteine residue in the extracellular domain that is involved in a disulfide bond which is essential for proper folding of the domain [186]. α-subunit mutations decrease interaction with β-1 (D1866Y), causing a right shift in the voltage dependence of inactivation and a greater persistent current, or can affect the voltage-dependence of inactivation (I1656M and R1657C) by uncoupling voltage sensor movements from fast inactivation [187-189]. Another form of epilepsy, severe myoclonic epilepsy of infancy (SMEI), has also been mapped to several sites on the *scn1a* (Nav1.1) gene [190]. Mutants causing this form of epilepsy are either non-functional or non-inactivating. Several missense mutations of Nav1.2 can also lead to GEFS [191] or benign familial neonatal-infantile seizures [192], while nonsense

mutations are correlated with intractable epilepsy such as SMEI [193]. Voltage-gated Na^+ channel mutations may also predispose individuals to autism [194].

Pharmacology

Several classes of toxins and small organic compounds bind to distinct sites on voltage-gated Na^+ channels, affecting channel permeation or inactivation. The first identified toxins that could specifically block Na^+ channels are tetrodotoxin (TTX) and saxitoxin (STX), which have varying affinities for different members of the voltage-gated Na^+ channel family. TTX is concentrated from marine bacteria by the *fugu* puffer fish, while STX is a poison from dinoflagellates, which are ingested by various shellfish. Both bind with low nanomolar affinity to the skeletal muscle and brain channels, and have much lower affinity for the cardiac and peripheral Na^+ channels Nav1.8 and 1.9. The TTX/STX binding site is determined by residues in the selectivity filter of the channel, as well as the β-subunit, and not surprisingly, these toxins block the channel pore. Both toxins contain a positively-charged guanidinium group that interacts with glutamate and aspartate residues in the SS2 regions. The μ-conotoxins are peptide toxins from the Conus marine snails and have a guanidinium group from an arginine residue that mediates binding to the same part of the channel as TTX and STX.

A second class of toxins is composed of lipid-soluble compounds such as the plant-derived aconitine, batrachotoxin (BTX), and grayanotoxin (GTX), and veratridine, which is secreted by the skin of poisonous frogs from the *Phyllobates* genus. Unlike TTX, STX and μ-conotoxins, these lipid-soluble toxins are activators of Na^+ channels that shift voltage activation to more negative potentials and inhibit fast inactivation.

Ciguatoxins (CTX) and brevetoxin (PbTx), both derived from marine dinoflagellates, make up another class of lipid-soluble toxins that activate voltage-gated Na^+ channels by shifting the voltage-dependence of activation to more hyperpolarized potentials and by inhibiting fast inactivation. The type-I sea anemone toxin, scorpion α-toxins, and Australian funnel-web spider-derived atracotoxins prevent fast inactivation of voltage-gated Na^+ channels by binding extracellular S3-S4 and S5-S6 linkers [195]. The peptide scorpion β-toxins bind to the extracellular end of S4DII and the S3-S4DII loop, and likely stabilize the open conformation of the voltage-sensing S4 transmembrane domain [196].

Other activators of voltage-gated Na^+ channels include the pyrethroid insecticides, such as dichlorodiphenyltrichloroethane (DDT). Anti-epileptic drugs like phenytoin, lamotrigine, and carbamazepine are blockers of voltage-gated Na^+ channels, and the Na^+ channel blocking action of antidepressants such as imipramine, amitriptyline, and maprotiline may mediate sedative and arrhythmogenic side effects of these drugs. Antiarrhythmic drugs of class 1b, such as mexiletine, as well as local anesthetics, have been useful treatments for paramyotonia congenita and potassium-aggravated myotonia, and can be neuroprotective in some cases. Antiarrhythmic drugs have not been as useful as one might hope, however, on account of their side effects: their tendency to promote arrhythmias in many patients is of particular concern.

Local anesthetics make up a class of voltage-gated Na^+ channel blockers that act on nociceptive fibers of the peripheral nervous system. These compounds are lipid-soluble, and include lidocaine, bupivacaine, benzocaine, and many other compounds. They cross the membrane in order to reach their site of action at the cytoplasmic mouth

of the channel, where they display use-dependent block: that is, successive depolarizations increase access of local anesthetics to their binding site on the channel [197]. Unlike the blockers TTX and STX, there is relatively little variability in local anesthetic affinity among the members of the voltage-gated Na^+ channel family. Affinities do not necessarily correlate with analgesic efficacy, since repetitive firing, not current amplitude, is what underlies nociceptive transmission [198].

Calcium channels

Voltage-gated Ca^{2+} channels are essential for mediating cellular responses to electrical activity, exemplified by the fundamental requirement of these channels in neurotransmitter release and muscle contraction. Intracellular calcium ion concentration is highly regulated and normally maintained around 100 nM, as prolonged elevation of calcium levels can trigger cell death. Voltage-gated Ca^{2+} channels play a major role in controlling intracellular calcium concentrations. The influx of calcium into a cell induced by the opening of a voltage-gated Ca^{2+} channel can cause over a 1,000-fold increase in localized calcium concentration, resulting in profound changes in cellular function.

Over the decades, an impressive body of work has examined the physiological impact of calcium currents and the proteins involved in shaping these currents. The initial cloning of a voltage-gated Ca^{2+} channel as well as the biochemical isolation of an α-subunit with its auxiliary subunits occurred in 1987 [199, 200]. Over the years, a total of ten pore forming $\alpha 1$- subunits from humans have been cloned along with a wide array of auxiliary subunits: four $\alpha 2\delta$-, four β-, and eight γ-subunits.

Like voltage-gated sodium channels, the voltage-gated Ca^{2+} channel's pore-forming α-subunit gene encodes a 24 transmembrane protein divided into four 6 TMS pseudo-repeating domains. This pore-forming α1-subunit interacts noncovalently with the auxiliary subunits α2δ, β, and sometimes γ at non-overlapping domains of the α1 subunit to form a voltage-gated Ca^{2+} channel complex.

The interactions of these subunits can have a profound impact on the function, localization, and stability of the Ca^{2+} channel. Ultrastructural studies using electron microscopy and single particle analysis of the skeletal muscle Ca^{2+} channel (Cav1.1, α2δ-1, β-1a, γ-1) and cardiac Ca^{2+} channel (Cav1.2, α2δ-1, β-2 or 3) at nanometer resolution have provided some insight into the physical association of the voltage-gated Ca^{2+} channel subunits, corroborating information gleaned from biochemical studies over the past few years [201]. High resolution crystal structures of Ca^{2+} channel components are an enticing but challenging goal that has not been fully realized. Obtaining a more structurally refined image of the Ca^{2+} channel will provide greater insight into the channel's mechanics, function, and provide a guide for the development of drugs to alter Ca^{2+} channel activity.

Recently, the first crystal structures of a voltage-gated Ca^{2+} channel domain were published, depicting the 18 amino acid stretch of the cytoplasmic domain I-II linker site where the β-subunits interact with the α1-subunit, known as the α1 interaction domain (AID) bound to different β-subunits at high resolution [202-204]. These structures reveal that the AID is an amphipathic helix. The highly conserved hydrophobic residues of the AID form a complement to the hydrophobic groove of the β-subunit that is most intimate

with the AID. Unlike the β subunit, it is not clear where α2δ- or γ- interact with the Cavα1-subunit.

There is great diversity among voltage-gated Ca^{2+} channels. From the sheer number of possible subunit combinations that assemble to form a functional channel to the range of signaling pathways involved in these channels, great challenges and opportunities exist in pharmacologically controlling these channels. Buoyed by the early success of blocking voltage-gated Ca^{2+} channels to treat hypertension, continued efforts are underway to better understand specific roles of voltage-gated Ca^{2+} channels and to develop new and better pharmacological tools.

α subunit

The broadest classifications among the ten cloned α subunits are the high voltage activated (HVA) and the low voltage activated (LVA) classes of subunits [205]. The HVA Ca^{2+} channels require a large depolarization to open in normal physiological conditions. Further classification of HVA channels is now possible based upon their pharmacological profile: dihydropyridine (DHP) sensitive channels (L-type, Cav1.1 – 1.4), ω–agatoxin IVA sensitive channels (P- and Q- type, Cav2.1), ω–conotoxin GVIA sensitive channels (N-type, Cav2.2), and SNX482 sensitive channels (R type, Cav2.3) [8]. The remaining three cloned Ca^{2+} channels are the LVA type channels (Cav3.1 – 3.3), also known as T-type channels, and have no known specific blockers at this time. These channels open at membrane potentials close to rest and have a small single channel conductance [206, 207], but can collectively influence the excitability and signaling properties of a neuron.

Voltage-gated Ca^{2+} channels are able to selectively allow calcium entry through the cell membrane and exclude the passage of other ions, including sodium, which is roughly the same size as a calcium ion. A ring of four glutamates, one from the pore lining P-loop of each pseudo-repeat, is the crucial site for calcium selectivity and is conserved among all of the HVA α subunits [208]. The acidic side chains of this EEEE ring motif are believed to project into the pore interior of the Ca^{2+} channel, allowing the negatively charged carboxylate oxygens to coordinate a calcium ion. Even a subtle mutation of a single glutamate to aspartate or glutamine reduces the calcium affinity of the voltage-gated Ca^{2+} channel [209]. LVA Cav3 channels have a similar selectivity ring, but with two glutamates and two aspartates instead of four glutamates forming the ring.

There is a proposed hinged-lid model for the fast inactivation of voltage-gated Ca^{2+} channels [210]. S6 of DI-IV acts as a docking site for the DI-II linker region to block the conduction of calcium reminiscent of the ball and chain model seen in sodium and potassium voltage-gated channels.

β-subunits

Of the four known cytosolic β-subunits, β-1a was the first discovered when it was copurified with the initial isolation of Cav1.1 in skeletal muscle [211] . Over the years, characterizations of the four β-subunits have revealed numerous splice variants with distinct properties [212]. β-1b and β-2a for example, have the ability to independently associate with the plasma membrane via acidic motifs or palmitoylation [213, 214].

Sequence analysis and the recent crystal structures of β-2, β-3, and β-4 show that β subunits are part of the membrane-associated guanylate kinase (MAGUK) family

[215]. SH3, a protein-protein binding motif, and a guanylate kinase motif the two main motifs of MAGUK proteins, although the enzymatic capability of the guanylate kinase has been modified in β-subunits and is now involved in establishing protein-protein interfaces that modulate Cav-α1 Ca^{2+} channel function.

The ability of β-subunits to physically interact with the AID was thought to be primarily mediated by a 41 amino acid region of the β-subunit known as the β-interacting domain [216]. However, crystal structures of the AID bound to a β-subunit have revealed a more accurate portrayal of this region that binds to the AID, dubbed the AID binding pocket (ABP). The ABP is located at the ATP-coordination site of the GK domain, but a conserved tryptophan in the AID allows the β-subunit to bind to the α-subunit instead of ATP.

β-subunits have a number of profound effects on the trafficking, kinetics, and voltage properties of the voltage-gated Ca^{2+} channel [217]. With the exception of some truncated splice variants, β-subunits increase the functional expression of HVA Ca^{2+} channels. Almost all voltage-gated Ca^{2+} channel α-subunits have an ER retention signal located in the I-II cytoplasmic loop and β-subunits shield this signal to promote exit from the ER and surface expression of the channel [218]. β-subunits also influence Ca^{2+} channels at the plasma membrane and are capable of increasing the mean open time of Ca^{2+} channels as well as shifting the voltage dependence of HVA Ca^{2+} channel activation, making the Ca^{2+} channel more apt to open when a cell depolarizes. The voltage dependence of steady state inactivation is also shifted to more hyperpolarized potentials by β-subunits, with the exception of N-terminal palmitoylated β-2a. Palmitoylated β-2a retards the inactivation of Cav1.2, 2.2, and 2.3.

α2δ-subunits

There are four known mammalian α2δ-subunits that interact with voltage-gated Ca^{2+} channel α-subunits. Expanding on this molecular diversity, at least five splice variants of α2δ-1 (α2δ-1a to α2δ-1e) and three of α2δ-2 (α2δ-2a to α2δ-2c) have been detected with a tissue-specific distribution pattern. A salient feature of the α2δ-subunit is that it is proteolytically cleaved and the resulting α2- and δ- peptides are linked together via disulfide bridges. The entire α2-subunit is located extracellulary and the δ-subunit is a single transmembrane protein that acts as its anchor [219].

α2 is heavily glycosylated and presumably this glycosylation ultimately influences the trafficking and stability of the voltage-gated Ca^{2+} channel. Indeed, α2δ generally increases the surface expression level of voltage-gated Ca^{2+} channels [220]. Depending on the Cav α1- and β- subunits coexpressed with α2δ in a heterologous expression system, α2δ is also capable of accelerating both the activation and inactivation of calcium current. Like the β-subunit, α2δ also shifts the voltage dependence of the Ca^{2+} channels to more hyperpolarized potentials. It is not clear how α2δ modulates these biophysical properties of the voltage-gated Ca^{2+} channel.

γ-subunits

The primary focus of research on γ-subunits involved in Ca^{2+} channel function has been on its role in skeletal muscle, the only tissue known to express calcium γ-subunits until recently. Since the discovery that the spontaneous mutation in the *stargazer*

mouse line is a neuronal γ-subunit [221], the number of γ-subunits cloned has expanded to eight, and a number of these are expressed in the brain [222].

γ-subunits have four transmembrane domains with intracellular amino- and carboxyl- termini. Features of some of the neuronal γ-subunits are a cAMP/cGMP phosphorylation consensus site and potential sites for N-linked glycosylation. The γ-subunits are unique among the auxiliary subunits in not having a known influence on voltage-gated Ca^{2+} channel surface density. They also do not interfere with the α2δ- or β-subunits' interactions with the Cav α-subunit. The impact of γ-subunits on voltage-gated Ca^{2+} channel electrophysiology has not been robust or clearly understood. The general consensus is that γ-subunits lower the current of Ca^{2+} channels by causing a hyperpolarizing shift in the voltage dependence of inactivation.

Voltage-gated Ca^{2+} channels: Function and Pharmacology

Voltage-gated Ca^{2+} channels are expressed in all excitable cells and play numerous functional roles in a variety of signaling pathways that encode electrical activity into cellular events [4]. Although voltage-gated Ca^{2+} channels share fundamental physiological properties, the different Cav α- and auxiliary subunits have specialized distributions, functions, and pharmacological sensitivities. For decades, Ca^{2+} channels have been manipulated by researchers using multivalent cations and small organic molecules. The repertoire of pharmacological manipulations has more recently been expanded using peptides mainly derived from the venoms of predatory creatures. There continue to be focused efforts on the discovery and synthesis of new compounds to influence voltage-gated Ca^{2+} channel behavior [223].

General Blockers

Certain metal ions are capable of nonselectively blocking voltage-gated Ca^{2+} channels. Cadmium ions block all HVA Ca^{2+} channels. Nickel ions were historically used to block LVA channels but only Cav3.2 of the LVA family as well as a number of HVA channels are actually blocked by nickel [224]. Trivalent cations such as lanthanum, yttrium, and holmium are potent blockers of all voltage-gated Ca^{2+} channels. These multivalent ions block voltage-gated Ca^{2+} channels primarily by occlusion of the $\alpha 1$ pore region containing the EEEE ring of glutamic acid residues. These ions also have secondary effects outside of the pore region that influence the biophysical properties of voltage-gated Ca^{2+} channel.

Cav1 Family

Cav1.1 expressed in skeletal muscle is directly coupled with ryanodine receptors that line the sarcoplasmic reticulum which stores intracellular calcium. Depolarization of skeletal muscle plasma membrane opens Cav1.1 with slow kinetics, causing activation of ryanodine receptors and leading to intracellular release of calcium. The released calcium from the internal stores binds to proteins such as troponin and ultimately allows myosin to generate the force necessary for contraction. Mutations of Cav1.1 have been associated with malignant hyperthermia, a condition in which a normally healthy individual can experience a life threatening release of calcium from the sarcoplasmic reticulum when given anesthetics or muscle relaxants [225]. The mutation is a substitution of an arginine to histidine or cysteine in the cytoplasmic III-IV linker that appears to lower the

depolarization threshold needed to induce the ryanodine receptor to release calcium from the sarcoplasmic reticulum stores [226].

The Cav1 family is important in cardiac and smooth muscle function. Cav1.2 and Cav1.3 are involved in pacemaking activity for the heart by controlling rhythmic entry of calcium in the sinoatrial and atrioventricular nodes. They also have roles in neurons along with the classical neuronal Cav2 family in regulating synaptic activity and gene expression. Unlike the predominantly axonal distribution of Cav2 channels, Cav1.2-1.4 have a more somatodendritic distribution in neurons. Cav1 channels possess a binding site for calmodulin, a calcium binding protein that can activate many signaling pathways in a calcium dependent manner. Synaptic activity that leads to Cav1 channel opening can initiate nuclear signaling and activation of transcription factors such as cyclic AMP response element binding (CREB) protein, leading to changes in gene transcription. Cav1 channels are able to both recruit and activate calmodulin by providing a calmodulin binding site as well as a calcium ion source from the open channel. Calcium-bound calmodulin is capable of activating a number of kinase pathways including ones that phosphorylate CREB, encouraging its nuclear entry and activity as a regulator of transcription [227].

Cav1.4, the most recently cloned of the Cav1 family, is the least understood, but a channelopathy, incomplete congenital stationary night blindness (CSNB2), caused by mutations in Cav1.4 has illuminated one of the roles of this channel. CSNB2 presents itself with a combination of symptoms such as myopia, nystagmus, reduced visual acuity, or night blindness. Over 40 mutations in Cav1.4, ranging from amino acid substitutions to truncations, have been identified in CSNB2 patients [228]. It is not clear how these

particular mutations of Cav1.4 compromise channel function. Cav1.4 is ideally suited for controlling tonic neurotransmitter release because it has a rather low threshold for activation at around -40 mV and inactivates slowly. Moreover, Cav1.4 is expressed in the retina and electroretinograms of CSNB2 patients indicate a defect in the tonic neurotransmission that occurs between photoreceptors and second order neurons [229].

The most varied and clinically useful Ca^{2+} channel pharmacological agents are those that block Cav1 channels to treat hypertension, angina, and certain arrhythmias [230]. The actions of dihydropyridines on Cav1 channels have been studied since the 1980s and their influences on the channel are complex. The ability of dihydropyridines to interact with Cav1 channels is state-dependent; dihydropyridines are inferior blockers when Cav1 Ca^{2+} channels are closed during hyperpolarizing conditions. There is also evidence that dihydropyridines promote the Ca^{2+} channel to be in an inactive state, reducing the channel's current [231]. The sites of dihydropyridine interaction with Cav1 have been isolated using mutagenesis studies, and a key conserved site is a threonine in S5 of domain III in Cav1.2 [232] . Moreover, a number of sites in domains III and IV also contribute to Cav1's dihydropyridine sensitivity [233, 234].

Like cardiac and skeletal muscle, vascular smooth muscle utilizes voltage-gated Ca^{2+} channels for regulating intracellular calcium levels that are responsible for muscular contraction. Using the dihydropyridine group of drugs has been clinically useful to treat hypertension by blocking Cav1 [235]. Reducing Cav1 channel activity reduces calcium entry into vascular smooth muscle and consequently reduces vascular pressure.

Cav2 Family

The members of the Cav2 family are expressed in a range of organs such as the pancreas, heart, and testis. However, their widespread presence in the central nervous system and their importance in neuronal function has been the overriding focus of Cav2 channel studies. The three Cav2 channel types have different pharmacological sensitivity profiles and specialized roles, but a common trait among them is their regulation of neurotransmitter release. Located at the presynaptic end of an axon, Cav2 channels open and allow calcium to enter the axonal terminal when an action potential pulse reaches the end of its path along an axon. Calcium ions that enter through Ca^{2+} channels and the channels themselves are key players in second messenger pathways leading to presynaptic release of neurotransmitters [236]. Cav2.1 and Cav2.2 contain a synaptic protein interaction motif in the II-III intracellular loop that binds with various proteins that are part of the neurotransmitter release machinery such as synaptotagmin I, syntaxin I, and SNAP-25 [237]. This voltage-gated Ca^{2+} channel involvement in linking electrical activity with exocytic release is also utilized in other physiological contexts such as hormone release [238].

Unlike the Cav1 family, individual Cav2 α subunits have specific blockers. The best known pharmacological modulators of the Cav2 family are peptides derived from the venom of predatory animals. These 20-30 amino acid peptides can be rather specific, capable of binding to a particular Cav2 subunit at nanomolar concentrations.

The most specific blocker of Cav2.1 is the 48 amino acid ω-agatoxin isolated from the American funnel spider *Agenelopsis aperta*. However, it also blocks Cav2.2 with low affinity, as well as Cav2.3. Blockade by ω-agatoxin is irreversible and likely interferes with the Cav2.1 voltage sensor. The S3-S4 region of DIV is the major site

where ω-agatoxin interacts with Cav2.1 [239]. P- and Q- type calcium currents arise from different splice variants of Cav2.1. The Q-type Cav2.1 splice variant has an addition of an aspargine and proline in the agatoxin interaction region, resulting in a lower agatoxin binding affinity.

The venom from the sea snail *Conus geopgraphus* contains a 27 amino acid peptide ω-conotoxin GVIA that is a selective, irreversible blocker of Cav2.2 N-type channels. Ω-conotoxin GVIA blocks Cav2.2 by physically occluding the pore [240]. Other selective N-type blocking peptides are ω-conotoxin MVIIA and MVIIC from the *Conus magus* snail, and the ω-conotoxin CVID isolated from *Conus catus*.

The therapeutic and commercial success of Cav1 channel blockers has inspired the possibility that specific Cav2 channel blockers have therapeutic potential as well. The most promising application is to use the Cav2 channel blockers for pain treatment. The impetus for finding pharmacological modulators of Cav2 channels is that the channels are highly expressed in the superficial layer of the dorsal horn of the spinal cord, an area where nociceptive signaling is transmitted. It is hoped that blocking Cav2 channels will block mediators of nociceptive signaling such as substance P [241]. The promise of this strategy is supported by Cav2.2 knock out mice having lowered sensitivity to neuropathic and inflammatory pain and current μ-opioid receptor agonists used for pain relief, such as morphine, partially block Cav2 channels [242, 243]. Ziconotide, a compound derived from ω-conotoxin MVIIA, has been approved for clinical use by the F.D.A. and the European Commission for treating severe chronic pain. Currently, ziconotide can only be administered intrathecally and there are some cases of severe side effects such as unruly behavior and hypotension [244]. More toxin-derived Cav2 channel blockers are in

various stages of development for pain treatment [245]. In addition, small organic molecules that specifically target Cav2 have the advantage of being orally administered and are also being developed and reviewed for pain treatment [246].

Until recently, there were no known pharmacologically blockers of Cav2.3 Ca^{2+} channels, but it is now known that these channels are blocked by SNX-482, a compound isolated from the venom of the tarantula *Hysterocrates gigas* [247]. SNX-482 also partially inhibits Cav1 channels with low affinity, but SNX-482 is the best Cav2.3 blocker to date [248].

Cav3 Family

The Cav3 family is the least understood among the voltage-gated channels but its members are known to be expressed in many tissues. Opening at potentials near the resting membrane potential, Cav3 channels can influence the membrane potential of the cell at rest. There is also evidence that Cav3 channels affect rhythmic neuronal firing.

Despite years of intense effort, there are still no specific and effective pharmacological blockers of Cav3 channels. As a result, studies of Cav3 have been hindered but there is growing evidence for functional roles of Cav3 channels and the potential benefits of developing specific Cav3 pharmacological targets.

Like Cav2.2, Cav3.2 and Cav3.3 are expressed in the dorsal root ganglion neurons of the superficial lamina. Given Cav3's low activation threshold kinetics, blocking these channels can reduce the overall excitability of a neuron. A number of pain models suggest an increase in excitability of nociceptive neurons contributes to pain perception.

Blocking Cav3 neurons could hamper these neurons' excitability and subsequently suppress nociceptive signaling [245].

Auxiliary subunit modulators

Given the substantial functional modifications that auxiliary subunits can have on voltage-gated Ca^{2+} channel properties, drugs that bind to these Ca^{2+} channel auxiliary subunits may also lead to alterations in Ca^{2+} channel function. One such example is the anticonvulsant drug gabapentin. Gabapentin interacts with a number of proteins, including $\alpha 2\delta$-1 [249]. Both the $\alpha 2$- and δ- subunits are required for gabapentin binding, but it is not known how this binding alters voltage-gated Ca^{2+} channel function. The general effect of gabapentin on voltage-gated Ca^{2+} channels is a reduction in macroscopic current. Besides the anticonvulsant properties of gabapentin, it has also been found to relieve neuropathic pain. Gabapentin's analgesic properties may be attributable to its block of Cav2.2 current in the dorsal root ganglia.

Other Voltage-Gated Channels

The superfamily of voltage-gated cation channels contains several other important channel types, including the cyclic nucleotide-gated (CNG) channels, the hyperpolarization-activated channels (HCN), and the transient receptor potential (TRP) channels. CNG channels are non-selective cation channels, and are crucial for the receptor-mediated transduction of visual and olfactory information through cyclic nucleotide second messenger pathways [250]. HCN channels are non-selective, gated by cyclic nucleotides, and are opened at voltages hyperpolarized to the resting potential.

They play a role in pacemaker activity of neurons and of the heart [251]. TRP channels are non-selective and only weakly voltage-sensitive. They are more distantly related to Kv channels than the HCN or CNG families. These channels play a role in a variety of sensory systems, including nociception, thermosensation, and taste sensation [252].

Other unrelated classes of voltage-gated ion channels include voltage-gated proton channels and voltage-gated chloride channels. The voltage-gated proton channel is an essential part of the oxidative burst of phagocytic cells of the immune system, providing a cationic shunt for the large, anionic superoxide flux generated by NADPH oxidase [253]. This channel has not yet been cloned. Voltage-gated chloride channels, or ClC channels, are a subset of anion channels that is entirely unrelated structurally to cation channels. These channels modulate muscle cell excitability, endosomal and vesicular acidification, epithelial transport, bone resorption, and cell swelling [254].

References

1. Noda, M., S. Shimizu, T. Tanabe, T. Takai, T. Kayano, T. Ikeda, H. Takahashi, H. Nakayama, Y. Kanaoka, N. Minamino, et al. (1984). Primary structure of Electrophorus electricus sodium channel deduced from cDNA sequence. *Nature*, 312:121-127.

2. Papazian, D. M., T. L. Schwarz, B. L. Tempel, Y. N. Jan, L. Y. Jan (1987). Cloning of genomic and complementary DNA from Shaker, a putative potassium channel gene from Drosophila. *Science*, 237:749-753.

3. Tempel, B. L., D. M. Papazian, T. L. Schwarz, Y. N. Jan, L. Y. Jan (1987). Sequence of a probable potassium channel component encoded at Shaker locus of Drosophila. *Science*, 237:770-775.

4. Hille, B., *Ion channels of excitable membranes*, 3rd ed. Sinauer. Sunderland, Mass., 2001

5. Paidhungat, M., S. Garrett (1997). A homolog of mammalian, voltage-gated calcium channels mediates yeast pheromone-stimulated Ca2+ uptake and exacerbates the cdc1(Ts) growth defect. *Mol Cell Biol*, 17:6339-6347.

6. Ren, D., B. Navarro, H. Xu, L. Yue, Q. Shi, D. E. Clapham (2001). A prokaryotic voltage-gated sodium channel. *Science*, 294:2372-2375.

7. Catterall, W. A., A. L. Goldin, S. G. Waxman (2003). International Union of Pharmacology. XXXIX. Compendium of voltage-gated ion channels: sodium channels. *Pharmacol Rev*, 55:575-578.

8. Catterall, W. A., J. Striessnig, T. P. Snutch, E. Perez-Reyes (2003). International Union of Pharmacology. XL. Compendium of voltage-gated ion channels: calcium channels. *Pharmacol Rev*, 55:579-581.

9. Gutman, G. A., K. G. Chandy, J. P. Adelman, J. Aiyar, D. A. Bayliss, D. E. Clapham, M. Covarriubias, G. V. Desir, K. Furuichi, B. Ganetzky, M. L. Garcia, S. Grissmer, L. Y. Jan, A. Karschin, D. Kim, S. Kuperschmidt, Y. Kurachi, M. Lazdunski, F. Lesage, H. A. Lester, D. McKinnon, C. G. Nichols, I. O'Kelly, J. Robbins, G. A. Robertson, B. Rudy, M. Sanguinetti, S. Seino, W. Stuehmer, M. M. Tamkun, C. A. Vandenberg, A. Wei, H. Wulff, R. S. Wymore (2003). International Union of Pharmacology. XLI. Compendium of voltage-gated ion channels: potassium channels. *Pharmacol Rev*, 55:583-586.

10. Doyle, D. A., J. Morais Cabral, R. A. Pfuetzner, A. Kuo, J. M. Gulbis, S. L. Cohen, B. T. Chait, R. MacKinnon (1998). The structure of the potassium channel: molecular basis of K+ conduction and selectivity. *Science*, 280:69-77.

11. Jiang, Y., A. Lee, J. Chen, M. Cadene, B. T. Chait, R. MacKinnon (2002). The open pore conformation of potassium channels. *Nature*, 417:523-526.

12. Jiang, Y., A. Lee, J. Chen, V. Ruta, M. Cadene, B. T. Chait, R. MacKinnon (2003). X-ray structure of a voltage-dependent K+ channel. *Nature*, 423:33-41.

13. Cohen, B. E., M. Grabe, L. Y. Jan (2003). Answers and questions from the KvAP structures. *Neuron*, 39:395-400.

14. Heginbotham, L., Z. Lu, T. Abramson, R. MacKinnon (1994). Mutations in the K+ channel signature sequence. *Biophys J*, 66:1061-1067.

15. Noskov, S. Y., S. Berneche, B. Roux (2004). Control of ion selectivity in potassium channels by electrostatic and dynamic properties of carbonyl ligands. *Nature*, 431:830-834.

16. Armstrong, C. M., F. Bezanilla (1973). Currents related to movement of the gating particles of the sodium channels. *Nature*, 242:459-461.

17. Papazian, D. M., L. C. Timpe, Y. N. Jan, L. Y. Jan (1991). Alteration of voltage-dependence of Shaker potassium channel by mutations in the S4 sequence. *Nature*, 349:305-310.

18. Papazian, D. M., X. M. Shao, S. A. Seoh, A. F. Mock, Y. Huang, D. H. Wainstock (1995). Electrostatic interactions of S4 voltage sensor in Shaker K+ channel. *Neuron*, 14:1293-1301.

19. Cha, A., G. E. Snyder, P. R. Selvin, F. Bezanilla (1999). Atomic scale movement of the voltage-sensing region in a potassium channel measured via spectroscopy. *Nature*, 402:809-813.

20. Glauner, K. S., L. M. Mannuzzu, C. S. Gandhi, E. Y. Isacoff (1999). Spectroscopic mapping of voltage sensor movement in the Shaker potassium channel. *Nature*, 402:813-817.

21. Jiang, Y., V. Ruta, J. Chen, A. Lee, R. MacKinnon (2003). The principle of gating charge movement in a voltage-dependent K+ channel. *Nature*, 423:42-48.

22. Liu, Y., M. Holmgren, M. E. Jurman, G. Yellen (1997). Gated access to the pore of a voltage-dependent K+ channel. *Neuron*, 19:175-184.

23. Webster, S. M., D. Del Camino, J. P. Dekker, G. Yellen (2004). Intracellular gate opening in Shaker K+ channels defined by high-affinity metal bridges. *Nature*, 428:864-868.

24. Zhou, M., J. H. Morais-Cabral, S. Mann, R. MacKinnon (2001). Potassium channel receptor site for the inactivation gate and quaternary amine inhibitors. *Nature*, 411:657-661.

25. Kuo, A., J. M. Gulbis, J. F. Antcliff, T. Rahman, E. D. Lowe, J. Zimmer, J. Cuthbertson, F. M. Ashcroft, T. Ezaki, D. A. Doyle (2003). Crystal structure of the potassium channel KirBac1.1 in the closed state. *Science*, 300:1922-1926.

26. Tristani-Firouzi, M., J. Chen, M. C. Sanguinetti (2002). Interactions between S4-S5 linker and S6 transmembrane domain modulate gating of HERG K+ channels. *J Biol Chem*, 277:18994-19000.

27. Long, S. B., E. B. Campbell, R. Mackinnon (2005). Voltage sensor of Kv1.2: structural basis of electromechanical coupling. *Science*, 309:903-908.

28. Demo, S. D., G. Yellen (1991). The inactivation gate of the Shaker K+ channel behaves like an open-channel blocker. *Neuron*, 7:743-753.

29. Gulbis, J. M., M. Zhou, S. Mann, R. MacKinnon (2000). Structure of the cytoplasmic beta subunit-T1 assembly of voltage-dependent K+ channels. *Science*, 289:123-127.

30. Murrell-Lagnado, R. D., R. W. Aldrich (1993). Interactions of amino terminal domains of Shaker K channels with a pore blocking site studied with synthetic peptides. *J Gen Physiol*, 102:949-975.

31. Nagaya, N., D. M. Papazian (1997). Potassium channel alpha and beta subunits assemble in the endoplasmic reticulum. *J Biol Chem*, 272:3022-3027.

32. Campomanes, C. R., K. I. Carroll, L. N. Manganas, M. E. Hershberger, B. Gong, D. E. Antonucci, K. J. Rhodes, J. S. Trimmer (2002). Kv beta subunit oxidoreductase activity and Kv1 potassium channel trafficking. *J Biol Chem*, 277:8298-8305.

33. An, W. F., M. R. Bowlby, M. Betty, J. Cao, H. P. Ling, G. Mendoza, J. W. Hinson, K. I. Mattsson, B. W. Strassle, J. S. Trimmer, K. J. Rhodes (2000). Modulation of A-type potassium channels by a family of calcium sensors. *Nature*, 403:553-556.

34. Shibata, R., H. Misonou, C. R. Campomanes, A. E. Anderson, L. A. Schrader, L. C. Doliveira, K. I. Carroll, J. D. Sweatt, K. J. Rhodes, J. S. Trimmer (2003). A fundamental role for KChIPs in determining the molecular properties and trafficking of Kv4.2 potassium channels. *J Biol Chem*, 278:36445-36454.

35. Sesti, F., S. A. Goldstein (1998). Single-channel characteristics of wild-type IKs channels and channels formed with two minK mutants that cause long QT syndrome. *J Gen Physiol*, 112:651-663.

36. Deschenes, I., G. F. Tomaselli (2002). Modulation of Kv4.3 current by accessory subunits. *FEBS Lett*, 528:183-188.

37. McCrossan, Z. A., A. Lewis, G. Panaghie, P. N. Jordan, D. J. Christini, D. J. Lerner, G. W. Abbott (2003). MinK-related peptide 2 modulates Kv2.1 and Kv3.1 potassium channels in mammalian brain. *J Neurosci*, 23:8077-8091.

38. Birnbaum, S. G., A. W. Varga, L. L. Yuan, A. E. Anderson, J. D. Sweatt, L. A. Schrader (2004). Structure and function of Kv4-family transient potassium channels. *Physiol Rev*, 84:803-833.

39. Vasilyev, D. V., M. E. Barish (2003). Regulation of an inactivating potassium current (IA) by the extracellular matrix protein vitronectin in embryonic mouse hippocampal neurones. *J Physiol*, 547:859-871.

40. Sheng, M., M. Wyszynski (1997). Ion channel targeting in neurons. *Bioessays*, 19:847-853.

41. Wang, H., D. D. Kunkel, T. M. Martin, P. A. Schwartzkroin, B. L. Tempel (1993). Heteromultimeric K+ channels in terminal and juxtaparanodal regions of neurons. *Nature*, 365:75-79.

42. Wang, H., D. D. Kunkel, P. A. Schwartzkroin, B. L. Tempel (1994). Localization of Kv1.1 and Kv1.2, two K channel proteins, to synaptic terminals, somata, and dendrites in the mouse brain. *J Neurosci*, 14:4588-4599.

43. Feng, J., B. Wible, G. R. Li, Z. Wang, S. Nattel (1997). Antisense oligodeoxynucleotides directed against Kv1.5 mRNA specifically inhibit ultrarapid delayed rectifier K+ current in cultured adult human atrial myocytes. *Circ Res*, 80:572-579.

44. Lin, C. S., R. C. Boltz, J. T. Blake, M. Nguyen, A. Talento, P. A. Fischer, M. S. Springer, N. H. Sigal, R. S. Slaughter, M. L. Garcia, et al. (1993). Voltage-gated potassium channels regulate calcium-dependent pathways involved in human T lymphocyte activation. *J Exp Med*, 177:637-645.

45. Du, J., J. H. Tao-Cheng, P. Zerfas, C. J. McBain (1998). The K+ channel, Kv2.1, is apposed to astrocytic processes and is associated with inhibitory postsynaptic membranes in hippocampal and cortical principal neurons and inhibitory interneurons. *Neuroscience*, 84:37-48.

46. Hwang, P. M., M. Fotuhi, D. S. Bredt, A. M. Cunningham, S. H. Snyder (1993). Contrasting immunohistochemical localizations in rat brain of two novel K+ channels of the Shab subfamily. *J Neurosci*, 13:1569-1576.

47. Kramer, J. W., M. A. Post, A. M. Brown, G. E. Kirsch (1998). Modulation of potassium channel gating by coexpression of Kv2.1 with regulatory Kv5.1 or Kv6.1 alpha-subunits. *Am J Physiol*, 274:C1501-1510.

48. Salinas, M., J. de Weille, E. Guillemare, M. Lazdunski, J. P. Hugnot (1997). Modes of regulation of shab K+ channel activity by the Kv8.1 subunit. *J Biol Chem*, 272:8774-8780.

49. Rudy, B., C. J. McBain (2001). Kv3 channels: voltage-gated K+ channels designed for high-frequency repetitive firing. *Trends Neurosci*, 24:517-526.

50. Erisir, A., D. Lau, B. Rudy, C. S. Leonard (1999). Function of specific K(+) channels in sustained high-frequency firing of fast-spiking neocortical interneurons. *J Neurophysiol*, 82:2476-2489.

51. Li, W., L. K. Kaczmarek, T. M. Perney (2001). Localization of two high-threshold potassium channel subunits in the rat central auditory system. *J Comp Neurol*, 437:196-218.

52. Sheng, M., M. L. Tsaur, Y. N. Jan, L. Y. Jan (1992). Subcellular segregation of two A-type K+ channel proteins in rat central neurons. *Neuron*, 9:271-284.

53. Song, W. J., T. Tkatch, G. Baranauskas, N. Ichinohe, S. T. Kitai, D. J. Surmeier (1998). Somatodendritic depolarization-activated potassium currents in rat neostriatal cholinergic interneurons are predominantly of the A type and attributable to coexpression of Kv4.2 and Kv4.1 subunits. *J Neurosci*, 18:3124-3137.

54. Hoffman, D. A., J. C. Magee, C. M. Colbert, D. Johnston (1997). K+ channel regulation of signal propagation in dendrites of hippocampal pyramidal neurons. *Nature*, 387:869-875.

55. Yuan, L. L., J. P. Adams, M. Swank, J. D. Sweatt, D. Johnston (2002). Protein kinase modulation of dendritic K+ channels in hippocampus involves a mitogen-activated protein kinase pathway. *J Neurosci*, 22:4860-4868.

56. Barry, D. M., H. Xu, R. B. Schuessler, J. M. Nerbonne (1998). Functional knockout of the transient outward current, long-QT syndrome, and cardiac remodeling in mice expressing a dominant-negative Kv4 alpha subunit. *Circ Res*, 83:560-567.

57. Rosati, B., Z. Pan, S. Lypen, H. S. Wang, I. Cohen, J. E. Dixon, D. McKinnon (2001). Regulation of KChIP2 potassium channel beta subunit gene expression underlies the gradient of transient outward current in canine and human ventricle. *J Physiol*, 533:119-125.

58. Maylie, B., E. Bissonnette, M. Virk, J. P. Adelman, J. G. Maylie (2002). Episodic ataxia type 1 mutations in the human Kv1.1 potassium channel alter hKvbeta 1-induced N-type inactivation. *J Neurosci*, 22:4786-4793.

59. Zasorin, N. L., R. W. Baloh, L. B. Myers (1983). Acetazolamide-responsive episodic ataxia syndrome. *Neurology*, 33:1212-1214.

60. Brundel, B. J., I. C. Van Gelder, R. H. Henning, A. E. Tuinenburg, M. Wietses, J. G. Grandjean, A. A. Wilde, W. H. Van Gilst, H. J. Crijns (2001). Alterations in potassium channel gene expression in atria of patients with persistent and paroxysmal atrial fibrillation: differential regulation of protein and mRNA levels for K+ channels. *J Am Coll Cardiol*, 37:926-932.

61. Kirsch, G. E., C. C. Shieh, J. A. Drewe, D. F. Vener, A. M. Brown (1993). Segmental exchanges define 4-aminopyridine binding and the inner mouth of K+ pores. *Neuron*, 11:503-512.

62. Fedida, D. (1997). Gating charge and ionic currents associated with quinidine block of human Kv1.5 delayed rectifier channels. *J Physiol*, 499 (Pt 3):661-675.

63. Beeton, C., H. Wulff, J. Barbaria, O. Clot-Faybesse, M. Pennington, D. Bernard, M. D. Cahalan, K. G. Chandy, E. Beraud (2001). Selective blockade of T lymphocyte K(+) channels ameliorates experimental autoimmune encephalomyelitis, a model for multiple sclerosis. *Proc Natl Acad Sci U S A*, 98:13942-13947.

64. Koo, G. C., J. T. Blake, K. Shah, M. J. Staruch, F. Dumont, D. Wunderler, M. Sanchez, O. B. McManus, A. Sirotina-Meisher, P. Fischer, R. C. Boltz, M. A. Goetz, R. Baker, J. Bao, F. Kayser, K. M. Rupprecht, W. H. Parsons, X. C. Tong, I. E. Ita, J. Pivnichny, S. Vincent, P. Cunningham, D. Hora, Jr., W. Feeney, G. Kaczorowski, et al. (1999). Correolide and derivatives are novel immunosuppressants blocking the lymphocyte Kv1.3 potassium channels. *Cell Immunol*, 197:99-107.

65. Vennekamp, J., H. Wulff, C. Beeton, P. A. Calabresi, S. Grissmer, W. Hansel, K. G. Chandy (2004). Kv1.3-blocking 5-phenylalkoxypsoralens: a new class of immunomodulators. *Mol Pharmacol*, 65:1364-1374.

66. Marrion, N. V., S. J. Tavalin (1998). Selective activation of Ca2+-activated K+ channels by co-localized Ca2+ channels in hippocampal neurons. *Nature*, 395:900-905.

67. Lovell, P. V., D. P. McCobb (2001). Pituitary control of BK potassium channel function and intrinsic firing properties of adrenal chromaffin cells. *J Neurosci*, 21:3429-3442.

68. Ramanathan, K., T. H. Michael, G. J. Jiang, H. Hiel, P. A. Fuchs (1999). A molecular mechanism for electrical tuning of cochlear hair cells. *Science*, 283:215-217.

69. Ruttiger, L., M. Sausbier, U. Zimmermann, H. Winter, C. Braig, J. Engel, M. Knirsch, C. Arntz, P. Langer, B. Hirt, M. Muller, I. Kopschall, M. Pfister, S. Munkner, K. Rohbock, I. Pfaff, A. Rusch, P. Ruth, M. Knipper (2004). Deletion of the Ca2+-activated potassium (BK) alpha-subunit but not the BKbeta1-subunit leads to progressive hearing loss. *Proc Natl Acad Sci U S A*, 101:12922-12927.

70. Amberg, G. C., A. D. Bonev, C. F. Rossow, M. T. Nelson, L. F. Santana (2003). Modulation of the molecular composition of large conductance, Ca(2+) activated K(+) channels in vascular smooth muscle during hypertension. *J Clin Invest*, 112:717-724.

71. Ahluwalia, J., A. Tinker, L. H. Clapp, M. R. Duchen, A. Y. Abramov, S. Pope, M. Nobles, A. W. Segal (2004). The large-conductance Ca2+-activated K+ channel is essential for innate immunity. *Nature*, 427:853-858.

72. Jensen, B. S. (2002). BMS-204352: a potassium channel opener developed for the treatment of stroke. *CNS Drug Rev*, 8:353-360.

73. Tanaka, M., K. Takahashi, T. Saika, I. Kobayashi, T. Ueno, J. Kumazawa (1998). Development of fluoroquinolone resistance and mutations involving GyrA and ParC proteins among Neisseria gonorrhoeae isolates in Japan. *J Urol*, 159:2215-2219.

74. Archer, S. L. (2002). Potassium channels and erectile dysfunction. *Vascul Pharmacol*, 38:61-71.

75. Brugnara, C., L. de Franceschi, S. L. Alper (1993). Inhibition of Ca(2+)-dependent K+ transport and cell dehydration in sickle erythrocytes by clotrimazole and other imidazole derivatives. *J Clin Invest*, 92:520-526.

76. Ghanshani, S., H. Wulff, M. J. Miller, H. Rohm, A. Neben, G. A. Gutman, M. D. Cahalan, K. G. Chandy (2000). Up-regulation of the IKCa1 potassium channel during T-cell activation. Molecular mechanism and functional consequences. *J Biol Chem*, 275:37137-37149.

77. Fanger, C. M., H. Rauer, A. L. Neben, M. J. Miller, H. Wulff, J. C. Rosa, C. R. Ganellin, K. G. Chandy, M. D. Cahalan (2001). Calcium-activated potassium channels sustain calcium signaling in T lymphocytes. Selective blockers and manipulated channel expression levels. *J Biol Chem*, 276:12249-12256.

78. Jensen, B. S., M. Hertz, P. Christophersen, L. S. Madsen (2002). The Ca2+-activated K+ channel of intermediate conductance:a possible target for immune suppression. *Expert Opin Ther Targets*, 6:623-636.

79. Wulff, H., M. J. Miller, W. Hansel, S. Grissmer, M. D. Cahalan, K. G. Chandy (2000). Design of a potent and selective inhibitor of the intermediate-conductance Ca2+-activated K+ channel, IKCa1: a potential immunosuppressant. *Proc Natl Acad Sci U S A*, 97:8151-8156.

80. Brugnara, C., L. De Franceschi, C. C. Armsby, N. Saadane, M. Trudel, Y. Beuzard, A. Rittenhouse, N. Rifai, O. Platt, S. L. Alper (1995). A new therapeutic approach for sickle cell disease. Blockade of the red cell Ca(2+)-activated K+ channel by clotrimazole. *Ann N Y Acad Sci*, 763:262-271.

81. Shieh, C. C., M. Coghlan, J. P. Sullivan, M. Gopalakrishnan (2000). Potassium channels: molecular defects, diseases, and therapeutic opportunities. *Pharmacol Rev*, 52:557-594.

82. Stocker, M. (2004). Ca(2+)-activated K+ channels: molecular determinants and function of the SK family. *Nat Rev Neurosci*, 5:758-770.

83. Messier, C., C. Mourre, B. Bontempi, J. Sif, M. Lazdunski, C. Destrade (1991). Effect of apamin, a toxin that inhibits Ca(2+)-dependent K+ channels, on learning and memory processes. *Brain Res*, 551:322-326.

84. Ikeda, M., D. Dewar, J. McCulloch (1991). Selective reduction of [125I]apamin binding sites in Alzheimer hippocampus: a quantitative autoradiographic study. *Brain Res*, 567:51-56.

85. Nagayama, T., Y. Fukushima, M. Yoshida, M. Suzuki-Kusaba, H. Hisa, T. Kimura, S. Satoh (2000). Role of potassium channels in catecholamine secretion in the rat adrenal gland. *Am J Physiol Regul Integr Comp Physiol*, 279:R448-454.

86. Tomita, H., V. G. Shakkottai, G. A. Gutman, G. Sun, W. E. Bunney, M. D. Cahalan, K. G. Chandy, J. J. Gargus (2003). Novel truncated isoform of SK3 potassium channel is a potent dominant-negative regulator of SK currents: implications in schizophrenia. *Mol Psychiatry*, 8:524-535, 460.

87. Koronyo-Hamaoui, M., Y. Danziger, A. Frisch, D. Stein, S. Leor, N. Laufer, C. Carel, S. Fennig, M. Minoumi, A. Apter, B. Goldman, G. Barkai, A. Weizman, E. Gak (2002). Association between anorexia nervosa and the hsKCa3 gene: a family-based and case control study. *Mol Psychiatry*, 7:82-85.

88. Auguste, P., M. Hugues, B. Grave, J. C. Gesquiere, P. Maes, A. Tartar, G. Romey, H. Schweitz, M. Lazdunski (1990). Leiurotoxin I (scyllatoxin), a peptide ligand for Ca2(+)-activated K+ channels. Chemical synthesis, radiolabeling, and receptor characterization. *J Biol Chem*, 265:4753-4759.

89. Xu, C. Q., L. L. He, B. Brone, M. F. Martin-Eauclaire, E. Van Kerkhove, Z. Zhou, C. W. Chi (2004). A novel scorpion toxin blocking small conductance Ca2+ activated K+ channel. *Toxicon*, 43:961-971.

90. Ishii, T. M., J. Maylie, J. P. Adelman (1997). Determinants of apamin and d-tubocurarine block in SK potassium channels. *J Biol Chem*, 272:23195-23200.

91. Rosa, J. C., D. Galanakis, C. R. Ganellin, P. M. Dunn, D. H. Jenkinson (1998). Bis-quinolinium cyclophanes: 6,10-diaza-3(1,3),8(1,4)-dibenzena-1,5(1,4)-diquinolinacyclodecaphane (UCL 1684), the first nanomolar, non-peptidic blocker of the apamin-sensitive Ca(2+)-activated K+ channel. *J Med Chem*, 41:2-5.

92. Pedarzani, P., J. Mosbacher, A. Rivard, L. A. Cingolani, D. Oliver, M. Stocker, J. P. Adelman, B. Fakler (2001). Control of electrical activity in central neurons by modulating the gating of small conductance Ca2+-activated K+ channels. *J Biol Chem*, 276:9762-9769.

93. Wang, Q., M. E. Curran, I. Splawski, T. C. Burn, J. M. Millholland, T. J. VanRaay, J. Shen, K. W. Timothy, G. M. Vincent, T. de Jager, P. J. Schwartz, J. A. Toubin, A. J. Moss, D. L. Atkinson, G. M. Landes, T. D. Connors, M. T. Keating (1996). Positional cloning of a novel potassium channel gene: KVLQT1 mutations cause cardiac arrhythmias. *Nat Genet*, 12:17-23.

94. Schroeder, B. C., S. Waldegger, S. Fehr, M. Bleich, R. Warth, R. Greger, T. J. Jentsch (2000). A constitutively open potassium channel formed by KCNQ1 and KCNE3. *Nature*, 403:196-199.

95. Nicolas, M., D. Dememes, A. Martin, S. Kupershmidt, J. Barhanin (2001). KCNQ1/KCNE1 potassium channels in mammalian vestibular dark cells. *Hear Res*, 153:132-145.

96. Ashcroft, F. M., *Ion channels and disease : channelopathies*. Academic Press. San Diego, 2000

97. Kharkovets, T., J. P. Hardelin, S. Safieddine, M. Schweizer, A. El-Amraoui, C. Petit, T. J. Jentsch (2000). KCNQ4, a K+ channel mutated in a form of dominant deafness, is expressed in the inner ear and the central auditory pathway. *Proc Natl Acad Sci U S A*, 97:4333-4338.

98. Nouvian, R., J. Ruel, J. Wang, M. J. Guitton, R. Pujol, J. L. Puel (2003). Degeneration of sensory outer hair cells following pharmacological blockade of cochlear KCNQ channels in the adult guinea pig. *Eur J Neurosci*, 17:2553-2562.

99. Kubisch, C., B. C. Schroeder, T. Friedrich, B. Lutjohann, A. El-Amraoui, S. Marlin, C. Petit, T. J. Jentsch (1999). KCNQ4, a novel potassium channel expressed in sensory outer hair cells, is mutated in dominant deafness. *Cell*, 96:437-446.

100. Van Hauwe, P., P. J. Coucke, R. J. Ensink, P. Huygen, C. W. Cremers, G. Van Camp (2000). Mutations in the KCNQ4 K+ channel gene, responsible for autosomal dominant hearing loss, cluster in the channel pore region. *Am J Med Genet*, 93:184-187.

101. Wang, H. S., Z. Pan, W. Shi, B. S. Brown, R. S. Wymore, I. S. Cohen, J. E. Dixon, D. McKinnon (1998). KCNQ2 and KCNQ3 potassium channel subunits: molecular correlates of the M-channel. *Science*, 282:1890-1893.

102. Cooper, E. C., L. Y. Jan (2003). M-channels: neurological diseases, neuromodulation, and drug development. *Arch Neurol*, 60:496-500.

103. Peters, H. C., H. Hu, O. Pongs, J. F. Storm, D. Isbrandt (2005). Conditional transgenic suppression of M channels in mouse brain reveals functions in neuronal excitability, resonance and behavior. *Nat Neurosci*, 8:51-60.

104. Schroeder, B. C., C. Kubisch, V. Stein, T. J. Jentsch (1998). Moderate loss of function of cyclic-AMP-modulated KCNQ2/KCNQ3 K+ channels causes epilepsy. *Nature*, 396:687-690.

105. Robbins, J. (2001). KCNQ potassium channels: physiology, pathophysiology, and pharmacology. *Pharmacol Ther*, 90:1-19.

106. Tamargo, J., R. Caballero, R. Gomez, C. Valenzuela, E. Delpon (2004). Pharmacology of cardiac potassium channels. *Cardiovasc Res*, 62:9-33.

107. Yang, I. C., M. W. Scherz, A. Bahinski, P. B. Bennett, K. T. Murray (2000). Stereoselective interactions of the enantiomers of chromanol 293B with human voltage-gated potassium channels. *J Pharmacol Exp Ther*, 294:955-962.

108. Busch, A. E., G. L. Busch, E. Ford, H. Suessbrich, H. J. Lang, R. Greger, K. Kunzelmann, B. Attali, W. Stuhmer (1997). The role of the IsK protein in the specific pharmacological properties of the IKs channel complex. *Br J Pharmacol*, 122:187-189.

109. Wang, H. S., B. S. Brown, D. McKinnon, I. S. Cohen (2000). Molecular basis for differential sensitivity of KCNQ and I(Ks) channels to the cognitive enhancer XE991. *Mol Pharmacol*, 57:1218-1223.

110. Seebohm, G., J. Chen, N. Strutz, C. Culberson, C. Lerche, M. C. Sanguinetti (2003). Molecular determinants of KCNQ1 channel block by a benzodiazepine. *Mol Pharmacol*, 64:70-77.

111. Schnee, M. E., B. S. Brown (1998). Selectivity of linopirdine (DuP 996), a neurotransmitter release enhancer, in blocking voltage-dependent and calcium-activated potassium currents in hippocampal neurons. *J Pharmacol Exp Ther*, 286:709-717.

112. van Dyck, C. H., C. H. Lin, R. Robinson, J. Cellar, E. O. Smith, J. C. Nelson, A. F. Arnsten, P. B. Hoffer (1997). The acetylcholine releaser linopirdine increases parietal regional cerebral blood flow in Alzheimer's disease. *Psychopharmacology (Berl)*, 132:217-226.

113. Dost, R., A. Rostock, C. Rundfeldt (2004). The anti-hyperalgesic activity of retigabine is mediated by KCNQ potassium channel activation. *Naunyn Schmiedebergs Arch Pharmacol*, 369:382-390.

114. Overholt, J. L., E. Ficker, T. Yang, H. Shams, G. R. Bright, N. R. Prabhakar (2000). HERG-Like potassium current regulates the resting membrane potential in glomus cells of the rabbit carotid body. *J Neurophysiol*, 83:1150-1157.

115. Chiesa, N., B. Rosati, A. Arcangeli, M. Olivotto, E. Wanke (1997). A novel role for HERG K+ channels: spike-frequency adaptation. *J Physiol*, 501 (Pt 2):313-318.

116. Sanguinetti, M. C., C. Jiang, M. E. Curran, M. T. Keating (1995). A mechanistic link between an inherited and an acquired cardiac arrhythmia: HERG encodes the IKr potassium channel. *Cell*, 81:299-307.

117. Smith, P. L., T. Baukrowitz, G. Yellen (1996). The inward rectification mechanism of the HERG cardiac potassium channel. *Nature*, 379:833-836.

118. Papa, M., F. Boscia, A. Canitano, P. Castaldo, S. Sellitti, L. Annunziato, M. Taglialatela (2003). Expression pattern of the ether-a-gogo-related (ERG) K+ channel-

encoding genes ERG1, ERG2, and ERG3 in the adult rat central nervous system. *J Comp Neurol*, 466:119-135.

119. Sacco, T., A. Bruno, E. Wanke, F. Tempia (2003). Functional roles of an ERG current isolated in cerebellar Purkinje neurons. *J Neurophysiol*, 90:1817-1828.

120. Pardo, L. A., D. del Camino, A. Sanchez, F. Alves, A. Bruggemann, S. Beckh, W. Stuhmer (1999). Oncogenic potential of EAG K(+) channels. *Embo J*, 18:5540-5547.

121. Farias, L. M., D. B. Ocana, L. Diaz, F. Larrea, E. Avila-Chavez, A. Cadena, L. M. Hinojosa, G. Lara, L. A. Villanueva, C. Vargas, E. Hernandez-Gallegos, I. Camacho-Arroyo, A. Duenas-Gonzalez, E. Perez-Cardenas, L. A. Pardo, A. Morales, L. Taja-Chayeb, J. Escamilla, C. Sanchez-Pena, J. Camacho (2004). Ether a go-go potassium channels as human cervical cancer markers. *Cancer Res*, 64:6996-7001.

122. Smith, G. A., H. W. Tsui, E. W. Newell, X. Jiang, X. P. Zhu, F. W. Tsui, L. C. Schlichter (2002). Functional up-regulation of HERG K+ channels in neoplastic hematopoietic cells. *J Biol Chem*, 277:18528-18534.

123. Pardo, L. A., A. Bruggemann, J. Camacho, W. Stuhmer (1998). Cell cycle-related changes in the conducting properties of r-eag K+ channels. *J Cell Biol*, 143:767-775.

124. Tristani-Firouzi, M., M. C. Sanguinetti (2003). Structural determinants and biophysical properties of HERG and KCNQ1 channel gating. *J Mol Cell Cardiol*, 35:27-35.

125. Rajamani, S., C. L. Anderson, B. D. Anson, C. T. January (2002). Pharmacological rescue of human K(+) channel long-QT2 mutations: human ether-a-go-go-related gene rescue without block. *Circulation*, 105:2830-2835.

126. Vandenberg, J. I., B. D. Walker, T. J. Campbell (2001). HERG K+ channels: friend and foe. *Trends Pharmacol Sci*, 22:240-246.

127. VerNooy, R. A., J. P. Mounsey (2004). Antiarrhythmic drug therapy of atrial fibrillation. *Cardiol Clin*, 22:21-34.

128. Gurrola, G. B., B. Rosati, M. Rocchetti, G. Pimienta, A. Zaza, A. Arcangeli, M. Olivotto, L. D. Possani, E. Wanke (1999). A toxin to nervous, cardiac, and endocrine ERG K+ channels isolated from Centruroides noxius scorpion venom. *Faseb J*, 13:953-962.

129. Korolkova, Y. V., S. A. Kozlov, A. V. Lipkin, K. A. Pluzhnikov, J. K. Hadley, A. K. Filippov, D. A. Brown, K. Angelo, D. Strobaek, T. Jespersen, S. P. Olesen, B. S. Jensen, E. V. Grishin (2001). An ERG channel inhibitor from the scorpion Buthus eupeus. *J Biol Chem*, 276:9868-9876.

130. Ouadid-Ahidouch, H., X. Le Bourhis, M. Roudbaraki, R. A. Toillon, P. Delcourt, N. Prevarskaya (2001). Changes in the K+ current-density of MCF-7 cells during progression through the cell cycle: possible involvement of a h-ether.a-gogo K+ channel. *Receptors Channels*, 7:345-356.

131. Gavrilova-Ruch, O., K. Schonherr, G. Gessner, R. Schonherr, T. Klapperstuck, W. Wohlrab, S. H. Heinemann (2002). Effects of imipramine on ion channels and proliferation of IGR1 melanoma cells. *J Membr Biol*, 188:137-149.

132. Goldstein, S. A., D. Bockenhauer, I. O'Kelly, N. Zilberberg (2001). Potassium leak channels and the KCNK family of two-P-domain subunits. *Nat Rev Neurosci*, 2:175-184.

133. Talley, E. M., Q. Lei, J. E. Sirois, D. A. Bayliss (2000). TASK-1, a two-pore domain K+ channel, is modulated by multiple neurotransmitters in motoneurons. *Neuron*, 25:399-410.

134. Patel, A. J., E. Honore, F. Lesage, M. Fink, G. Romey, M. Lazdunski (1999). Inhalational anesthetics activate two-pore-domain background K+ channels. *Nat Neurosci*, 2:422-426.

135. Koishi, R., H. Xu, D. Ren, B. Navarro, B. W. Spiller, Q. Shi, D. E. Clapham (2004). A superfamily of voltage-gated sodium channels in bacteria. *J Biol Chem*, 279:9532-9538.

136. Hodgkin, A. L., A. F. Huxley (1952). Currents carried by sodium and potassium ions through the membrane of the giant axon of Loligo. *J Physiol*, 116:449-472.

137. Narahashi, T., J. W. Moore, W. R. Scott (1964). Tetrodotoxin Blockage of Sodium Conductance Increase in Lobster Giant Axons. *J Gen Physiol*, 47:965-974.

138. Kao, C. Y., A. Nishiyama (1965). Actions of saxitoxin on peripheral neuromuscular systems. *J Physiol*, 180:50-66.

139. West, J. W., D. E. Patton, T. Scheuer, Y. Wang, A. L. Goldin, W. A. Catterall (1992). A cluster of hydrophobic amino acid residues required for fast Na(+)-channel inactivation. *Proc Natl Acad Sci U S A*, 89:10910-10914.

140. McPhee, J. C., D. S. Ragsdale, T. Scheuer, W. A. Catterall (1995). A critical role for transmembrane segment IVS6 of the sodium channel alpha subunit in fast inactivation. *J Biol Chem*, 270:12025-12034.

141. Hartshorne, R. P., D. J. Messner, J. C. Coppersmith, W. A. Catterall (1982). The saxitoxin receptor of the sodium channel from rat brain. Evidence for two nonidentical beta subunits. *J Biol Chem*, 257:13888-13891.

142. Chanda, B., O. K. Asamoah, F. Bezanilla (2004). Coupling interactions between voltage sensors of the sodium channel as revealed by site-specific measurements. *J Gen Physiol*, 123:217-230.

143. Bezanilla, F. (2002). Voltage sensor movements. *J Gen Physiol*, 120:465-473.

144. Sun, Y. M., I. Favre, L. Schild, E. Moczydlowski (1997). On the structural basis for size-selective permeation of organic cations through the voltage-gated sodium channel. Effect of alanine mutations at the DEKA locus on selectivity, inhibition by Ca2+ and H+, and molecular sieving. *J Gen Physiol*, 110:693-715.

145. Heinemann, S. H., H. Terlau, W. Stuhmer, K. Imoto, S. Numa (1992). Calcium channel characteristics conferred on the sodium channel by single mutations. *Nature*, 356:441-443.

146. Zhou, Y., J. H. Morais-Cabral, A. Kaufman, R. MacKinnon (2001). Chemistry of ion coordination and hydration revealed by a K+ channel-Fab complex at 2.0 A resolution. *Nature*, 414:43-48.

147. Patton, D. E., J. W. West, W. A. Catterall, A. L. Goldin (1992). Amino acid residues required for fast Na(+)-channel inactivation: charge neutralizations and deletions in the III-IV linker. *Proc Natl Acad Sci U S A*, 89:10905-10909.

148. Stuhmer, W., F. Conti, H. Suzuki, X. D. Wang, M. Noda, N. Yahagi, H. Kubo, S. Numa (1989). Structural parts involved in activation and inactivation of the sodium channel. *Nature*, 339:597-603.

149. McPhee, J. C., D. S. Ragsdale, T. Scheuer, W. A. Catterall (1994). A mutation in segment IVS6 disrupts fast inactivation of sodium channels. *Proc Natl Acad Sci U S A*, 91:12346-12350.

150. Tang, L., R. G. Kallen, R. Horn (1996). Role of an S4-S5 linker in sodium channel inactivation probed by mutagenesis and a peptide blocker. *J Gen Physiol*, 108:89-104.

151. Toib, A., V. Lyakhov, S. Marom (1998). Interaction between duration of activity and time course of recovery from slow inactivation in mammalian brain Na+ channels. *J Neurosci*, 18:1893-1903.

152. Vilin, Y. Y., P. C. Ruben (2001). Slow inactivation in voltage-gated sodium channels: molecular substrates and contributions to channelopathies. *Cell Biochem Biophys*, 35:171-190.

153. Garrido, J. J., F. Fernandes, A. Moussif, M. P. Fache, P. Giraud, B. Dargent (2003). Dynamic compartmentalization of the voltage-gated sodium channels in axons. *Biol Cell*, 95:437-445.

154. Fache, M. P., A. Moussif, F. Fernandes, P. Giraud, J. J. Garrido, B. Dargent (2004). Endocytotic elimination and domain-selective tethering constitute a potential mechanism of protein segregation at the axonal initial segment. *J Cell Biol*, 166:571-578.

155. Garrido, J. J., P. Giraud, E. Carlier, F. Fernandes, A. Moussif, M. P. Fache, D. Debanne, B. Dargent (2003). A targeting motif involved in sodium channel clustering at the axonal initial segment. *Science*, 300:2091-2094.

156. Wood, S. J., C. R. Slater (1998). beta-Spectrin is colocalized with both voltage-gated sodium channels and ankyrinG at the adult rat neuromuscular junction. *J Cell Biol*, 140:675-684.

157. Zhou, D., S. Lambert, P. L. Malen, S. Carpenter, L. M. Boland, V. Bennett (1998). AnkyrinG is required for clustering of voltage-gated Na channels at axon initial segments and for normal action potential firing. *J Cell Biol*, 143:1295-1304.

158. Lustig, M., G. Zanazzi, T. Sakurai, C. Blanco, S. R. Levinson, S. Lambert, M. Grumet, J. L. Salzer (2001). Nr-CAM and neurofascin interactions regulate ankyrin G and sodium channel clustering at the node of Ranvier. *Curr Biol*, 11:1864-1869.

159. Golding, N. L., W. L. Kath, N. Spruston (2001). Dichotomy of action-potential backpropagation in CA1 pyramidal neuron dendrites. *J Neurophysiol*, 86:2998-3010.

160. Stuart, G., M. Hausser (1994). Initiation and spread of sodium action potentials in cerebellar Purkinje cells. *Neuron*, 13:703-712.

161. Bischofberger, J., P. Jonas (1997). Action potential propagation into the presynaptic dendrites of rat mitral cells. *J Physiol*, 504 (Pt 2):359-365.

162. Vega-Saenz de Miera, E. C., B. Rudy, M. Sugimori, R. Llinas (1997). Molecular characterization of the sodium channel subunits expressed in mammalian cerebellar Purkinje cells. *Proc Natl Acad Sci U S A*, 94:7059-7064.

163. Baker, M. D., H. Bostock (1997). Low-threshold, persistent sodium current in rat large dorsal root ganglion neurons in culture. *J Neurophysiol*, 77:1503-1513.

164. Cummins, T. R., S. D. Dib-Hajj, J. A. Black, A. N. Akopian, J. N. Wood, S. G. Waxman (1999). A novel persistent tetrodotoxin-resistant sodium current in SNS-null and wild-type small primary sensory neurons. *J Neurosci*, 19:RC43.

165. Raman, I. M., B. P. Bean (1997). Resurgent sodium current and action potential formation in dissociated cerebellar Purkinje neurons. *J Neurosci*, 17:4517-4526.

166. Raman, I. M., L. K. Sprunger, M. H. Meisler, B. P. Bean (1997). Altered subthreshold sodium currents and disrupted firing patterns in Purkinje neurons of Scn8a mutant mice. *Neuron*, 19:881-891.

167. Toledo-Aral, J. J., B. L. Moss, Z. J. He, A. G. Koszowski, T. Whisenand, S. R. Levinson, J. J. Wolf, I. Silos-Santiago, S. Halegoua, G. Mandel (1997). Identification of PN1, a predominant voltage-dependent sodium channel expressed principally in peripheral neurons. *Proc Natl Acad Sci U S A*, 94:1527-1532.

168. Benn, S. C., M. Costigan, S. Tate, M. Fitzgerald, C. J. Woolf (2001). Developmental expression of the TTX-resistant voltage-gated sodium channels Nav1.8 (SNS) and Nav1.9 (SNS2) in primary sensory neurons. *J Neurosci*, 21:6077-6085.

169. Yang, Y., Y. Wang, S. Li, Z. Xu, H. Li, L. Ma, J. Fan, D. Bu, B. Liu, Z. Fan, G. Wu, J. Jin, B. Ding, X. Zhu, Y. Shen (2004). Mutations in SCN9A, encoding a sodium channel alpha subunit, in patients with primary erythermalgia. *J Med Genet*, 41:171-174.

170. Cummins, T. R., S. D. Dib-Hajj, S. G. Waxman (2004). Electrophysiological properties of mutant Nav1.7 sodium channels in a painful inherited neuropathy. *J Neurosci*, 24:8232-8236.

171. Nassar, M. A., L. C. Stirling, G. Forlani, M. D. Baker, E. A. Matthews, A. H. Dickenson, J. N. Wood (2004). Nociceptor-specific gene deletion reveals a major role for Nav1.7 (PN1) in acute and inflammatory pain. *Proc Natl Acad Sci U S A*, 101:12706-12711.

172. Lai, J., M. S. Gold, C. S. Kim, D. Bian, M. H. Ossipov, J. C. Hunter, F. Porreca (2002). Inhibition of neuropathic pain by decreased expression of the tetrodotoxin-resistant sodium channel, NaV1.8. *Pain*, 95:143-152.

173. Waxman, S. G., J. D. Kocsis, J. A. Black (1994). Type III sodium channel mRNA is expressed in embryonic but not adult spinal sensory neurons, and is reexpressed following axotomy. *J Neurophysiol*, 72:466-470.

174. Boucher, T. J., K. Okuse, D. L. Bennett, J. B. Munson, J. N. Wood, S. B. McMahon (2000). Potent analgesic effects of GDNF in neuropathic pain states. *Science*, 290:124-127.

175. Dib-Hajj, S. D., L. Tyrrell, J. A. Black, S. G. Waxman (1998). NaN, a novel voltage-gated Na channel, is expressed preferentially in peripheral sensory neurons and down-regulated after axotomy. *Proc Natl Acad Sci U S A*, 95:8963-8968.

176. Craner, M. J., J. Newcombe, J. A. Black, C. Hartle, M. L. Cuzner, S. G. Waxman (2004). Molecular changes in neurons in multiple sclerosis: altered axonal expression of Nav1.2 and Nav1.6 sodium channels and Na+/Ca2+ exchanger. *Proc Natl Acad Sci U S A*, 101:8168-8173.

177. Maier, S. K., R. E. Westenbroek, T. T. Yamanushi, H. Dobrzynski, M. R. Boyett, W. A. Catterall, T. Scheuer (2003). An unexpected requirement for brain-type sodium channels for control of heart rate in the mouse sinoatrial node. *Proc Natl Acad Sci U S A*, 100:3507-3512.

178. Watanabe, E., A. Fujikawa, H. Matsunaga, Y. Yasoshima, N. Sako, T. Yamamoto, C. Saegusa, M. Noda (2000). Nav2/NaG channel is involved in control of salt-intake behavior in the CNS. *J Neurosci*, 20:7743-7751.

179. Yang, N., S. Ji, M. Zhou, L. J. Ptacek, R. L. Barchi, R. Horn, A. L. George, Jr. (1994). Sodium channel mutations in paramyotonia congenita exhibit similar biophysical phenotypes in vitro. *Proc Natl Acad Sci U S A*, 91:12785-12789.

180. Mitrovic, N., A. L. George, Jr., H. Lerche, S. Wagner, C. Fahlke, F. Lehmann-Horn (1995). Different effects on gating of three myotonia-causing mutations in the inactivation gate of the human muscle sodium channel. *J Physiol*, 487 (Pt 1):107-114.

181. Jurkat-Rott, K., N. Mitrovic, C. Hang, A. Kouzmekine, P. Iaizzo, J. Herzog, H. Lerche, S. Nicole, J. Vale-Santos, D. Chauveau, B. Fontaine, F. Lehmann-Horn (2000). Voltage-sensor sodium channel mutations cause hypokalemic periodic paralysis type 2 by enhanced inactivation and reduced current. *Proc Natl Acad Sci U S A*, 97:9549-9554.

182. Viswanathan, P. C., J. R. Balser (2004). Inherited sodium channelopathies: a continuum of channel dysfunction. *Trends Cardiovasc Med*, 14:28-35.

183. Wang, Q., J. Shen, I. Splawski, D. Atkinson, Z. Li, J. L. Robinson, A. J. Moss, J. A. Towbin, M. T. Keating (1995). SCN5A mutations associated with an inherited cardiac arrhythmia, long QT syndrome. *Cell*, 80:805-811.

184. Brugada, P., J. Brugada (1992). Right bundle branch block, persistent ST segment elevation and sudden cardiac death: a distinct clinical and electrocardiographic syndrome. A multicenter report. *J Am Coll Cardiol*, 20:1391-1396.

185. Tan, H. L., C. R. Bezzina, J. P. Smits, A. O. Verkerk, A. A. Wilde (2003). Genetic control of sodium channel function. *Cardiovasc Res*, 57:961-973.

186. Wallace, R. H., D. W. Wang, R. Singh, I. E. Scheffer, A. L. George, Jr., H. A. Phillips, K. Saar, A. Reis, E. W. Johnson, G. R. Sutherland, S. F. Berkovic, J. C. Mulley

(1998). Febrile seizures and generalized epilepsy associated with a mutation in the Na+-channel beta1 subunit gene SCN1B. *Nat Genet*, 19:366-370.

187. Spampanato, J., J. A. Kearney, G. de Haan, D. P. McEwen, A. Escayg, I. Aradi, B. T. MacDonald, S. I. Levin, I. Soltesz, P. Benna, E. Montalenti, L. L. Isom, A. L. Goldin, M. H. Meisler (2004). A novel epilepsy mutation in the sodium channel SCN1A identifies a cytoplasmic domain for beta subunit interaction. *J Neurosci*, 24:10022-10034.

188. Wallace, R. H., I. E. Scheffer, S. Barnett, M. Richards, L. Dibbens, R. R. Desai, T. Lerman-Sagie, D. Lev, A. Mazarib, N. Brand, B. Ben-Zeev, I. Goikhman, R. Singh, G. Kremmidiotis, A. Gardner, G. R. Sutherland, A. L. George, Jr., J. C. Mulley, S. F. Berkovic (2001). Neuronal sodium-channel alpha1-subunit mutations in generalized epilepsy with febrile seizures plus. *Am J Hum Genet*, 68:859-865.

189. Lossin, C., T. H. Rhodes, R. R. Desai, C. G. Vanoye, D. Wang, S. Carniciu, O. Devinsky, A. L. George, Jr. (2003). Epilepsy-associated dysfunction in the voltage-gated neuronal sodium channel SCN1A. *J Neurosci*, 23:11289-11295.

190. Rhodes, T. H., C. Lossin, C. G. Vanoye, D. W. Wang, A. L. George, Jr. (2004). Noninactivating voltage-gated sodium channels in severe myoclonic epilepsy of infancy. *Proc Natl Acad Sci U S A*, 101:11147-11152.

191. Sugawara, T., Y. Tsurubuchi, K. L. Agarwala, M. Ito, G. Fukuma, E. Mazaki-Miyazaki, H. Nagafuji, M. Noda, K. Imoto, K. Wada, A. Mitsudome, S. Kaneko, M. Montal, K. Nagata, S. Hirose, K. Yamakawa (2001). A missense mutation of the Na+ channel alpha II subunit gene Na(v)1.2 in a patient with febrile and afebrile seizures causes channel dysfunction. *Proc Natl Acad Sci U S A*, 98:6384-6389.

192. Heron, S. E., K. M. Crossland, E. Andermann, H. A. Phillips, A. J. Hall, A. Bleasel, M. Shevell, S. Mercho, M. H. Seni, M. C. Guiot, J. C. Mulley, S. F. Berkovic, I. E. Scheffer (2002). Sodium-channel defects in benign familial neonatal-infantile seizures. *Lancet*, 360:851-852.

193. Kamiya, K., M. Kaneda, T. Sugawara, E. Mazaki, N. Okamura, M. Montal, N. Makita, M. Tanaka, K. Fukushima, T. Fujiwara, Y. Inoue, K. Yamakawa (2004). A nonsense mutation of the sodium channel gene SCN2A in a patient with intractable epilepsy and mental decline. *J Neurosci*, 24:2690-2698.

194. Weiss, L. A., A. Escayg, J. A. Kearney, M. Trudeau, B. T. MacDonald, M. Mori, J. Reichert, J. D. Buxbaum, M. H. Meisler (2003). Sodium channels SCN1A, SCN2A and SCN3A in familial autism. *Mol Psychiatry*, 8:186-194.

195. Tejedor, F. J., W. A. Catterall (1988). Site of covalent attachment of alpha-scorpion toxin derivatives in domain I of the sodium channel alpha subunit. *Proc Natl Acad Sci U S A*, 85:8742-8746.

196. Cestele, S., Y. Qu, J. C. Rogers, H. Rochat, T. Scheuer, W. A. Catterall (1998). Voltage sensor-trapping: enhanced activation of sodium channels by beta-scorpion toxin bound to the S3-S4 loop in domain II. *Neuron*, 21:919-931.

197. Courtney, K. R. (1975). Mechanism of frequency-dependent inhibition of sodium currents in frog myelinated nerve by the lidocaine derivative GEA. *J Pharmacol Exp Ther*, 195:225-236.

198. Scholz, A. (2002). Mechanisms of (local) anaesthetics on voltage-gated sodium and other ion channels. *Br J Anaesth*, 89:52-61.

199. Tanabe, T., H. Takeshima, A. Mikami, V. Flockerzi, H. Takahashi, K. Kangawa, M. Kojima, H. Matsuo, T. Hirose, S. Numa (1987). Primary structure of the receptor for calcium channel blockers from skeletal muscle. *Nature*, 328:313-318.

200. Takahashi, M., M. J. Seagar, J. F. Jones, B. F. Reber, W. A. Catterall (1987). Subunit structure of dihydropyridine-sensitive calcium channels from skeletal muscle. *Proc Natl Acad Sci U S A*, 84:5478-5482.

201. Wang, M. C., A. Dolphin, A. Kitmitto (2004). L-type voltage-gated calcium channels: understanding function through structure. *FEBS Lett*, 564:245-250.

202. Van Petegem, F., K. A. Clark, F. C. Chatelain, D. L. Minor, Jr. (2004). Structure of a complex between a voltage-gated calcium channel beta-subunit and an alpha-subunit domain. *Nature*, 429:671-675.

203. Opatowsky, Y., C. C. Chen, K. P. Campbell, J. A. Hirsch (2004). Structural analysis of the voltage-dependent calcium channel beta subunit functional core and its complex with the alpha 1 interaction domain. *Neuron*, 42:387-399.

204. Chen, Y. H., M. H. Li, Y. Zhang, L. L. He, Y. Yamada, A. Fitzmaurice, Y. Shen, H. Zhang, L. Tong, J. Yang (2004). Structural basis of the alpha1-beta subunit interaction of voltage-gated Ca2+ channels. *Nature*, 429:675-680.

205. Carbone, E., H. D. Lux (1984). A low voltage-activated, fully inactivating Ca channel in vertebrate sensory neurones. *Nature*, 310:501-502.

206. Bean, B. P. (1985). Two kinds of calcium channels in canine atrial cells. Differences in kinetics, selectivity, and pharmacology. *J Gen Physiol*, 86:1-30.

207. Hagiwara, N., H. Irisawa, M. Kameyama (1988). Contribution of two types of calcium currents to the pacemaker potentials of rabbit sino-atrial node cells. *J Physiol*, 395:233-253.

208. Varadi, G., M. Strobeck, S. Koch, L. Caglioti, C. Zucchi, G. Palyi (1999). Molecular elements of ion permeation and selectivity within calcium channels. *Crit Rev Biochem Mol Biol*, 34:181-214.

209. Ellinor, P. T., J. Yang, W. A. Sather, J. F. Zhang, R. W. Tsien (1995). Ca2+ channel selectivity at a single locus for high-affinity Ca2+ interactions. *Neuron*, 15:1121-1132.

210. Stotz, S. C., S. E. Jarvis, G. W. Zamponi (2004). Functional roles of cytoplasmic loops and pore lining transmembrane helices in the voltage-dependent inactivation of HVA calcium channels. *J Physiol*, 554:263-273.

211. Curtis, B. M., W. A. Catterall (1984). Purification of the calcium antagonist receptor of the voltage-sensitive calcium channel from skeletal muscle transverse tubules. *Biochemistry*, 23:2113-2118.

212. Helton, T. D., W. A. Horne (2002). Alternative splicing of the beta 4 subunit has alpha1 subunit subtype-specific effects on Ca2+ channel gating. *J Neurosci*, 22:1573-1582.

213. Chien, A. J., T. Gao, E. Perez-Reyes, M. M. Hosey (1998). Membrane targeting of L-type calcium channels. Role of palmitoylation in the subcellular localization of the beta2a subunit. *J Biol Chem*, 273:23590-23597.

214. Bogdanov, Y., N. L. Brice, C. Canti, K. M. Page, M. Li, S. G. Volsen, A. C. Dolphin (2000). Acidic motif responsible for plasma membrane association of the voltage-dependent calcium channel beta1b subunit. *Eur J Neurosci*, 12:894-902.

215. Richards, M. W., A. J. Butcher, A. C. Dolphin (2004). Ca2+ channel beta-subunits: structural insights AID our understanding. *Trends Pharmacol Sci*, 25:626-632.

216. Walker, D., M. De Waard (1998). Subunit interaction sites in voltage-dependent Ca2+ channels: role in channel function. *Trends Neurosci*, 21:148-154.

217. Dolphin, A. C. (2003). Beta subunits of voltage-gated calcium channels. *J Bioenerg Biomembr*, 35:599-620.

218. Bichet, D., V. Cornet, S. Geib, E. Carlier, S. Volsen, T. Hoshi, Y. Mori, M. De Waard (2000). The I-II loop of the Ca2+ channel alpha1 subunit contains an endoplasmic reticulum retention signal antagonized by the beta subunit. *Neuron*, 25:177-190.

219. Gurnett, C. A., M. De Waard, K. P. Campbell (1996). Dual function of the voltage-dependent Ca2+ channel alpha 2 delta subunit in current stimulation and subunit interaction. *Neuron*, 16:431-440.

220. Felix, R., C. A. Gurnett, M. De Waard, K. P. Campbell (1997). Dissection of functional domains of the voltage-dependent Ca2+ channel alpha2delta subunit. *J Neurosci*, 17:6884-6891.

221. Letts, V. A., R. Felix, G. H. Biddlecome, J. Arikkath, C. L. Mahaffey, A. Valenzuela, F. S. Bartlett, 2nd, Y. Mori, K. P. Campbell, W. N. Frankel (1998). The mouse stargazer gene encodes a neuronal Ca2+-channel gamma subunit. *Nat Genet*, 19:340-347.

222. Black, J. L., 3rd (2003). The voltage-gated calcium channel gamma subunits: a review of the literature. *J Bioenerg Biomembr*, 35:649-660.

223. Doering, C. J., G. W. Zamponi (2003). Molecular pharmacology of high voltage-activated calcium channels. *J Bioenerg Biomembr*, 35:491-505.

224. Zamponi, G. W., E. Bourinet, T. P. Snutch (1996). Nickel block of a family of neuronal calcium channels: subtype- and subunit-dependent action at multiple sites. *J Membr Biol*, 151:77-90.

225. Jurkat-Rott, K., H. Lerche, F. Lehmann-Horn (2002). Skeletal muscle channelopathies. *J Neurol*, 249:1493-1502.

226. Weiss, R. G., K. M. O'Connell, B. E. Flucher, P. D. Allen, M. Grabner, R. T. Dirksen (2004). Functional analysis of the R1086H malignant hyperthermia mutation in the DHPR reveals an unexpected influence of the III-IV loop on skeletal muscle EC coupling. *Am J Physiol Cell Physiol*, 287:C1094-1102.

227. Deisseroth, K., P. G. Mermelstein, H. Xia, R. W. Tsien (2003). Signaling from synapse to nucleus: the logic behind the mechanisms. *Curr Opin Neurobiol*, 13:354-365.

228. Striessnig, J., J. C. Hoda, A. Koschak, F. Zaghetto, C. Mullner, M. J. Sinnegger-Brauns, C. Wild, K. Watschinger, A. Trockenbacher, G. Pelster (2004). L-type Ca2+ channels in Ca2+ channelopathies. *Biochem Biophys Res Commun*, 322:1341-1346.

229. Tremblay, F., R. G. Laroche, I. De Becker (1995). The electroretinographic diagnosis of the incomplete form of congenital stationary night blindness. *Vision Res*, 35:2383-2393.

230. Eisenberg, M. J., A. Brox, A. N. Bestawros (2004). Calcium channel blockers: an update. *Am J Med*, 116:35-43.

231. Sun, J., D. J. Triggle (1995). Calcium channel antagonists: cardiovascular selectivity of action. *J Pharmacol Exp Ther*, 274:419-426.

232. Ito, H., N. Klugbauer, F. Hofmann (1997). Transfer of the high affinity dihydropyridine sensitivity from L-type To non-L-type calcium channel. *Mol Pharmacol*, 52:735-740.

233. Wappl, E., J. Mitterdorfer, H. Glossmann, J. Striessnig (2001). Mechanism of dihydropyridine interaction with critical binding residues of L-type Ca2+ channel alpha 1 subunits. *J Biol Chem*, 276:12730-12735.

234. Yamaguchi, S., Y. Okamura, T. Nagao, S. Adachi-Akahane (2000). Serine residue in the IIIS5-S6 linker of the L-type Ca2+ channel alpha 1C subunit is the critical determinant of the action of dihydropyridine Ca2+ channel agonists. *J Biol Chem*, 275:41504-41511.

235. Opie, L. H. (1997). Calcium channel blockers for hypertension: dissecting the evidence for adverse effects. *Am J Hypertens*, 10:565-577.

236. Dolphin, A. C. (2003). G protein modulation of voltage-gated calcium channels. *Pharmacol Rev*, 55:607-627.

237. Zamponi, G. W. (2003). Regulation of presynaptic calcium channels by synaptic proteins. *J Pharmacol Sci*, 92:79-83.

238. Fisher, T. E., C. W. Bourque (2001). The function of Ca(2+) channel subtypes in exocytotic secretion: new perspectives from synaptic and non-synaptic release. *Prog Biophys Mol Biol*, 77:269-303.

239. Bourinet, E., T. W. Soong, K. Sutton, S. Slaymaker, E. Mathews, A. Monteil, G. W. Zamponi, J. Nargeot, T. P. Snutch (1999). Splicing of alpha 1A subunit gene

generates phenotypic variants of P- and Q-type calcium channels. *Nat Neurosci*, 2:407-415.

240. McDonough, S. I., K. J. Swartz, I. M. Mintz, L. M. Boland, B. P. Bean (1996). Inhibition of calcium channels in rat central and peripheral neurons by omega-conotoxin MVIIC. *J Neurosci*, 16:2612-2623.

241. Smith, M. T., P. J. Cabot, F. B. Ross, A. D. Robertson, R. J. Lewis (2002). The novel N-type calcium channel blocker, AM336, produces potent dose-dependent antinociception after intrathecal dosing in rats and inhibits substance P release in rat spinal cord slices. *Pain*, 96:119-127.

242. Saegusa, H., T. Kurihara, S. Zong, A. Kazuno, Y. Matsuda, T. Nonaka, W. Han, H. Toriyama, T. Tanabe (2001). Suppression of inflammatory and neuropathic pain symptoms in mice lacking the N-type Ca2+ channel. *Embo J*, 20:2349-2356.

243. Hatakeyama, S., M. Wakamori, M. Ino, N. Miyamoto, E. Takahashi, T. Yoshinaga, K. Sawada, K. Imoto, I. Tanaka, T. Yoshizawa, Y. Nishizawa, Y. Mori, T. Niidome, S. Shoji (2001). Differential nociceptive responses in mice lacking the alpha(1B) subunit of N-type Ca(2+) channels. *Neuroreport*, 12:2423-2427.

244. Penn, R. D., J. A. Paice (2000). Adverse effects associated with the intrathecal administration of ziconotide. *Pain*, 85:291-296.

245. Altier, C., G. W. Zamponi (2004). Targeting Ca2+ channels to treat pain: T-type versus N-type. *Trends Pharmacol Sci*, 25:465-470.

246. Hu, L. Y., T. R. Ryder, S. S. Nikam, E. Millerman, B. G. Szoke, M. F. Rafferty (1999). Synthesis and biological evaluation of substituted 4-(OBz)phenylalanine

derivatives as novel N-type calcium channel blockers. *Bioorg Med Chem Lett*, 9:1121-1126.

247. Newcomb, R., B. Szoke, A. Palma, G. Wang, X. Chen, W. Hopkins, R. Cong, J. Miller, L. Urge, K. Tarczy-Hornoch, J. A. Loo, D. J. Dooley, L. Nadasdi, R. W. Tsien, J. Lemos, G. Miljanich (1998). Selective peptide antagonist of the class E calcium channel from the venom of the tarantula Hysterocrates gigas. *Biochemistry*, 37:15353-15362.

248. Bourinet, E., S. C. Stotz, R. L. Spaetgens, G. Dayanithi, J. Lemos, J. Nargeot, G. W. Zamponi (2001). Interaction of SNX482 with domains III and IV inhibits activation gating of alpha(1E) (Ca(V)2.3) calcium channels. *Biophys J*, 81:79-88.

249. Gee, N. S., J. P. Brown, V. U. Dissanayake, J. Offord, R. Thurlow, G. N. Woodruff (1996). The novel anticonvulsant drug, gabapentin (Neurontin), binds to the alpha2delta subunit of a calcium channel. *J Biol Chem*, 271:5768-5776.

250. Kaupp, U. B., R. Seifert (2002). Cyclic nucleotide-gated ion channels. *Physiol Rev*, 82:769-824.

251. Robinson, R. B., S. A. Siegelbaum (2003). Hyperpolarization-activated cation currents: from molecules to physiological function. *Annu Rev Physiol*, 65:453-480.

252. Moran, M. M., H. Xu, D. E. Clapham (2004). TRP ion channels in the nervous system. *Curr Opin Neurobiol*, 14:362-369.

253. Decoursey, T. E. (2003). Voltage-gated proton channels and other proton transfer pathways. *Physiol Rev*, 83:475-579.

254. Jentsch, T. J., V. Stein, F. Weinreich, A. A. Zdebik (2002). Molecular structure and physiological function of chloride channels. *Physiol Rev*, 82:503-568.

CHAPTER II

mTOR Mediates Neuronal Activity Suppression of Local Translation of Kv1.1 mRNA in Dendrites

Summary

Mammalian target of rapamycin (mTOR) has been implicated in synaptic plasticity and local translation in neuronal dendrites. Here we report that the mTOR inhibitor rapamycin increases Kv1.1 total protein in hippocampal neurons and promotes Kv1.1 surface expression on dendrites. Moreover, endogenous Kv1.1 mRNA as well as mRNA for fluorescently tagged Kv1.1 localize to hippocampal neuronal dendrites and soma. We further show local synthesis of Kv1.1 fused to the photo-convertible Kaede in hippocampal neuronal dendrites upon inhibition of mTOR, the upstream molecule PI3 kinase, or the N-methyl-D-aspartate (NMDA) glutamate receptor, suggesting that synaptic excitation may cause local suppression of dendritic Kv1 channels.

Results and Discussion

Pathways involving the mammalian target of rapamycin (mTOR) kinase are important for neuronal signaling. For example, the mTOR inhibitor rapamycin blocks brain-derived neurotrophin (BDNF)-induced synaptic potentiation, maintenance of long-term potentiation (LTP), and the ability of group 1 metabotropic glutamate receptors (mGluR1) to induce long-term depression (LTD) [1]. These different forms of synaptic plasticity depend on the PI3 kinase (PI3-K) /mTOR pathway [2-4]. Products of tumor suppressor genes linked to the disorders Tuberous sclerosis complex (TSC) and Peutz-Jeghers syndrome [5] TSC1, TSC2 and LKB1 are negative regulators of this pathway and have been implicated in controlling local synthesis in synaptodendritic compartments [4, 6-8], thereby providing a mechanism that enables a neuron to respond to synaptic activities by altering protein synthesis near the active synapses.

Whether the mTOR pathway regulates ion channel synthesis and localization is an interesting open question. Both positive and negative translational regulation of ion channels will alter channel density which in turn will influence the excitability of the neuron. Although mammalian homologs of Shaker voltage-gated K^+ (Kv) channels of the Kv1 family are primarily localized to the axons [9], α-dendrotoxin (DTX)-sensitive Kv1 channels also contribute to a fraction of the rapidly inactivating (A-type) and slowly inactivating (D-type) Kv channels in somatodendritic regions of various neurons in the central nervous system (CNS) ([10] and references therein). These channels are thus poised to control local excitability of dendritic branches [11, 12] and to restrict the generation of calcium spikes to the dendrites [13]. Whereas the T1 tetramerization domain of Kv1 channels can mediate axonal targeting [14], it is not known whether

specific mechanisms are employed for dendritic localization of Kv1 channels. In this study, we provide evidence for local synthesis of Kv1.1 in hippocampal neuronal dendrites.

In our pilot studies of the regulation of Kv channels by mTOR, we found that the mTOR inhibitor rapamycin led to the appearance of a prominent Kv1.1 immunoreactivity in the dendritic field of CA1 neurons in hippocampal slices (Fig. 1A). Whereas there was no significant alteration of Kv1.4 immunoreactivity in the same region in slices treated with rapamycin or the carrier DMSO, the Kv1.1 immunoreactivity of rapamycin-treated slices was 50 ± 14% greater than that of control slices treated with DMSO ($n = 3$, $p = 0.03$). Western blot analysis of cortical and hippocampal neuronal cultures verified the increase in Kv1.1 total protein level following mTOR inhibition by rapamycin, whereas the Kv1.4 protein and tubulin levels remained unchanged (Fig. 1B, 2A). As expected for the established mTOR signaling pathway in which the mTOR kinase, upon activation by PI3 kinase and its effector the Akt/PKB kinase, causes phosphorylation of key cap-dependent translation initiation factors as well as the p70 S6 kinase [6, 15], rapamycin inhibition of mTOR reduced the extent of phosphorylation of the downstream p70 S6 kinase but not the Akt kinase upstream of mTOR (Fig. 1B). Moreover, Kv1.1 total protein levels approximately doubled with 20 nM, 200 nM or 500 nM rapamycin (mean percent of control: 236 ± 12%, $n = 5$, $p < 0.05$ for 20 nM; 205± 7%, $n = 7$, $p < 0.05$ for 200 nM, Fig. 2; 280 ± 24%, $n = 3$, $p < 0.01$ for 500 nM; Fig. 1B). Whereas mTOR activity is generally associated with increased protein synthesis, it can also down regulate the level of certain proteins [2, 16-18], similar to the down regulation of Kv1.1 in our study (Fig. 1A, B).

Having found an increase of Kv1.1 expression in the dendritic field of CA1 neurons in hippocampal slices (Fig. 1A), we further examined Kv1.1 distribution in cultured hippocampl neurons with well resolved dendrites and axons, as revealed with the dendritic marker MAP2 (Fig. 1C) and the axonal marker Neural Filament M (Fig. 2B), and found that rapamycin increased Kv1.1 in dendrites without affecting the Kv1.1 level in axons. Interestingly, Kv1.1 appeared in distinct punctate structures in MAP2 positive dendrites upon inhibition of mTOR (Fig. 1C, 2B). Compared to control neurons treated with DMSO, rapamycin treatment significantly increased the Kv1.1 immunoreactivity of these puncta in the proximal dendrites (0 -50 μm from soma; 2.9 ± 0.6; n = 52 control dendrites; n = 50 dendrites treated with rapamycin; p = 0.002). Remarkably, for puncta localized to the primary apical dendrite (50 – 150 μm from soma), rapamycin increased Kv1.1 immunoreactivity dramatically by 12 fold (12.3 ± 3.68; n = 50 control dendrites; n = 49 dendrites treated with rapamycin; p = 0.002; Fig. 1C).

Moreover, using a monoclonal antibody against an extracellular epitope of Kv1.1 [19] to label Kv1.1-containing channels on the surface of hippocampal neurons without detergent permeabilization, we found high levels of Kv1.1 on the surface of proximal apical dendrites of neurons treated with rapamycin but not the carrier DMSO (Fig. 1D). Taken together, we found that the hippocampal neurons displayed mTOR activity as evidenced by the presence of phosphorylated Akt and p70 S6 kinase (Fig. 1B) and the rapamycin effect in decreasing p70 S6 kinase phosphorylation and increasing endogenous Kv1.1 (Fig. 1).

The unexpected finding of rapamycin-induced increase of Kv1.1 on the surface of dendrites (Fig. 1D) raised the possibility that mTOR regulates local synthesis of Kv1.1 in

dendrites. To explore this intriguing possibility, we first double labeled rapamycin treated cultured hippocampal neurons with antibodies against Kv1.1 and mTOR, and found that mTOR-containing granules were colocalized with a fraction of the Kv1.1 immuoreactive punctate structures (R_{coloc} = 60 ± 5%; Fig. 3A). Next, we looked for Kv1.1 mRNA in dendrites by *in situ* hybridization with endogenous Kv1.1 mRNA in cultured hippocampal neurons (Fig. 3C), as well as comparing the levels of mRNA from synaptosomes and those from whole hippocampi using two different measurements (Fig. 3B, table 1). In microarray analyses, we found the Kv1.1 mRNA in synaptosomes normalized by that in hippocampi to be greater than those for MAP2 and ARC, which are known to be targeted to dendrites, and substantially higher than those for the synaptic protein NSF and nuclear proteins such as histones (table 1). Similarly, in real time PCR measurements, the normalized (synaptosomes/total hippocampus) ratio for Kv1.1 mRNA (0.73 ± 0.08, n = 8) was comparable if not greater than that for MAP2 mRNA (0.47 ± 0.05, n = 9), which is targeted to the dendrites [20] (Fig. 3B). For comparison, the normalized ratio for Kv1.4 mRNA (n = 6) was only a fraction of that for Kv1.1 mRNA (15 ± 2%, $p < 0.001$) and MAP2 mRNA (23 ± 3%; $p < 0.001$) (Fig. 3B; Tukey multiple comparison test). To complement these quantitative comparisons of Kv1.1 with known dendritic messenger RNAs, we looked more closely at the subcellular distribution of Kv1.1 mRNA in cultured hippocampal neurons using MAP2 as a dendritic marker, and found significant levels of Kv1.1 mRNA along the length of major dendrites (Fig. 3C). Not only was endogenous Kv1.1 mRNA found in dendrites, *in situ* hybridization of hippocampal neurons infected with a Sindbis viral construct, which included cDNA for the fusion protein EGFP-Kv1.1 followed with the 3'UTR sequence for Kv1.1, revealed

significant signals in granules in dendrites up to 110 μm from the soma (Fig. 3D); the signal was abolished when the labeled EGFP anti-sense oligonucleotide probe was combined with excess unlabeled oligonucleotides. In contrast, when control neurons infected with Sindbis viral constructs for EGFP cDNA, with similar polyadenylation signal and poly A tail for transcript stabilization, were probed with the same EGFP anti-sense oligonucleotides, the signals that were above background levels only appeared within 10 to 20 μm from the soma (Fig. 3D). The finding of Kv1.1 mRNA targeting to neuronal dendrites, where punctate structures of endogenous Kv1.1 protein are found partially colocalized and near the vicinity of mTOR, is thus compatible with the possibility of Kv1.1 local synthesis in dendrites.

To ask whether Kv1.1 could be synthesized locally in dendrites, it is necessary to devise a method to distinguish Kv1.1 that is synthesized in dendrites from Kv1.1 that is synthesized in neuronal soma and then transported to dendrites. For this purpose, we developed a translation reporter by fusing Kaede, a photo-convertible fluorescence protein [21], to the N-terminus of the Kv1.1 coding sequence (Kaede-Kv1.1), followed with 3'UTR of Kv1.1. UV induces a specific proteolytic cleavage of Kaede, converting its fluorescence from green into red, allowing the Kaede-Kv1.1 that is newly synthesized following the UV exposure to be distinguished by its green chromophore (Fig. 4A). After verifying that the fusion protein Kaede-Kv1.1 appeared on the cell surface (Fig. 5A) and gave rise to functional channels with the same biophysical properties as Kv1.1 channels in *Xenopus* oocytes (Fig. 5B), we went on to express these fluorescent channels in hippocampal neurons via Sindbis virus-mediated infection.

To look for newly synthesized Kaede-Kv1.1 in neurons treated with the mTOR inhibitor rapamycin, PI3-K inhibitors, or the DMSO carrier as control, we imaged live neurons before and after UV-induced photo-conversion of existing Kaede-Kv1.1 into red fluorescent proteins (Fig. 4B). Following this UV treatment, newly synthesized Kaede-Kv1.1 appeared in the dendrites over the course of approximately one hour. To verify that the increase in pixel intensity of green fluorescence was due to newly synthesized Kaede-Kv1.1, we subjected the neuron to a second UV exposure (2^{nd} photo-conversion), which would convert the green fluorescence due to Kaede-Kv1.1—but not background fluorescence—into red fluorescence. This series of experiments revealed that treating neurons with rapamycin or either of two PI3-K inhibitors, wortmannin and LY294002, caused a marked increase in newly synthesized Kaede-Kv1.1 in the dendrites (Fig. 4B and data not shown).

The green Kaede-Kv1.1 in the dendrites that appeared following UV photo-conversion of existing Kaede-Kv1.1 is likely due to local dendritic protein synthesis, because movement of Kaede-Kv1.1 from the cell body to the dendrites was not detected over the course of one hour (Fig. 6). In fact, after photo-conversion of the Kaede fluorescence in a defined region of the dendritic branch of a neuron expressing Kaede-Kv1.1, very little green fluorescence appeared in the photoconverted region of the dendrite over 50 min (Fig. 6A, B). By contrast, in control neurons expressing Kaede fused to only the soluble N-terminal domain of Kv1.1, green protein was transported to the photoconverted region of the dendrite within 5 min (Fig. 6A, B). Furthermore, in the rare example of an observed channel movement, Kaede-Kv1.1 exhibited a slow transport rate of less than 15 μm/hour. Fusion of Kv1.1 to EGFP (EGFP-Kv1.1) also revealed

similar low mobility (data not shown). The slow traffic of fluorescently tagged Kv1.1 would be consistent with an insufficient amount of endogenous Kv1 α and/or β subunits that promote forward trafficking of Kv1.1-containing channels. In any case, we saw no indication of Kaede-Kv1.1 traffic from the cell body to the dendrites. Rather, the fluorescently tagged Kv1.1 was concentrated in stationary "hot spots" along the dendrite, reminiscent of the appearance of proteins locally translated in dendrites [8, 22]. In fact, in our time-lapse live imaging of dendrites, the newly synthesized Kaede-Kv1.1 was most prominent in those punctate hotspots that exhibited the strongest Kaede-Kv1.1 signal prior to photo-conversion (Fig. 4B, arrows); the Kaede-Kv1.1 fluorescence at these hot spots grew over time without detectable transport of Kaede-Kv1.1 along the dendrites, consistent with the notion that these puncta correspond to sites of local synthesis of Kv1.1 in dendrites.

To further test the possibility that Kaede-Kv1.1 was synthesized near the punctate structures in the dendrites, we quantified the appearance of newly synthesized Kaede-Kv1.1 over time, in puncta localized in the dendrite over 50 μm from the soma. Whereas the mean pixel intensity of green fluorescence in puncta of DMSO-treated control neurons exhibited a modest increase one hour after the UV exposure (119 ± 8% of the level immediately after photo-conversion; n = 24 puncta, 4 neurons), the increase of Kaede-Kv1.1 green fluorescence was significantly greater in neurons treated with rapamycin (162 ± 14%; n = 27 puncta, 5 neurons, $p < 0.05$), or with the PI3-K inhibitors, LY294002 (164 ± 17%; n = 21 puncta, 4 neurons, $p < 0.05$), or wortmannin (168 ± 10%; n = 24 puncta, 4 neurons, $p < 0.05$) (Fig. 4C). Moreover, the rapamycin-induced increase in Kaede-Kv1.1 (169 ± 6%; n = 48 puncta, 7 neurons) was greatly reduced by the protein

synthesis inhibitors anisomycin (aniso) (138 ± 5%; n = 45 puncta, 7 neurons, $p < 0.01$) and cycloheximide (CHX) (135% ± 6%; n = 34 puncta, 5 neurons, $p < 0.01$) (Fig. 7B, C). These findings provide further support for local synthesis of Kv1.1 in the dendrites.

Having obtained evidence for active signaling of the pathway involving PI3 kinase and mTOR (Fig. 1B)—as revealed by the presence of phosphorylated Akt and p70 S6 kinase (Fig. 1B)—and the involvement of this signaling pathway in local translation of Kaede-Kv1.1 in dendrites (Fig. 4 and 7B, C), we next asked how Kv1.1 local translation might be regulated by neuronal activity. To do this we examined hippocampal neuronal cultures with and without treatments with antagonists of the NMDA glutamate receptor and mGluR1/5 receptor (Fig. 7A). Interestingly, the NMDA receptor antagonist AP5 significantly increased the level of endogenous Kv1.1 but decreased mTOR phosphorylation (P-mTOR; Kv1.1 282 ± 52%, n = 4, p = 0.013; P-mTOR 46 ± 20%, n = 4, p = 0.035; Fig. 7A). Furthermore, when NMDA receptor activation is inhibited in neurons the ratio of Kv1.1 total protein and P- mTOR is approximately 11 fold greater than control neurons (10.9 ± 3.92, n = 4, p = 0.045; Fig. 7A). By contrast, the mGluR1/5 antagonist MCPG had no significant effect on endogenous Kv1.1 protein levels or P-mTOR (Kv1.1 162 ± 35%, n = 4, NS; P-mTOR 147 ± 48%, n = 3, NS; ratio 2.02 ± 0.45, n = 3, NS). It thus appears that NMDA receptor activity causes activation of mTOR and consequently suppresses Kv1.1 production. To determine whether NMDA receptor activity could affect Kv1.1 local synthesis, we tested the effect of AP5, in the presence or absence of the protein synthesis inhibitor anisomycin (aniso), on local synthesis of Kaede-Kv1.1. Indeed, the appearance of newly synthesized Kaede-Kv1.1 at preexisting "hot spots" along the dendrites requires protein synthesis (Fig. 7B, C; AP5 149% ± 5%; n

= 62 puncta, n = 10 neurons; AP5 + aniso 128% ± 5%; n = 24 puncta, n = 4 neurons, $p < 0.01$), indicating that NMDA receptors activated due to synaptic activity could locally regulate Kv1.1 synthesis in dendritic locations near the active synapse.

In summary, we have found Kv1.1 mRNA in the dendrites of hippocampal neurons (Fig. 3B, C, table 1). Moreover, mRNA for fluorescently tagged Kv1.1 is targeted to the dendrites (Fig. 3D) and can be translated locally (Fig. 4B, C). We further show that the activity of NMDA receptor and mTOR of cultured hippocampal neurons is important for suppression of local synthesis of Kaede-Kv1.1 (Fig. 7B, C) and for controlling endogenous Kv1.1 protein level (Fig. 1B, 7A), thereby down regulating dendritic Kv1.1 (Fig. 1C) and Kv1.1-containing channel density on the surface of hippocampal dendrites (Fig. 1D).

These unexpected findings raise a number of interesting questions. How might NMDA receptor activity be linked to the signaling pathway involving PI3 kinase and mTOR that is implicated in controlling Kv1.1 local synthesis? It is known that NMDA receptor-dependent LTP of EPSCs is associated with increased PI3 kinase activity in CA1 [23], likely due to the ability of NMDA receptor to increase Ca^{2+} and Ca^{2+}-loaded calmodulin so as to activate PI3 kinase associated with the AMPA glutamate receptor [24]. This PI3 kinase activation in turn causes phosphorylation of Akt and p70 S6 kinase, which are upstream and downstream of the mTOR kinase, respectively, and is essential for the expression but not the induction or maintenance of LTP of EPSC [23]. Thus, NMDA receptor activation could lead to direct activation of PI3 kinase locally at the active synapses, potentially causing local suppression of Kv1.1 synthesis in the dendrites via the mTOR signaling pathway, thereby contributing to EPSP-spike (E-S) potentiation

[12]. These considerations further raise the intriguing possibility this signaling pathway plays a role in EPSC LTP expression, perhaps by regulating local translation of AMPA receptor and/or other proteins for their surface expression [25-27].

How might mTOR regulate the local translation of Kv1.1 mRNA? One possibility is that when mTOR is inhibited, cap-dependent translation is inhibited, and the synapse shifts to cap-independent translation of transcripts with internal ribosome entry sites (IRES) [5]. However, Kv1.1 mRNA does not contain an IRES and our translation reporter Kaede-Kv1.1 lacking the 5'UTR is still regulated by mTOR inhibition. Interestingly, Kv1.1 mRNA has two putative AU rich elements (AREs) in the 3' UTR often found in early response genes and other molecules subject to rapid regulation, similar to the AREs in the ligatin mRNA reported to be under NMDA receptor regulation [28]. ARE binding proteins could either stabilize the mRNA for translation or promote the degradation of mRNA. Moreover, these positive and negative regulators can respond to signaling pathways often through phosphorylation and compete with one another for binding of mRNA, thus providing a way for rapid change [29]. It will be interesting to explore the possibility that NMDA receptor activation shifts Kv1.1 mRNA from a form readily accessible to translation to perhaps a different complex for silencing or degradation.

The suppression of Kv1.1 local synthesis via NMDA receptor activity uncovered in our study represents an interesting positive feedback mechanism that could specifically enhance the EPSP arising from previously active synapses, by increasing its ability to activate voltage-gated sodium and/or calcium channels thereby facilitating EPSP summation and making it more likely that the membrane potential will reach the

threshold for action potential generation [11, 30]. In addition, hippocampal neuronal dendrites exhibit uneven distribution of Kv channels [11, 31], with one fifth of these dendritic Kv channels sensitive to not only 4-aminopyridine (4-AP) but also the Kv1-specific α-DTX [11], so as to effectively prevent action potential initiation in dendrites and dampen back propagated action potentials [11, 13]. Given the interesting findings of clustered D-type Kv channels on the CA1 dendrite [31] and the local increase of dendritic excitability and calcium influx within the dendritic branch with potentiated EPSC [12], it would be interesting to explore in future studies the possibility that synaptic activities along the dendrites dynamically regulate the size and distribution of microdomains of Kv1 channels, thereby varying the extent of integration and plasticity of synaptic inputs impinging in the vicinity of the previously active synapses and to adjust the quality and capacity of information storage [30]. It will also be important to elucidate homeostasis mechanisms of Kv1.1 local synthesis regulation for the resetting of local excitability.

Materials and methods

DNA constructs

The 3'UTR of Kv1.1 was cloned by RT-PCR from rat brain cDNA, using a primer specific for the coding sequence of Kv1.1 (cattcaccgcatcgataacaccacag) in the forward direction and an oligo dT primer in the reverse direction. The 3'UTR was inserted into Kv1.1 cDNA at the Cla I site within the coding sequence and the Not I (blunt) site within the multiple cloning site of pcDNA3 (Invitrogen). The 3'UTR equivalent to the 3'UTR cloned for this study is reported in Genbank (accession number M26161).

Kaede was initially cloned into the EGFP-N1 vector (Clontech) by replacing the EGFP cDNA inserted at the BamH1 and Not I (blunt) sites. Kaede-Kv1.1 and EGFP-Kv1.1 were generated by PCR using a primer specific for the EGFP-N1 vector in the forward direction (aggcgtgtacggtgggaggtctatata) and a primer that contained the last 15 nucleotides of the cDNA before the stop codon, of either Kaede or EGFP, with the addition of a Nhe I site at the 3' end (Kaede: cccggccgctagccttgacgttgtcc; EGFP: cggccgctagccttgtacagctcgtccatgccgaga) in the reverse direction. The PCR product was digested with Nhe I and inserted into a Nhe I site of the Kv1.1 cDNA at the start codon that was previously engineered into the sequence by the Quick Change Site Directed Mutagenesis Kit (Strategene).

Sindbis virus generation

Kaede/EGFP-Kv1.1 was subcloned by a blunt end ligation into the Stu I site of the SinRep5 virus vector (Invitrogen) and pseudovirions produced according to the

manufacturer's directions. Virus was concentrated by ultracentrifugation for 90 minutes at 100,000 x g.

Brain slice preparation

Brains from 15-25 days old Sprague-Dawley rats (Charles River, CA) were removed and immersed into cold dissection buffer containing 87 mM NaCl, 25 mM $NaHCO_3$, 75 mM Sucrose, 10 mM Glucose, 2.5 mM KCl, 1 mM NaH_2PO_4, 0.5 mM $CaCl_2$, 7 mM $MgCl_2$ and equilibrated with 95% O_2 and 5% CO_2. Hippocampal slices of ~400 µm thickness were prepared with vibratome (Leica), transferred to a holding chamber with the ACSF solution containing 119 mM NaCl, 2.5 mM KCl, 2.5 mM $CaCl_2$, 1.3 mM $MgCl_2$, 26.2 mM $NaHCO_3$, 1 mM NaH_2PO_4, 11 mM glucose and bubbled with 95%O_2/5% CO_2 at 37° C.

Primary neuronal cultures

Cortical and Hippocampal neurons were prepared by the method described by Ma et al. [32, 33] with the exception that the high density cultures were plated at approximately 600,000 cells / 35 mm plate. Three days after plating the media was changed to neurobasal media (Invitrogen) supplemented with 1X B-27, 100 units/ml of penicillin-streptomycin, 2 mM L-glutamine and 2.5 µM cytosine.

Antibodies

Rabbit and monoclonal antibodies against Kv1.1 were a kind gift from Dr. James Trimmer [19, 34], Kv1.4 antibodies have been previously described by Sheng *et. al* [35],

Rabbit MAP2 and NFM antibodies were purchased from Chemicon, Phospho-p70 S6 kinase (Thr 389), Phospho Akt, and Phopho mTOR (Ser 2448) antibodies were purchased from Cell Signaling, mTOR antibody was purchased from AbCam, and anti-tubulin was purchased from Sigma.

Antibody dilutions used in immunostaining: mouse anti-Kv1.1, 1:500, mouse anti Kv1.1e, 1:500; rabbit anti-Kv1.4, 1:100; rabbit anti-MAP2, 1:1000; rabbit anti-mTOR, 1:100. Antibody dilutions used in western blotting experiments: rabbit anti-Kv1.1, 1:1000; mouse anti Kv1.1, 1:1000; rabbit anti-Kv1.4, 1:100; mouse anti-tubulin, 1:1000; mouse anti-phospho-p70 S6 kinase (Thr 389), 1:100; rabbit anti-phospho Akt, 1:100, rabbit anti-phospho mTOR (Ser 2448), 1:500.

Western Blot Analysis

SDS-PAGE and Western Blotting were performed as previously described [36]. High-density hippocampal or cortical cultures were washed and treated for 75 minutes in pre-warmed HEPES-based artificial CSF (ACSF: 150 mM NaCl, 10 mM HEPES [pH 7.4], 3mM KCl, 2 mM $CaCl_2$, 1 mM $MgCl_2$, 10 mM glucose) containing either DMSO as carrier control, or 20 nM, 200 nM (hippocampal neurons, Fig. 3A), or 500 nM rapamycin (cortical neurons, Fig. 1B). For neuronal activity experiments hippocampal neurons (DIV 21 – 30) were treated with DMSO, 200 μm DL-2-amino-5-phophonopentanoic acid (AP5), or 50 μm (+)-alpha-methyl-4-carboxyphenylglcine (MCPG; hippocampal neurons, Fig. 7A) for 75 minutes. Neurons were lysed using RIPA buffer (150 mM NaCl, 10 mM Tris [pH 7.2], 0.1% SDS, 1.0% Triton X-100, 1.0% Deoxycholate, 5 mM EDTA) plus 1X complete protease inhibitor (Boehringer Mannheim). Lysates were collected and

centrifuged at 4 °C for 20 minutes at 20,000 x g. SDS sample buffer was added and the samples were separated by SDS-PAGE and transferred to ECL-hybond nitrocellulose (Amersham). The membranes were incubated with primary antibodies followed by horseradish peroxidase-conjugated anti-rabbit or anti-mouse IgG (1:1000; Jackson laboratories). Proteins were detected using SuperSignal® West Femto Maximum Sensitivity Substrate (Pierce) that was diluted 2 fold with double distilled water. Densitometry was performed by scanning films with an Alpha Imager Imaging system and the band intensity was analyzed with Alpha Imager software. Signals for each lane were normalized against the tubulin signal.

Immunostaining

Acute slices were treated with or without rapamycin (200 nM) in oxygenated ACSF for 75 minutes at 37 °C. Slices were fixed in 4% paraformaldehyde overnight at 4°C. Slices were washed 3X in PBS-T (PBS + 0.3% Triton X-100), blocked overnight in 5% goat serum, PBS-T, incubated with primary antibody in the blocking buffer overnight at 4°C. Slices were washed four times in PBS-T for 30 minutes/wash at 4°C, and then incubated with fluorophore-conjugated secondary antibodies (Jackson Laboratories) at 1:400 dilution overnight at 4°C. Slices were washed at least four times in PBS-T for 30 minutes/wash at 4°C followed by a final wash at 4°C overnight. Slices were mounted using GEL/MOUNT™ (biomeda) and imaged at 4X using a Texas Instruments epifluorescent e800 microscope. For each condition, three slices from 3 rats were quantified in the hippocampal slice experiment. For signal quantification, digitized

images were analyzed with NIH IMAGE J software for mean signal intensity for both Kv1.1 and Kv1.4 in the same slice.

Cultured neurons were treated as described above for western blotting. Neurons were fixed and stained as previously described [33]. Neurons were imaged using a Texas Instruments epifluorescence e800 microscope. All dendrites of each neuron in control and rapamycin treated were analyzed. Puncta were defined as peaks that exceeded the mean control signal intensity plus two standard deviations using NIH Image J software (http://rsb.info.nih.gov/ij). Mean signal intensities of the punctae were compared between control neurons and rapamycin treated neurons between 0 – 50 μm and 50 – 150 μm from the soma. Mean signal intensity of the axons was determined by tracing the axon 150 μm from the soma.

A modified method as outlined by Tiffany *et al.* (2000) was used for surface staining of Kv1.1. In brief, hippocampal neurons (DIV 21) were treated for one hour and 45 minutes in HEPES based ACSF containing either DMSO or rapamycin (200 nM) and then fixed in 4% paraformaldehyde in PBS for 20 minutes at 4°C. Neurons were then washed 3X in TBS (50 mM Tris-HCl, pH 7.4 and 150 mM NaCl), blocked in BLOTTO (3% nonfat dry milk powder in TBS) for 1 hour at room temperature, and incubated overnight at 4°C with an antibody against an extracellular epitope of Kv1.1. Neurons were then washed 6 times with TBS for a total of one hour before permeabilization with 0.1% Triton X-100, and one hour incubation at room temperature with rabbit anti-MAP2. Kv1.1 and MAP2 were detected using cy3 and cy5 conjugated goat anti-mouse and goat anti-rabbit antibodies, respectively. Quantification of surface signal in dendrites was carried out by using NIH Image J software to obtain the background subtracted pixel

intensity by tracing a dendrite for 120 μm from the soma and an equal area adjacent to the dendrite (background). Background subtracted pixel intensity was averaged every 10 μm and plotted against distance from the soma.

For co-localization experiments of Kv1.1 and mTOR, neurons in culture for 28 days were treated with rapamycin for 75 minutes to induce synthesis of dendritic Kv1.1. Neurons were fixed and stained as outline above. Images were acquired with a Zeiss confocal microscope (Zeiss Axioskop 2 FS mot) using a water immersion lens (IR-Achroplan 63x/0.90 W). Pearson's coefficient for colocalization (R_{coloc}) was determined by analyzing two dendrites from 13 neurons using the co-localization test included in NIH Image J software.

Microarray Analysis

Oligonucleotide microarrays representing 8800 genes in the rat genome (Rat genome U34A) were used (Affymetrix). Probes for microarray hybridization were generated from RNA that was purified from total hippocampi and from the synaptosomal fraction of hippocampi from twenty P70 rats. Synaptosomes were prepared as outlined in Raab-Graham and Vandenberg [36]. Total RNA from the synaptosomal fraction and the total hippocampal fraction was isolated by RNeasy kit (Qiagen). cDNA was generated from 1 μg of total RNA using the SMART cDNA synthesis kit (Clontech) with a modified oligo dT primer that included the T7 bacterial phage sequence for subsequent *in vitro* transcription of cDNA (ggccagtgaattgtaatacgactcactatagggaggcggttttttttttttttttttttttt). Biotin-labeled cRNA was generated by *in vitro* transcription using the T7 Ampliscribe kit in the presence of biotin-CTP and biotin-UTP. A single microarray was used for each

condition for the sole purpose of identifying putative mRNAs that are near or at the synapse to be verified by quantitative Real Time PCR and *in situ* hybridization. Raw data for two accession numbers per gene that are relevant to this study are reported in table 1.

Quantitative Real Time PCR

Synaptosomal RNA and toal hippocampal RNA were isolated as outlined above for microarray analysis. Total RNA yield was determined by RiboGreen® RNA Quantitation Kit (Molecular probes). RT-PCR was performed using Superscript II (Invitrogen) with an oligo-dT primer. A second strand was synthesized according to the manufacteurer's instructions. cDNA was incubated with RNase One (Promega) to remove all RNA. cDNA was quantified using PicoGreen® dsDNA Quantitation Kit against a set of known standards in order to ensure that equal amounts of cDNA were used for Real time PCR. Real time PCR was performed in the presence of SYBR-green DNA binding dye (Molecular Probes) using an icycler Real time PCR machine (BIORAD). Each sample was run in duplicate at the time of the experiment. Each experiment was performed at least six times using four independent RNA preparations. The primers used had a Tm of at least 60 °C and were HPLC purified. The primer sequences are listed below 5' to 3':

Kv1.1	Forward:	agcaagctcctgaccgatgtttaaa
	Reverse:	gttgggtttttttttttctttttgct
Kv1.4	Forward:	cggaggaggaggcgacagcgaac
	Reverse:	cctcctcctcgctcagctccctaag
MAP2	Forward:	gccgcagcgccaatggatttc

	Reverse:	agctctccgttgatcccgttctctttg
NSF	Forward:	ggccttctcagtgggacagcagcttg
	Reverse:	gcgattttccttggttttagccttgc

***In situ* Hybridiztion**

Fluorescence *in situ* hybridization (FISH) was performed using a method developed by combining protocols described by http://www.singerlab.org/protocols and Wells et al. [37] with the following modifications: Low density cultured hippocampal neurons (28 days in vitro) were fixed in 4% paraformaldehyde, 4% sucrose for 18 minutes on ice. Neurons were washed 3X in PBS and 1X in SSC for 5 minutes. Neurons were permeabilized with 1% Triton-X 100, 1X SSC for 30 minutes at room temperature. Digoxigenin labeled cRNA corresponding to the sense and antisense strand of Kv1.1 3' UTR (nucleotides 1523 – 1746, accession number M26161) was hybridized overnight at 50 ° C followed by a 2 hour incubation at 37 ° C before washing as outlined in protocol. DIG-labled cRNA was detected with a monoclonal mouse anti-digoxygenin antibody (1:100; Boehringer Mannheim) overnight at 4 °C followed by a cy5-conjugated anti mouse secondary antibody (1:200) for 2 hours at room temperature. Quantification of punctate signal (mRNA granules) was carried out as described above for dendritic Kv1.1 puncta.

For *in situ* hybridization of infected neurons, cultures (DIV 21) were infected with Sindbis virus encoding either EGFP-Kv1.1 or EGFP. 18 hours post infection *in situ* hybridization (*ISH*) was performed as described above using an EGFP antisense DIG labeled oligo as described by Wells et al. [37] and hybridized overnight at 37 °C. ISH

signal was normalized for each neuron by taking the ratio of the mean hybridization signal every 10 μm along the dendrite and the mean of the hybridization signal of 3 μm within the first 10 μm from the soma at the point at which the signal was not saturated.

Preparation, electrophysiology, and imaging of oocytes

Xenopus oocytes were prepared and maintained as previously described [38]. Oocytes were injected with 5 ng of cRNA coding for Kaede-Kv1.1 or Kv1.1. Currents were measured using standard two electrode voltage-clamp recording (Degan Amplifier; pCLAMP software). Oocytes were bathed in ND96 solution, held at –80 mV and Kv1.1 currents were recorded with 200 msec voltage pulses ramping from –70 mV to +70 mV in 10 mV increments, before and after the perfusion of 100 nM DTX-K. After recording, oocytes were fixed in 4% paraformaldehyde for 30 min, washed three times in PBS and mounted using GEL/MOUNT™ (biomeda). Twenty-five confocal images of oocytes in 2 μm z-section steps were acquired using an upright microscope (Leica TCS SP2) with a 20X oil immersion lens (HC PL APO 20x/0.70 imm/corr). Kaede-Kv1.1 or wildtype Kv1.1 was excited at 488 nm and green emission was detected at 500 – 550 nm.

Live imaging and analysis

Primary culture of neurons (14 – 28 DIV) was placed in a custom made temperature controlled, closed chamber stage (Brook Industries) containing HEPES based ACSF with DMSO, rapamycin (200 nM), LY294002 (50 μM), wortmannin (50 nM), or AP5 (200 μM) and maintained at 36.5°C. Two-photon excitation imaging was accomplished using an upright scope (Zeiss Axioskop 2 FS mot) with a water immersion

lens (IR-Achroplan 63x/0.90 W). A Ti:sapphire laser (Coherent Chameleon) was tuned to 930 nm to excite Kaede-Kv1.1 and green emission was detected at 500 – 535 nm. Serial 1.2 μm z-sections of a neuron expressing Kaede-Kv1.1 were acquired then photo-converted using a DAPI filter for 2 min. After the initial photo-conversion, images were acquired at 20 min intervals for 1 h, followed with a second photo-conversion and then a final image acquisition.

Live imaging experiments in Figure 4 were performed as above except a water immersion lens (Achroplan 20x/0.50 W) was used and the duration of photo-conversion was reduced to 30 sec. Neurons treated with anisomycin (40 nM) or cycloheximide (5.5 μg/ml) were washed 3x with ACSF and stored in a 37 °C incubator for 20 min in ACSF with anisomycin or cycloheximide before being placed in the chamber stage.

Eight-bit images of the maximum signal from z-compressed stacks were used for data analysis. For each neuron, the mean intensity of 5 -8 puncta more than 50 μm from the soma was measured. The magnitude of new protein synthesis was calculated from the fold increase of the mean green pixel intensity of puncta 1 h after photo-conversion as compared to that immediately after photo-conversion.

For trafficking experiments (partial photo-conversion; Fig. 6) neurons expressing either Kaede-Kv1.1 or Kaede-Kv1.1 N-terminal domain were imaged as described above with the following modifications: A fraction of the dendrite was photo-converted using a DAPI filter for 30sec. Afterwhich images were taken every 5 min for 55 minutes using a water immersion lens (Achroplan 20x/0.50 W).

Eight-bit images of the maximum signal from z-compressed stacks were used for data analysis. The green pixel intensity of the photo-converted dendrites was normalized to the green pixel intensity before photo-conversion.

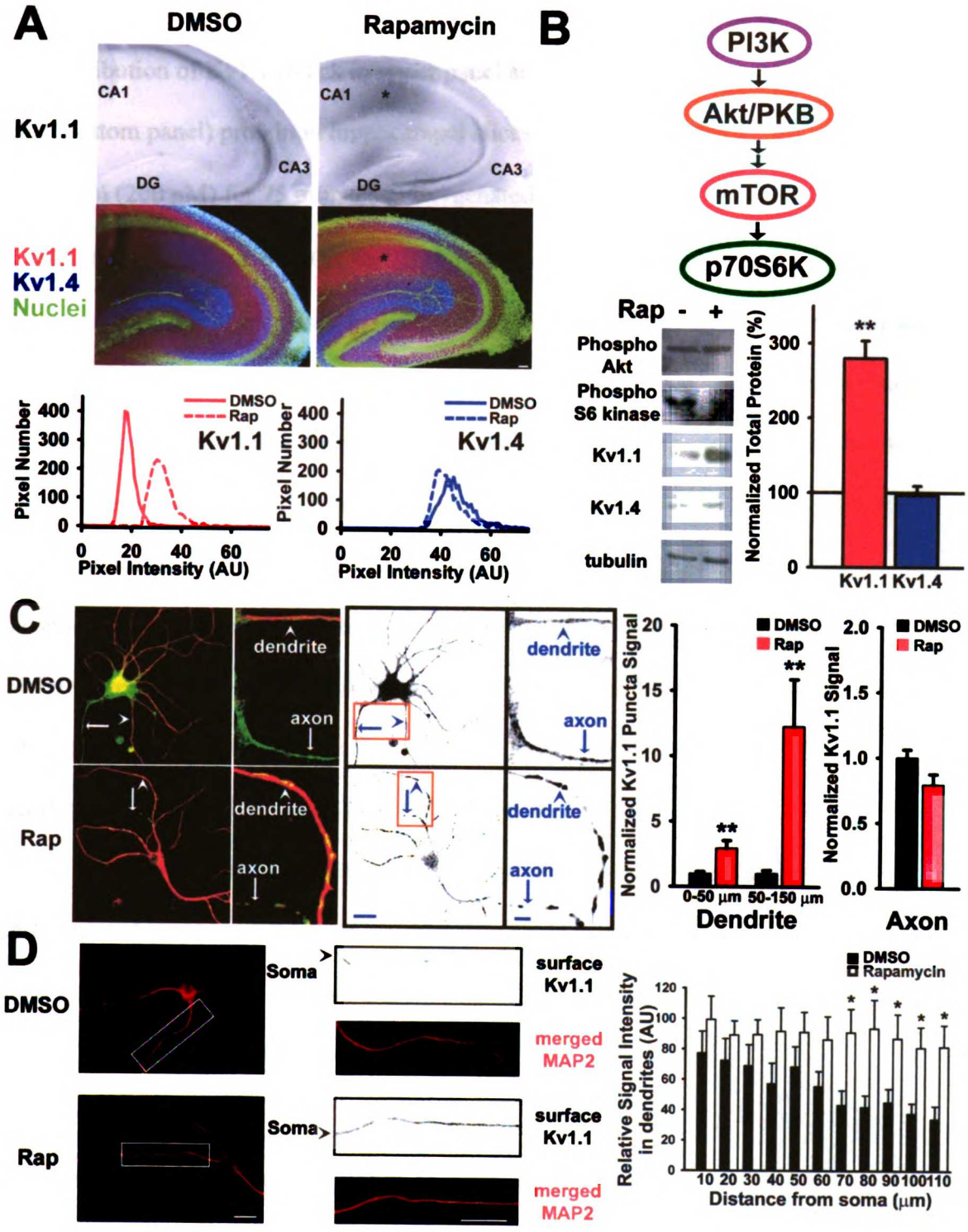
A
DMSO
Rapamycin
Kv1.1
CA1
CA3
DG
Kv1.1
Kv1.4
Nuclei
Pixel Number
Pixel Intensity (AU)
DMSO
Rap
Kv1.1
Kv1.4
B
PI3K
Akt/PKB
mTOR
p70S6K
Rap - +
Phospho Akt
Phospho S6 kinase
Kv1.1
Kv1.4
tubulin
Normalized Total Protein (%)
Kv1.1 Kv1.4
C
DMSO
Rap
dendrite
axon
Normalized Kv1.1 Puncta Signal
0-50 µm
50-150 µm
Dendrite
Normalized Kv1.1 Signal
Axon
D
DMSO
Rap
Soma
surface Kv1.1
merged MAP2
Rapamycin
Relative Signal Intensity in dendrites (AU)
Distance from soma (µm)

Figure 1. Inhibition of mTOR increases Kv1.1 protein in central neuronal dendrites. (A) Distribution of Kv1.1 (black in upper panel and red in bottom panel) and Kv1.4 (blue, bottom panel) protein in hippocampal slices treated with either DMSO (control) or rapamycin (200 nM) for 75 minutes in oxygenated ACSF at 37 °C. Nuclei were stained with the fluorescent dye SYTOX for DNA (green). Scale bar = 100 μm. The Kv1.1 immunoreactivity was increased in the CA1 dendritic field of the rapamycin-treated slice (* in upper right panel indicates regions of increase) (red dash line) compared to control (red solid line), as shown in the histogram below. By contrast, the histogram of the Kv1.4 signal (blue lines) was not altered by the rapamycin treatment. DG, dentate gyrus. (B) Schematic for the PI3-K/Akt/mTOR pathway. Below schematic, immunoblot of phospho-Akt, phospho-S6 kinase, Kv1.1, Kv1.4, and tubulin of cultured cortical neurons (30 DIV) treated with either DMSO (control) or rapamycin. Right, after normalization by the level of tubulin in the sample, the total Kv1.1 but not Kv1.4 protein level was significantly increased by rapamycin (500 nM) (Kv1.1, 280% ± 24%, p = 0.002; Kv1.4, 97% ± 12%, NS; Rapamycin-treated/DMSO control; 3 independent experiments). (C) Left, cultured hippocampal neurons treated with DMSO (control) or rapamycin (Rap; 200 nM) were double labeled with antibodies against Kv1.1 (green) and the dendritic marker MAP2 (red), revealing an increase in dendritic Kv1.1 punctate structures in the rapamycin treated neurons. Scale bar = 20 μm. Right, quantification of Kv1.1 puncta signal intensity in all dendrites 0 - 50 μm and 50 -150 μm from the soma and in axons (dendrites: 0 - 50 μm, DMSO 1 ± 0.2, n = 52 dendrites, Rap 3 ± 0.6, p = 0.002, n = 50 dendrites; 50 -150 μm, DMSO 1 ± 0.25, n = 51, Rap 12.3 ± 3.7, n = 49, p = 0.002; axons: DMSO 1 ± 0.06, n = 17, Rap 0.8 ± 0.08, n = 21, NS). (D) Left, staining of surface Kv1.1

of unpermeabilized cultured hippocampal neurons (DIV 21) treated with DMSO (control) or rapamycin (Rap; 200 nM) with primary antibody against an extracellular epitope of Kv1.1 (green), followed by permeabilization and detection of the dendritic marker MAP2 (red), revealing an increase of surface Kv1.1 in the distal dendrites. Scale bar represents 20 μm. Right, quantification of surface expression of Kv1.1 in DMSO versus rapamycin treated neurons. Mean signal intensities were averaged every 10 μm along the dendrite as indicated by the end point designated on the x axis (DMSO versus Rapamycin: 61-70 μm: 55.4 ± 30.1 versus 86.4 ± 45.4, $p = 0.02$; 71-80 μm: 43.2 ± 29.3 versus 91.1 ± 46.1, $p = 0.02$; 81-90 μm: 42.0 ± 23.1 versus 93.7 ± 56.4, $p = 0.04$; 91-100 μm: 45.1 ± 26.8 versus 87.1 ± 47.8, $p = 0.01$; 101-110 μm: 37.8 ± 20.2 versus 81.2 ± 40.7, $p = 0.01$; $n = 9$ neurons per treatment processed in parallel; 1 dendrite per neuron) * indicates $p < 0.05$.

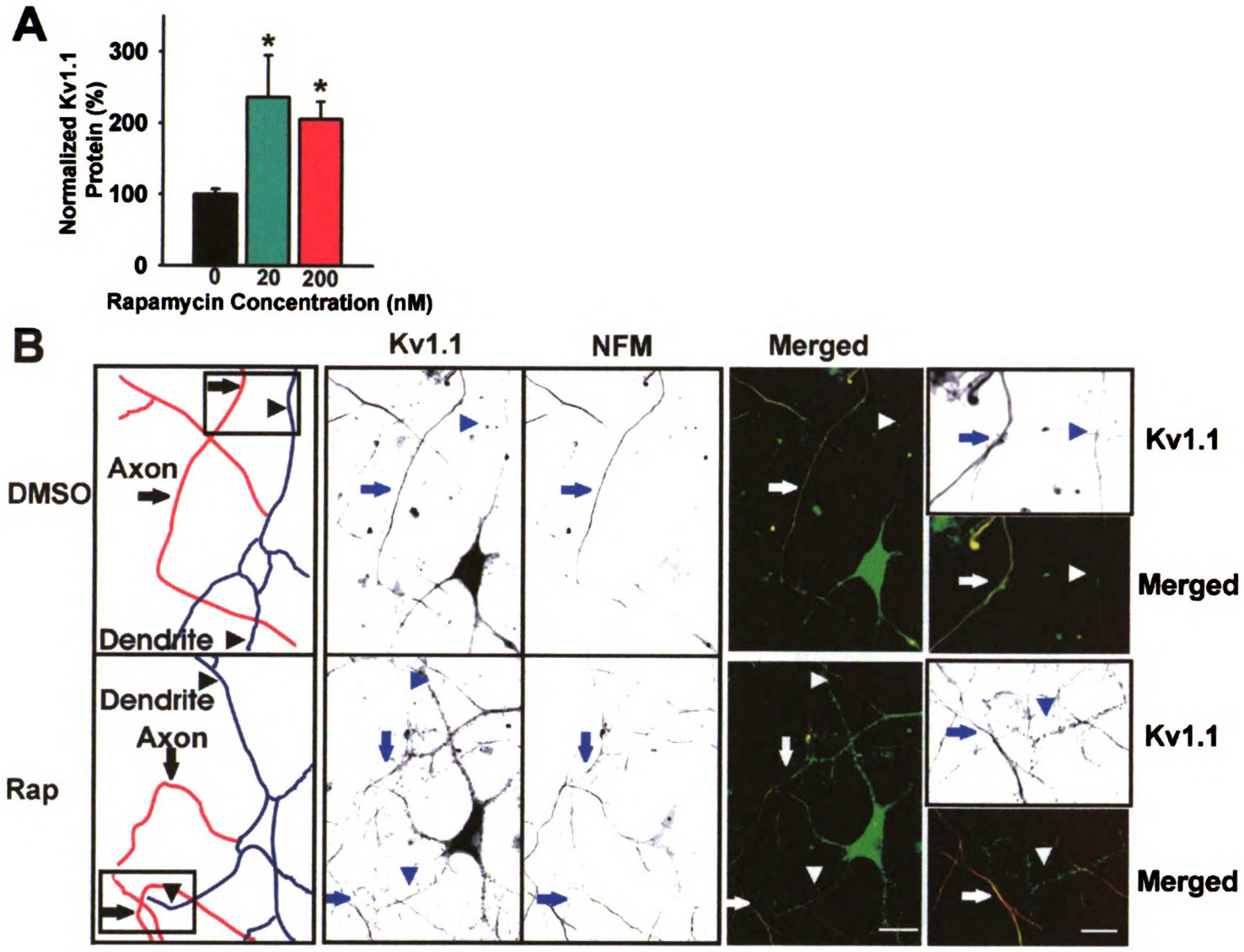
A
Normalized Kv1.1 Protein (%)
300
200
100
0
*
*
0
20
200
Rapamycin Concentration (nM)
B
Kv1.1
NFM
Merged
DMSO
Axon
Dendrite
Rap
Dendrite
Axon
Kv1.1
Merged
Kv1.1
Merged

Figure 2. Inhibition of mTOR by 20 and 200 nM increased Kv1.1 total protein in the dendrites of hippocampal neurons. (A) After normalization by the level of tubulin in the sample, the total Kv1.1 level was significantly increased by treating hippocampal neurons with 20 nM and 200 nM rapamycin (DMSO = 100 ± 6%, n = 7; 20 nM = 236% ± 12%, n = 5; 200 nM, 205 ± 7%, n = 7). Statistical significance was determined by one-way ANOVA with reference to control (0 nM) group. Error bars are SEM. * indicates $p < 0.05$. (B) Cultured hippocampal neurons treated with DMSO (control) or rapamycin (Rap; 200 nM) were double labeled with antibodies against Kv1.1 (green) and the axonal marker neurofilament M (NFM) (red), revealing an increase in dendritic Kv1.1 punctate structures in the rapamycin treated neurons in NFM minus dendrites. Left, sketch of neuron to clearly indicate axons (red) and dendrites (blue). Magnified dendrites and axons are indicated by the box (sketched neuron) and by the arrow (axon) or the arrowhead (dendrite) in parent neuron on left. Scale bar = 20 μm.

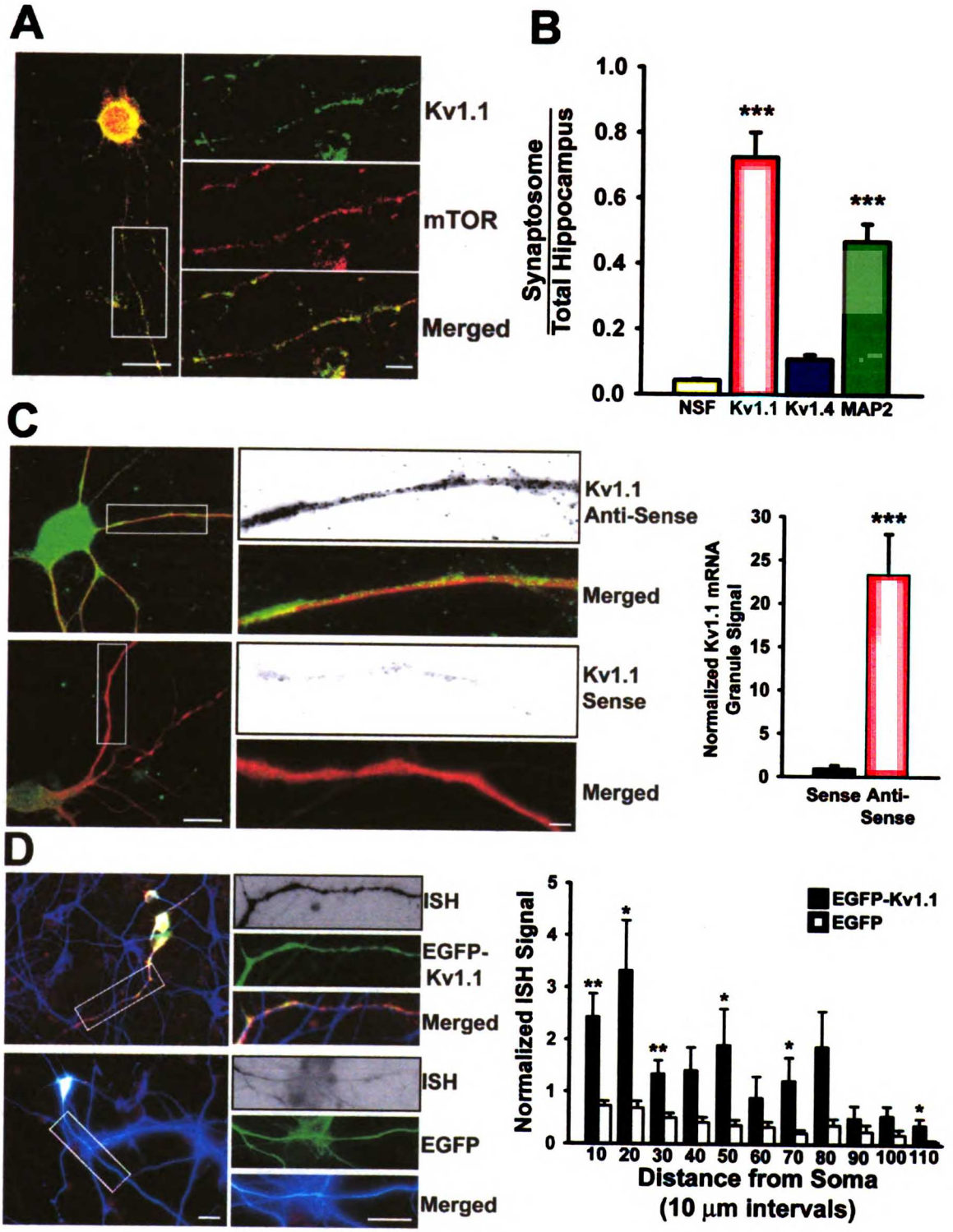
A
Kv1.1
mTOR
Merged
B
Synaptosome / Total Hippocampus
1.0
0.8
0.6
0.4
0.2
0.0
***
***
NSF
Kv1.1
Kv1.4
MAP2
C
Kv1.1 Anti-Sense
Merged
Kv1.1 Sense
Merged
Normalized Kv1.1 mRNA Granule Signal
30
25
20
15
10
5
0
***
Sense
Anti-Sense
D
ISH
EGFP-Kv1.1
Merged
ISH
EGFP
Merged
Normalized ISH Signal
5
4
3
2
1
0
EGFP-Kv1.1
EGFP
**
*
**
*
*
*
10 20 30 40 50 60 70 80 90 100 110
Distance from Soma
(10 μm intervals)

Figure 3. Dendritic Kv1.1 partially co-localizes with mTOR in hippocampal neuronal dendrites containing Kv1.1 mRNA. (A) Co-localization of dendritic Kv1.1 (green) and mTOR (red) in rapamycin (200 nM) treated hippocampal neurons. Boxed dendrites are shown at higher magnification on the right. Scale bar represents 20 μm on the left and 5 μm on the right. (B) Real time PCR measurements revealed that the ratio of synaptosomal mRNA and total hippocampal mRNA (synaptosome/ total hippocampus) for Kv1.1 mRNA (0.73 ± 0.08, n = 8) is greater than that for MAP2 mRNA (0.47 ± 0.05, n = 9), Kv1.4 mRNA (0.11 ± 0.01, n = 6) and NSF mRNA (0.04 ± 0.04, n = 10). **: significant difference compared to NSF according to one way ANOVA test (Kv1.1 vs. NSF, $p < 0.001$, MAP2 vs. NSF, $p < 0.001$, Kv1.4 vs. NSF, NS). (C) Kv1.1 mRNA is present in the dendrites of hippocampal neurons. Left, in situ hybridization images. Boxed dendrite is shown in high magnification on the right. *In situ* hybridization of cultured hippocampal neurons (DIV 28) was performed by using a DIG labeled antisense probe against the 3' UTR of Kv1.1 to detect endogenous Kv1.1 mRNA (green in top panels, also shown in black in top panel on the right) in MAP2 positive dendrites. As a negative control, neurons were hybridized with a sense probe corresponding to the same region as the antisense probe (neuron in bottom panels and corresponding high magnification images on the right). Right, the Kv1.1 mRNA granule signal in the dendrites is normalized by the average background signal in the control using the sense probe (sense n = 8 dendrites, anti-sense n = 9 dendrites). Scale bar represents 20 μm on the left and 5 μm in high magnification images. (D) Left, dendritic localization of EGFP-Kv1.1 RNA with poly-adenylation (top) but not EGFP RNA with poly-adenylation sequence, as revealed by *in situ* hybridization (ISH) using the same antisense probe for

EGFP coding sequences. The boxed dendrites are shown at high magnification in panels on the right. Note granular distribution of EGFP-Kv1.1 RNA. RNA (ISH): black, top; red in merged panel; EGFP: green; MAP2: blue. Scale bar = 20 μm for both low and high magnification images. Right, normalized ISH signal of EGFP-Kv1.1 mRNA (solid bars) and EGFP mRNA (open bars). Mean signal intensities were averaged every 10 μm along the dendrite. To normalize for expression for each neuron, these signals were divided by hybridization signals within the first 10 μm from the soma where the signal was not saturated. End point is designated on the x axis. Significance was determined by the student's t-test to compare Kv1.1-EGFP mean ISH signal to EGFP mean ISHsignal for 10 μm intervals (n = 13 dendrites). Error bars represent SEM * indicates $p < 0.05$; ** indicates $p < 0.01$; *** indicates $p < 0.001$.

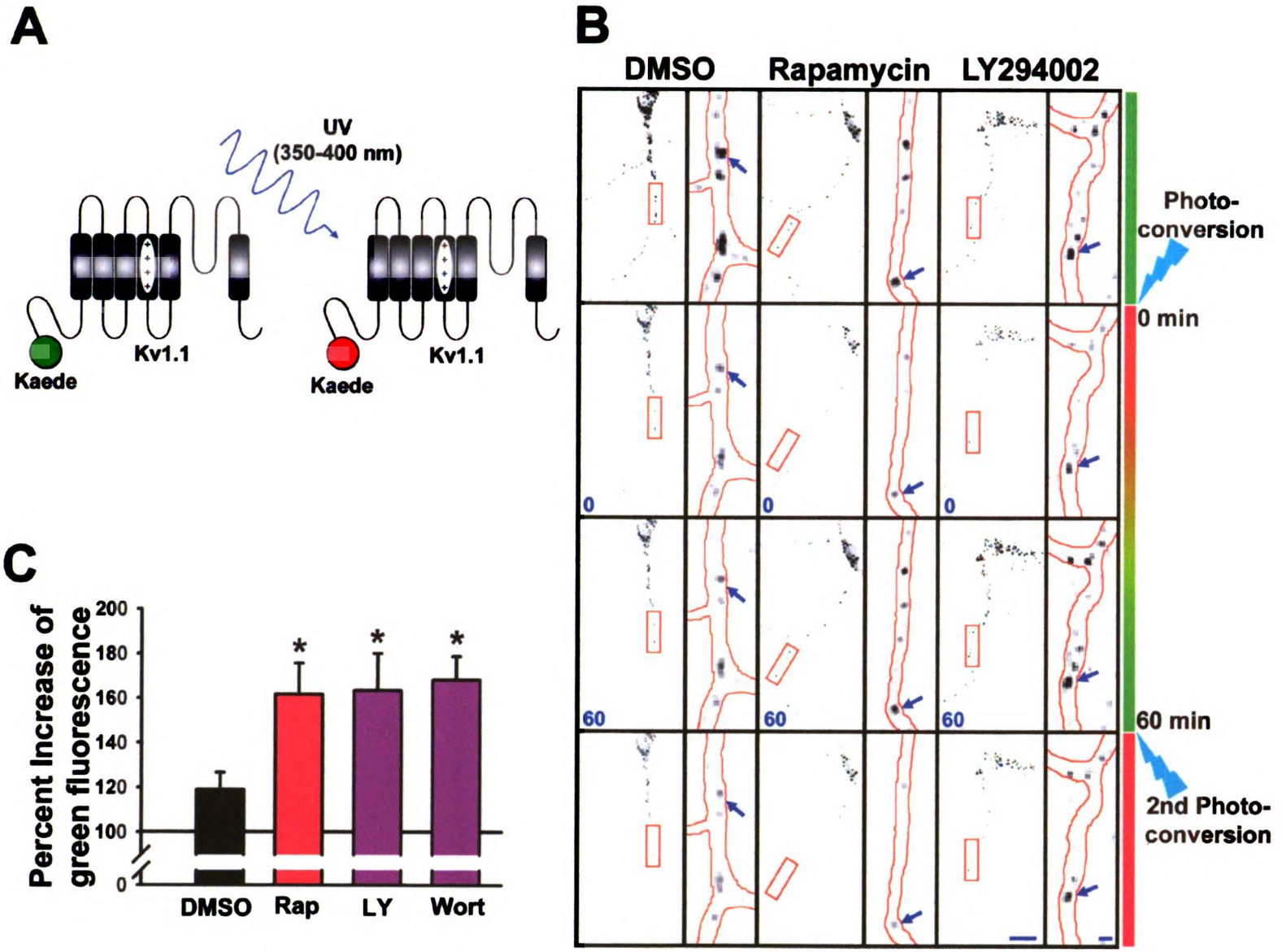
A
UV
(350-400 nm)
Kv1.1
Kaede
Kv1.1
Kaede
B
DMSO
Rapamycin
LY294002
Photo-
conversion
0 min
0
0
0
60
60
60
60 min
2nd Photo-
conversion
C
Percent Increase of
green fluorescence
200
180
160
140
120
100
0
*
*
*
DMSO
Rap
LY
Wort

Figure 4. Inhibition of PI3-K or mTOR increased local translation of Kaede-Kv1.1, revealed by live imaging of newly synthesized Kaede-Kv1.1 in dendrites. (A) Schematic of photo-convertable Kaede-Kv1.1. (B) By monitoring neurons in ACSF containing DMSO (control), rapamycin (200 nM), LY294002 (50 μM), or wortmannin (50 nM) before photo-conversion, immediately after (0 min), or sixty minutes after (60 min) the first UV exposure to photo-convert existing Kaede-Kv1.1 into red fluorescent protein, newly synthesized Kaede-Kv1.1 appeared as green fluorescence, which was then transformed into red fluorescence by the second photo-conversion (2nd Photo-conversion). Left, representative grey scale images of green fluorescence of neurons have orange rectangle indicating magnified view of neuron. Scale bar = 20 μm. Right, dendrite is outlined (orange) and arrowhead follows the fluorescence of an individual Kaede-Kv1.1 punctum. Scale bar = 2 μm. (C) Percent increase of newly synthesized Kaede-Kv1.1 (green fluorescence pixel intensity) in individual puncta greater than 50 μm from the soma, over the course of 1 hour, is stimulated by treatment with rapamycin (162 ± 14%, n = 27 puncta, 5 neurons), LY (163 ± 17%, n = 21 puncta, 4 neurons), or wortmannin (168 ± 11%, n = 24 puncta, 4 neurons), as compared to DMSO control neurons (119 ± 8%, n = 24 puncta, 4 neurons) Error bars represent SEM. Significance was determined by one-way ANOVA with DMSO as the reference * indicating a $p < 0.05$.

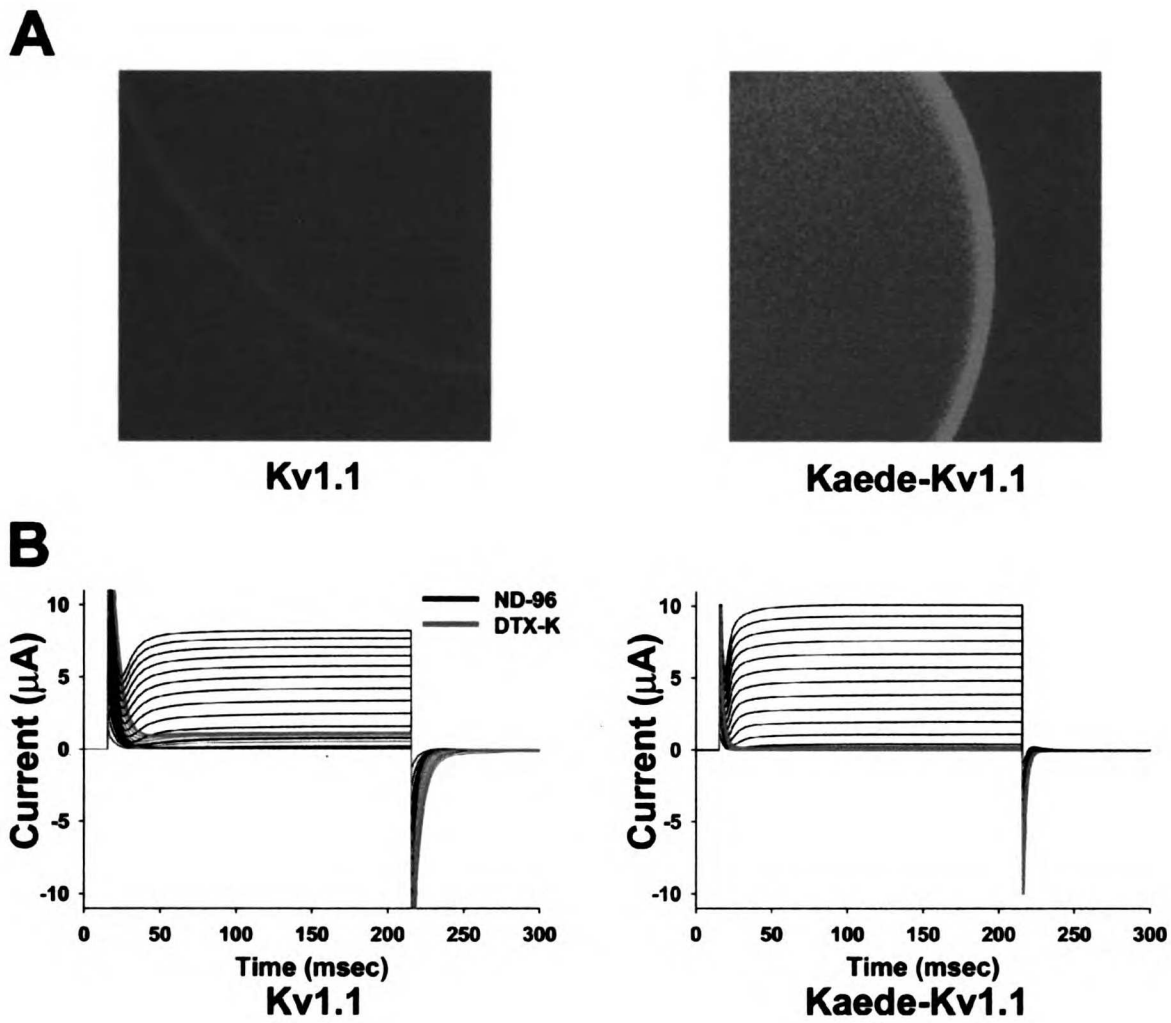
A
Kv1.1
Kaede-Kv1.1
B
ND-96
DTX-K
Current (μA)
10
5
0
-5
-10
0
50
100
150
200
250
300
Time (msec)
Kv1.1
Kaede-Kv1.1

Figure 5. Functional expression of Kaede-Kv1.1 in *Xenopus* oocytes (A) Surface expression of Kaede-Kv1.1 in *Xenopus* oocyte. Confocal image of *Xenopus* oocyte expressing Kv1.1 (left) or Kaede-Kv1.1 (right). (B) Kaede-Kv1.1 exhibits normal channel properties in *Xenopus* oocytes. Representative current traces (black) of voltage clamp recordings from Xenopus oocyte expressing Kv1.1 (left) or Kaede-Kv1.1 (right), and the background currents after blocking Kv1.1 with DTX-K (red).

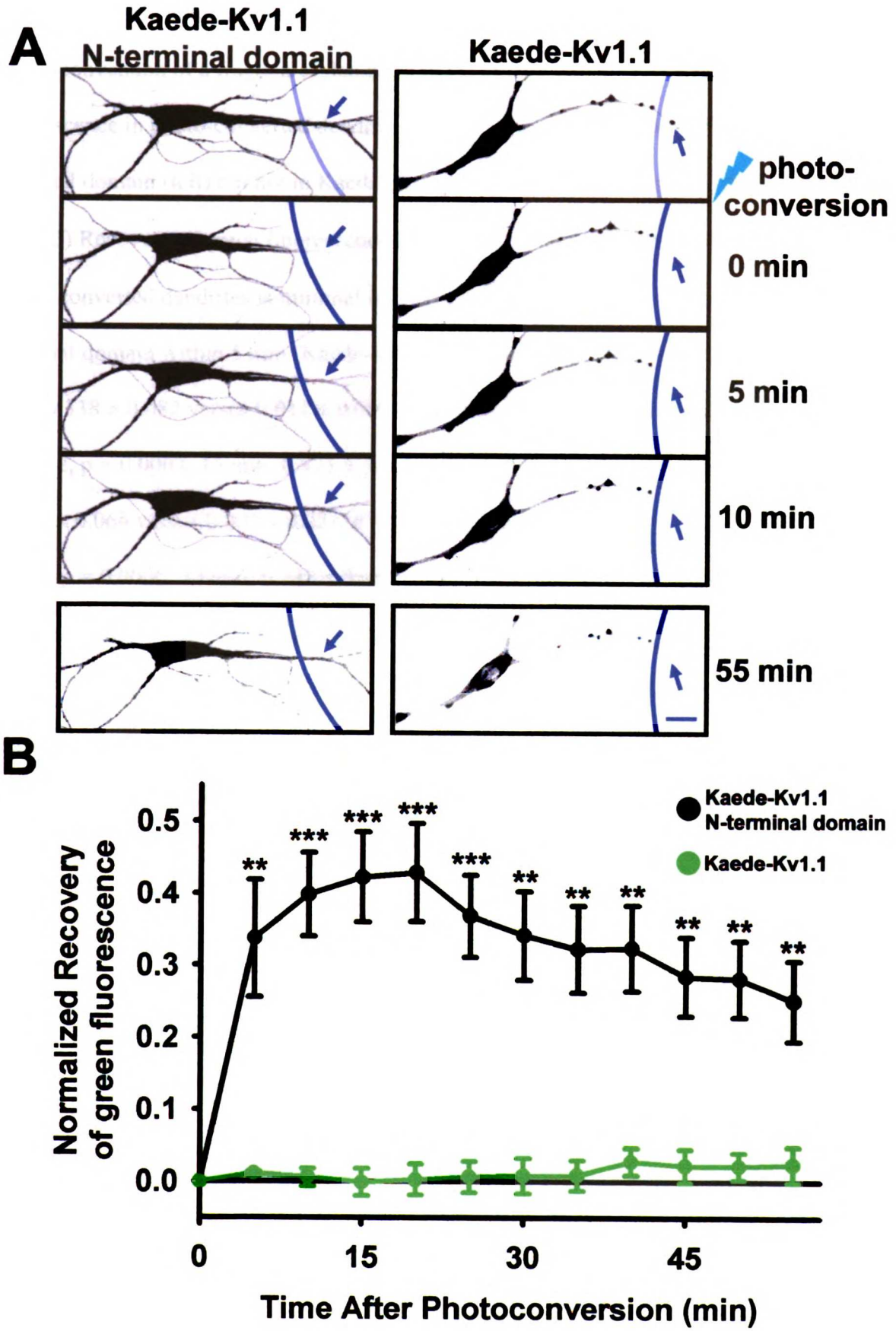
A
Kaede-Kv1.1
N-terminal domain
Kaede-Kv1.1
photo-
conversion
0 min
5 min
10 min
55 min
B
Kaede-Kv1.1
N-terminal domain
Kaede-Kv1.1
Normalized Recovery
of green fluorescence
0.5
0.4
0.3
0.2
0.1
0.0
0
15
30
45
Time After Photoconversion (min)

Figure 6. Little detectable movement of Kaede-Kv1.1. (A) Time-lapse imaging after photo-conversion of a fraction of dendrites (right of blue arc) reveals a recovery of green fluorescence in photo-converted dendrite (arrow) in neurons expressing Kaede-Kv1.1 N-terminal domain (left) but not in Kaede-Kv1.1 expressing neurons (right). Scale bar = 20 μm. (B) Recovery of green fluorescence (normalized recovery of green fluorescence) in photo-converted dendrites is minimal in Kaede-Kv1.1 compared to Kaede-Kv1.1 N-terminal domain within 5 min (Kaede-Kv1.1 N-terminal domain versus Kaede-Kv1.1: 5 min: 0.338 ± 0.082 versus 0.011 ± 0.003, $p = 0.005$; 10 min: 0.398 ± 0.058 versus 0.006 ± 0.012, $p = 0.0003$; 15 min: 0.423 ± 0.063 versus -0.001 ± 0.019, $p = 0.0003$; 20 min: 0.429 ± 0.068 versus 0.003 ± 0.021, $p = 0.0006$; 25 min: 0.369 ± 0.057 versus 0.007 ± 0.022, $p = 0.0006$; 30 min: 0.342 ± 0.061 versus 0.008 ± 0.024, $p = 0.001$; 35 min: 0.323 ± 0.060 versus 0.009 ± 0.021, $p = 0.002$; 40 min: 0.324 ± 0.059 versus 0.028 ± 0.019, $p = 0.002$; 45 min: 0.285 ± 0.054 versus 0.022 ± 0.023, $p = 0.003$; 50 min: 0.282 ± 0.053 versus 0.022 ± 0.019, $p = 0.002$; 55 min: 0.251 ± 0.055 versus 0.024 ± 0.025, $p = 0.007$; $n = 4$ neurons per construct) Error bars represent SEM ** indicates $p < 0.01$; *** indicates $p < 0.001$.

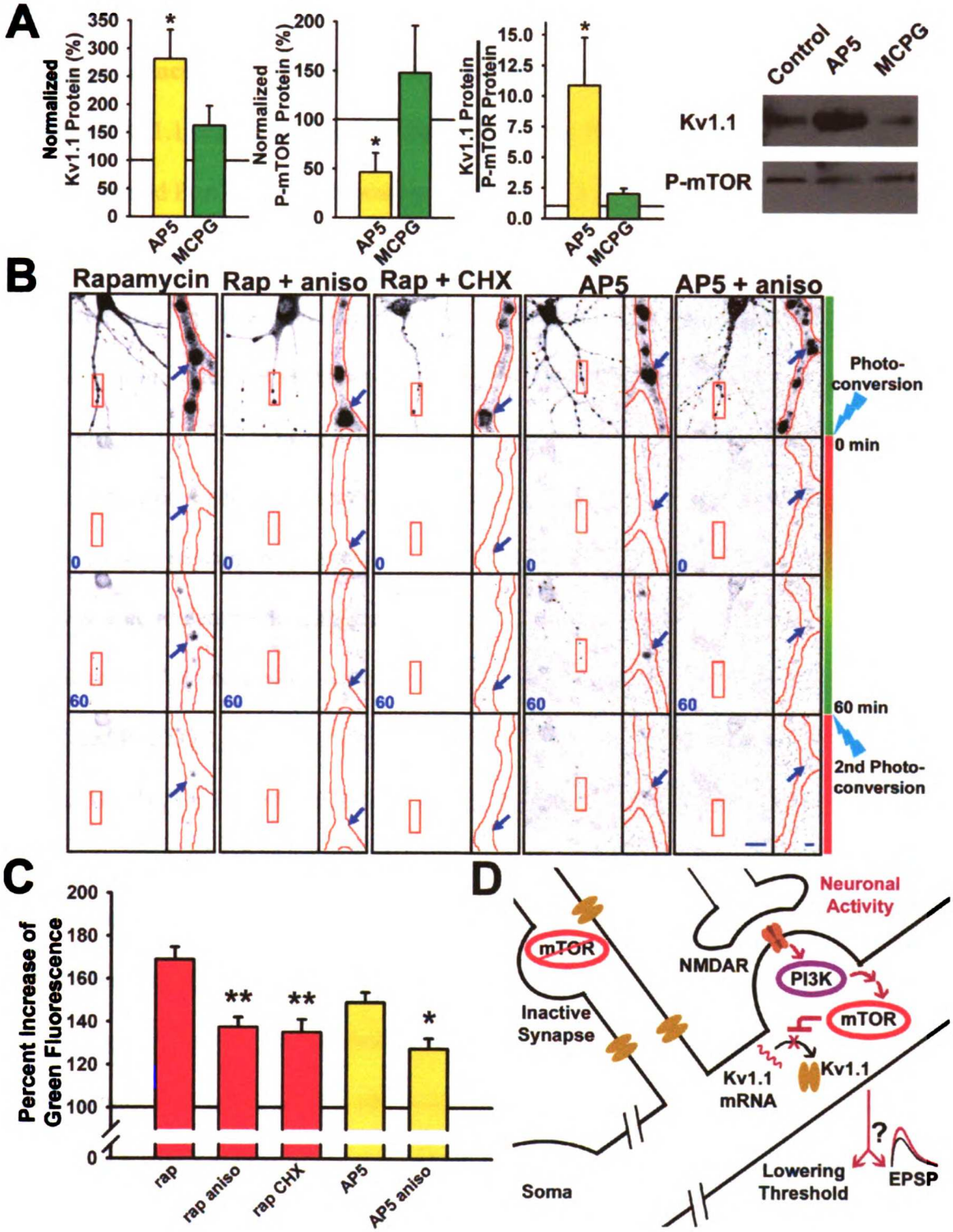
A
Normalized Kv1.1 Protein (%)
AP5
MCPG
Normalized P-mTOR Protein (%)
Kv1.1 Protein / P-mTOR Protein
Control
AP5
MCPG
Kv1.1
P-mTOR
B
Rapamycin
Rap + aniso
Rap + CHX
AP5
AP5 + aniso
Photo-conversion
0 min
60 min
2nd Photo-conversion
C
Percent Increase of Green Fluorescence
rap
rap aniso
rap CHX
AP5
AP5 aniso
D
Neuronal Activity
mTOR
NMDAR
PI3K
mTOR
Inactive Synapse
Kv1.1 mRNA
Kv1.1
Soma
Lowering Threshold
EPSP

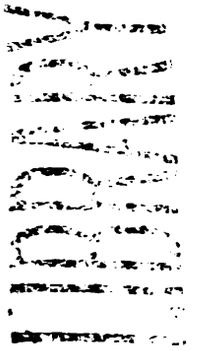

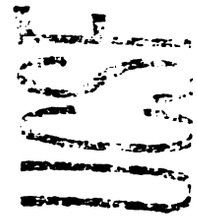

Figure 7. Inhibiting neuronal activity increases the local translation of dendritic Kv1.1 and reduces the phosphorylation of mTOR. (A) Left, quantification of normalized Kv1.1 protein, normalized Phospho-mTOR (P-mTOR), and the ratio of Kv1.1 total protein and P-mTOR of hippocampal neurons (DIV 21 – 30) treated for 75 minutes at 37 °C in ACSF containing DMSO (control), AP5 (200 μm), or MCPG (50 μm) demonstrating a significant increase of Kv1.1 total protein and a significant decrease in phosphorylation of mTOR in AP5 treated samples. By contrast there was no significant change in Kv1.1 or P-mTOR in MCPG treated samples. Samples were normalized by tubulin and ratios for Kv1.1 protein and phosphor-mTOR were determined for each sample. Treated neurons were compared to corresponding control sister culture. Student's t-test was used to determine significance between control and treated neurons (normalized Kv1.1 protein, AP5 282 ± 52%, $p = 0.013$; MCPG 163 ± 35%, NS; normalized P-mTOR, AP5 46 ± 20, $p = 0.038$; MCPG 148 ± 48%, NS; Kv1.1 protein/ P-mTOR, AP5 10.9 ± 3.9, $p = 0.046$; MCPG 2 ± 0.45, NS). Right, immunoblot of Kv1.1 (top panel) and P-mTOR (bottom panel) demonstrating that the ratio of Kv1.1 protein and P-mTOR in AP5 treated neurons is greater than that for either the control or MCPG treated neurons. (B) Left, live imaging of Kaede-Kv1.1 in the presence of rapamycin (200 nM), rapamycin plus the protein synthesis inhibitor anisomycin (40 nM) or cycloheximide (5.5 μg/ml) before photo-conversion, after photo-conversion (0 min), 60 minutes, and after a second photo-conversion demonstrating that the newly synthesized green Kaede-Kv1.1 when mTOR is inhibited by rapamycin is sensitive to protein synthesis inhibitors. Right, live imaging of Kaede-Kv1.1 demonstrates that blocking neuronal activity by AP5 (200 μm) increases green Kaede-Kv1.1 signal. Note the

presence of new green signal at translational hot spots in dendrites as indicated by arrows after 60 minutes. By contrast, note the absence of green signal at hot spots in neurons treated with the protein synthesis inhibitor anisomycin (40 nM) prior and during rapamycin or AP5 treatment as indicated by arrow at time point 60 minutes. Left, representative grey scale images of green fluorescence of neurons have orange rectangle indicating magnified view of neuron. Scale bar = 20 μm. Right, magnified view of neuron with dendrite outlined (orange). Scale bar = 2 μm. (C) Percent increase of newly synthesized Kaede-Kv1.1 (green fluorescence pixel intensity) in individual puncta greater than 50 μm from the soma, over the course of 1 hour, is stimulated by treatment with rapamycin (169 ± 6%, n = 48 puncta, 7 neurons), Rap + anisomycin (138 ± 4.6%, n = 45 puncta, 7 neurons) Rap + cycloheximide (135 ± 6.2%, n = 34 puncta, 5 neurons), AP5 (149 ± 4.8%, n = 62 puncta, 10 neurons), AP5 + anisomycin (128 ± 4.8%, n = 24 puncta, 4 neurons). Error bars represent SEM. Significance was determined by one-way ANOVA with Rap as the reference for Rap + aniso and Rap + CHX. Student t-test was used to determine the significance between AP5 and AP5 + aniso treated neurons. * indicating a $p < 0.05$ and ** indicating a $p < 0.01$. (D) Schematic of neuron showing an inactive synapse (left) where mTOR is not active, therefore permitting the local synthesis of Kv1.1 channels that are displayed on the dendritic surface. Right, dendritic branch shows that neuronal activity can activate NMDA receptors thereby activating the PI3kinase/mTOR pathway and suppressing the local translation of Kv1.1. This activity may lower the threshold required to propagate a dendritic action potential and/or increase the amplitude of the EPSP locally.

Table 1. Ratio of Kv1.1 mRNA in synaptosomes/hippocampi is greater than ratio for known dendritic mRNAs. Raw data collected from microarray experiment comparing mRNA isolated from the synaptosomal fraction of hippocampi to total hippocampi demonstrates that ratio for Kv1.1 is greater than known dendritic mRNAs such as CamKII α, Arc, and MAP2 as well as the synaptic protein NSF, and the nuclear protein Histone 2a.

References

1. Hou, L., E. Klann (2004). Activation of the phosphoinositide 3-kinase-Akt-mammalian target of rapamycin signaling pathway is required for metabotropic glutamate receptor-dependent long-term depression. *J Neurosci*, 24:6352-6361.

2. Klann, E., T. E. Dever (2004). Biochemical mechanisms for translational regulation in synaptic plasticity. *Nat Rev Neurosci*, 5:931-942.

3. Tang, S. J., G. Reis, H. Kang, A. C. Gingras, N. Sonenberg, E. M. Schuman (2002). A rapamycin-sensitive signaling pathway contributes to long-term synaptic plasticity in the hippocampus. *Proc Natl Acad Sci U S A*, 99:467-472.

4. Cammalleri, M., R. Lutjens, F. Berton, A. R. King, C. Simpson, W. Francesconi, P. P. Sanna (2003). Time-restricted role for dendritic activation of the mTOR-p70S6K pathway in the induction of late-phase long-term potentiation in the CA1. *Proc Natl Acad Sci U S A*, 100:14368-14373.

5. Inoki, K., M. N. Corradetti, K. L. Guan (2005). Dysregulation of the TSC-mTOR pathway in human disease. *Nat Genet*, 37:19-24.

6. Takei, N., N. Inamura, M. Kawamura, H. Namba, K. Hara, K. Yonezawa, H. Nawa (2004). Brain-derived neurotrophic factor induces mammalian target of rapamycin-dependent local activation of translation machinery and protein synthesis in neuronal dendrites. *J Neurosci*, 24:9760-9769.

7. Schratt, G. M., E. A. Nigh, W. G. Chen, L. Hu, M. E. Greenberg (2004). BDNF regulates the translation of a select group of mRNAs by a mammalian target of rapamycin-phosphatidylinositol 3-kinase-dependent pathway during neuronal development. *J Neurosci*, 24:7366-7377.

8. Aakalu, G., W. B. Smith, N. Nguyen, C. Jiang, E. M. Schuman (2001). Dynamic visualization of local protein synthesis in hippocampal neurons. *Neuron*, 30:489-502.

9. Trimmer, J. S., K. J. Rhodes (2004). Localization of voltage-gated ion channels in mammalian brain. *Annu Rev Physiol*, 66:477-519.

10. Guan, D., J. C. Lee, T. Tkatch, D. J. Surmeier, W. E. Armstrong, R. C. Foehring (2006). Expression and biophysical properties of Kv1 channels in supragranular neocortical pyramidal neurones. *J Physiol*, 571:371-389.

11. Hoffman, D. A., J. C. Magee, C. M. Colbert, D. Johnston (1997). K+ channel regulation of signal propagation in dendrites of hippocampal pyramidal neurons. *Nature*, 387:869-875.

12. Frick, A., J. Magee, D. Johnston (2004). LTP is accompanied by an enhanced local excitability of pyramidal neuron dendrites. *Nat Neurosci*, 7:126-135.

13. Golding, N. L., H. Y. Jung, T. Mickus, N. Spruston (1999). Dendritic calcium spike initiation and repolarization are controlled by distinct potassium channel subtypes in CA1 pyramidal neurons. *J Neurosci*, 19:8789-8798.

14. Gu, C., Y. N. Jan, L. Y. Jan (2003). A conserved domain in axonal targeting of Kv1 (Shaker) voltage-gated potassium channels. *Science*, 301:646-649.

15. Brown, E. J., S. L. Schreiber (1996). A signaling pathway to translational control. *Cell*, 86:517-520.

16. Pirola, L., S. Bonnafous, A. M. Johnston, C. Chaussade, F. Portis, E. Van Obberghen (2003). Phosphoinositide 3-kinase-mediated reduction of insulin receptor substrate-1/2 protein expression via different mechanisms contributes to the insulin-

induced desensitization of its signaling pathways in L6 muscle cells. *J Biol Chem*, 278:15641-15651.

17. Gebauer, F., M. W. Hentze (2004). Molecular mechanisms of translational control. *Nat Rev Mol Cell Biol*, 5:827-835.

18. Peng, T., T. R. Golub, D. M. Sabatini (2002). The immunosuppressant rapamycin mimics a starvation-like signal distinct from amino acid and glucose deprivation. *Mol Cell Biol*, 22:5575-5584.

19. Tiffany, A. M., L. N. Manganas, E. Kim, Y. P. Hsueh, M. Sheng, J. S. Trimmer (2000). PSD-95 and SAP97 exhibit distinct mechanisms for regulating K(+) channel surface expression and clustering. *J Cell Biol*, 148:147-158.

20. Blichenberg, A., B. Schwanke, M. Rehbein, C. C. Garner, D. Richter, S. Kindler (1999). Identification of a cis-acting dendritic targeting element in MAP2 mRNAs. *J Neurosci*, 19:8818-8829.

21. Mizuno, H., T. K. Mal, K. I. Tong, R. Ando, T. Furuta, M. Ikura, A. Miyawaki (2003). Photo-induced peptide cleavage in the green-to-red conversion of a fluorescent protein. *Mol Cell*, 12:1051-1058.

22. Steward, O., E. M. Schuman (2003). Compartmentalized synthesis and degradation of proteins in neurons. *Neuron*, 40:347-359.

23. Sanna, P. P., M. Cammalleri, F. Berton, C. Simpson, R. Lutjens, F. E. Bloom, W. Francesconi (2002). Phosphatidylinositol 3-kinase is required for the expression but not for the induction or the maintenance of long-term potentiation in the hippocampal CA1 region. *J Neurosci*, 22:3359-3365.

24. Man, H. Y., Q. Wang, W. Y. Lu, W. Ju, G. Ahmadian, L. Liu, S. D'Souza, T. P. Wong, C. Taghibiglou, J. Lu, L. E. Becker, L. Pei, F. Liu, M. P. Wymann, J. F. MacDonald, Y. T. Wang (2003). Activation of PI3-kinase is required for AMPA receptor insertion during LTP of mEPSCs in cultured hippocampal neurons. *Neuron*, 38:611-624.

25. Ju, W., W. Morishita, J. Tsui, G. Gaietta, T. J. Deerinck, S. R. Adams, C. C. Garner, R. Y. Tsien, M. H. Ellisman, R. C. Malenka (2004). Activity-dependent regulation of dendritic synthesis and trafficking of AMPA receptors. *Nat Neurosci*, 7:244-253.

26. Kacharmina, J. E., C. Job, P. Crino, J. Eberwine (2000). Stimulation of glutamate receptor protein synthesis and membrane insertion within isolated neuronal dendrites. *Proc Natl Acad Sci U S A*, 97:11545-11550.

27. Sutton, M. A., H. T. Ito, P. Cressy, C. Kempf, J. C. Woo, E. M. Schuman (2006). Miniature neurotransmission stabilizes synaptic function via tonic suppression of local dendritic protein synthesis. *Cell*, 125:785-799.

28. Jakoi, E. R., D. M. Panchision, C. M. Gerwin, R. J. DeLorenzo (1995). Post-transcriptional regulation of gene expression in hippocampal neurons by glutamate receptor activation. *Brain Res*, 693:124-132.

29. Barreau, C., L. Paillard, H. B. Osborne (2005). AU-rich elements and associated factors: are there unifying principles? *Nucleic Acids Res*, 33:7138-7150.

30. Frick, A., D. Johnston (2005). Plasticity of dendritic excitability. *J Neurobiol*, 64:100-115.

31. Chen, X., D. Johnston (2006). Voltage-gated ion channels in dendrites of hippocampal pyramidal neurons. *Pflugers Arch*.

32. Ma, D., N. Zerangue, K. Raab-Graham, S. R. Fried, Y. N. Jan, L. Y. Jan (2002). Diverse trafficking patterns due to multiple traffic motifs in G protein-activated inwardly rectifying potassium channels from brain and heart. *Neuron*, 33:715-729.

33. Banker, G., K. Goslin, *Culturing nerve cells*, 2nd ed. MIT Press. Cambridge, Mass., 1998

34. Rhodes, K. J., S. A. Keilbaugh, N. X. Barrezueta, K. L. Lopez, J. S. Trimmer (1995). Association and colocalization of K+ channel alpha- and beta-subunit polypeptides in rat brain. *J Neurosci*, 15:5360-5371.

35. Sheng, M., M. L. Tsaur, Y. N. Jan, L. Y. Jan (1992). Subcellular segregation of two A-type K+ channel proteins in rat central neurons. *Neuron*, 9:271-284.

36. Raab-Graham, K. F., C. A. Vandenberg (1998). Tetrameric subunit structure of the native brain inwardly rectifying potassium channel Kir 2.2. *J Biol Chem*, 273:19699-19707.

37. Wells, D. G., X. Dong, E. M. Quinlan, Y. S. Huang, M. F. Bear, J. D. Richter, J. R. Fallon (2001). A role for the cytoplasmic polyadenylation element in NMDA receptor-regulated mRNA translation in neurons. *J Neurosci*, 21:9541-9548.

38. Collins, A., H. Chuang, Y. N. Jan, L. Y. Jan (1997). Scanning mutagenesis of the putative transmembrane segments of Kir2.1, an inward rectifier potassium channel. *Proc Natl Acad Sci U S A*, 94:5456-5460.

39. We are grateful to J. Trimmer for Kv1.1 antibodies and A. Miyawaki for the Kaede construct. We thank S. Yurkovskaya and M. Jain for technical assistance. A NIMH grant (MH65334) to L. Y. Jan supported this work. K. F. Raab-Graham was supported in

CHAPTER III

Conclusion and Future Directions

Conclusion and Future Directions

Controlling the site of protein translation in a neuron offers a level of cellular regulation. In many types of cells the machinery to synthesize protein resides in the soma and the task of getting a protein synthesized in the soma to its desired location is relegated to protein transport machinery such as motor proteins [1]. For neurons, there could be some limitations in quickly and effectively localizing proteins, particularly if faced with transporting proteins through the long distances and complex paths of dendritic branches, in order to get them to distal dendrites, and to specific synapses in response to certain patterns of synaptic inputs.

A proposed method for a neuron to overcome the hurdle of properly targeting a protein to a discrete part of a dendrite in a timely manner would be to translate the protein near the site of its final destination, rather than the soma [2-4]. For local translation to occur, three categories of events have to take place: 1) the RNA needs to be transported to the dendrites, 2) translational machinery needs to be present in dendrites for translation, and 3) the initiation of translation has to be regulated so that local translation only occurs when necessary. Over the years, technological advances have given researchers the tools needed to peer into neurons with greater detail, allowing for more direct observations of the capacity and occurrence of local translation in neurons. Some of the key benefits of local translation over the conventional somatic synthesis and transport of protein is that the response to the need of increased protein levels at a precise location can be faster. Multiple protein products can also be generated from translation of a single transcript targeted to the dendrite, providing a source of signal amplification.

The list of mRNA transcripts that are found in neuronal processes is growing [5]. Our work has expanded the scope of the types of proteins that could be translated locally, to include a member of the voltage-gated ion channel family, Kv1.1. We focused on the regulation of translating Kv1.1 locally. An open question for future investigation is the process of localizing Kv1.1 mRNA to dendrites which is necessary for local translation. Our microarray experiment detected Kv1.1 transcripts in synaptosomes of naïve adult rats indicates that Kv1.1 mRNA is constitutively present. However, it is possible for the levels of Kv1.1 mRNA in neuronal processes to be modulated. The same signaling cascade that responds to neuronal activity to control local translation of Kv1.1 may also lead to regulation of the transport of Kv1.1 mRNA to dendrites in order to accommodate the demand for dendritic Kv1.1. The transcript of the immediate early gene Arc is well known for being sensitive to being trafficked to dendritic processes in an activity dependent manner [6, 7]. Kv1.1 mRNA may not respond the same way as Arc mRNA but they may share some similarities in RNA transport if there are universal features of trafficking mRNA to dendrites.

Only a select group of mRNA is translated locally in neurons. These transcripts, including Kv1.1, possess an intrinsic motif to dictate targeting to dendrites. The motifs that dictate the trafficking of mRNA to neuronal processes is an active research avenue and will be more tractable as more transcripts are detected in processes. One of the best characterized motifs for mRNA targeting to dendrites is found in the 3' UTR of CamKII [8]. However, most of the 3'UTR of CamKII is necessary for targeting its mRNA to dendrites. Finding the RNA sequence necessary and sufficient for the dendritic targeting of Kv1.1 mRNA may not be a trivial continuous stretch of RNA. Rather, it will likely

involve the secondary structure of RNA and may even be dependent on the RNA transport machinery available in the neuron. As more transcripts are discovered that target to dendrites, a common pattern may emerge from these mRNA sequences that signal the neuron to transport the transcript to dendrites. Investigations into the parts of the Kv1.1 transcript responsible for its dendritic targeting will help in determining the intrinsic signals of dendritically localized RNA.

Determining the proteins necessary for transporting Kv1.1 mRNA is also a potential future endeavor. The first indicator of translational machinery in dendrites was the detection of polyribosomes located in dendrites, preferentially below postsynaptic sites [4]. Although not identical to the machinery found in the soma, more ultrastructural studies have detected components of translational machinery in dendrites [9, 10]. There is even evidence of proteins involved in post translational modifications of proteins ascribed to the Golgi apparatus [11] and supports the possibility of integral membrane proteins being locally translated [12, 13].

RNA is transported from the soma to dendrites in neuronal granules that contain a collection of mRNA, components of translational machinery, and RNA binding proteins [14]. It would be interesting to see if Kv1.1 mRNA interacts with any known RNA binding proteins or those not yet discovered. The specificity of a neuronal granule for the transcripts it contains is not known, and there may be preferential co-transport of Kv1.1 mRNA with a particular subset of dendritically targeted mRNAs.

There has to be a mechanism in place to silence the translational machinery that travels with the mRNA in neuronal granules, to allow for occasions when local translation is not needed in the dendrites. We have found that mTOR activity suppresses

the local translation of Kv1.1. However, we do not know if this is a direct suppression of Kv1.1 synthesis, or that mTOR activity upregulates another protein that suppresses Kv1.1. It would be interesting to explore the effect of mTOR activity on neuronal granule function. mTOR may have a broad impact on many components of neuronal granules, even the granule itself.

Although the acceptance that neurons are capable of local translation has grown, there is still quite a bit of uncertainty on the physiological impact of local translation. The contributions of many research groups have demonstrated the phenomenon of local translation and are beginning to establish its functional significance. A particularly striking study highlighting the role of local translation involved generating a mouse with just the 3'UTR of CamKII knocked out [15]. With the signaling to target CamKII mRNA to the dendrites removed, there were a number of behavioral deficits in these mice such as impaired spatial memory, associative fear conditioning, and object recognition memory. These phenotypes are attributed to the inability of CamKIIa to be locally translated.

Decades of research have been devoted to the biophysical characterization of voltage-gated ion channels and their physiological roles. One of the joys and challenges of new biological discoveries is to judge their *in vivo* significance. An exciting prospect of future work will involve how the site of translation of voltage-gated ion channels in neurons impacts their physiological significance.

Autosomal dominant point mutations of Kv1.1 in humans can cause episodic ataxia, a disorder that can result in periods of ataxia and uncontrollable muscle movement often triggered by stress or fatigue [16]. Although there is not a genetically modified

mouse available that only disrupts the local translation of Kv1.1, a knockout mouse line of Kv1.1 has been generated [17]. These mice have a number of defects, the most salient being increased susceptibility to seizures. There is also a spontaneous 11 base pair deletion of Kv1.1, leading to a reading frameshift and introduction of an early stop codon that causes a 265 amino acid C-terminal truncation [18]. These mice have similar phenotypes as the Kv1.1 null mice such as epileptic seizures and hyperexcitable neurons. Moreover, these mice have enlarged brain volumes not seen in KCNA1 null mice and are a model for megencephaly. In the CA1 region of the hippocampus, there is a dramatically higher level of Kv1.1 mRNA in these megencephalic mice compared to wild type. Perhaps the truncated Kv1.1 interferes with a feedback signaling loop that regulates the level of Kv1.1 mRNA. mTOR, or one of its upstream regulators, may also be upregulated in megencephalic mice, causing a translational suppression and accumulation of Kv1.1 mRNA. It is interesting to note that mTOR activity is involved with cell growth and a negative regulator of mTOR is tuberous sclerosis complex, that when mutated, causes increased mTOR activity and abnormal increases in cell growth [19, 20].

mTOR is a prominent kinase regulated by a variety of cellular factors and the proteins it phosphorylates control a number of important cellular processes including translational regulation [21]. Given its role in cellular growth, it would be interesting to see if mTOR activity influences dendritic morphology in a manner correlated with its regulation of Kv1.1 translation. We observed the effect of mTOR suppression on a timescale of hours. The increase of Kv1.1 translation may be just one part of an orchestrated program to change the morphology and function of the dendrite over a longer time course than we observed.

As mentioned, one of the most extensively studied proteins for local translation is CamKII. Whereas NMDA receptor activity and mTOR suppress Kv1.1 local translation, CamKII translation is upregulated [22, 23]. mTOR is known to upregulate the translation of many transcripts, but it also selectively downregulates others [24]. The translational capacity in dendrites may be a limiting factor in the overall rate of dendritic translation [25]. To maximize the utilization of the translational machinery in dendrites, there may be a near constant rate of translation occurring but the selection of transcripts translated could be highly regulated. Perhaps there is a competition for the local translation of Kv1.1 and CamKII. Monitoring both CamKII and Kv1.1 local translation simultaneously to examine whether they are regulated in opposite ways may be interesting. If so, identifying the point of the signaling pathway that diverges in the translational regulation between CamKII and Kv1.1 could lead towards discovering the determinants of how mTOR regulates the translation of particular transcripts.

Voltage gated potassium channels are expressed throughout the brain and help in establishing the resting potential, shaping action potentials, and repolarizing neurons that can impact action potential frequency [26]. Kv1.1 is characterized as a delayed rectifier. They are more likely to open when the neuron depolarizes and do not rapidly inactivate. Depending on the other subunits Kv1.1 assembles with, the properties of the currents generated vary. For example, Kv1.1 channels associated with beta 1 subunits inactivate [27]. It is not known what the final subunit composition of the channels that incorporate the locally translated Kv1.1 and it could be worthwhile to determine the subunit composition and biophysical properties of the Kv1.1 channels that are created from locally translated Kv1.1.

Before the molecular cloning of ion channels, the channels responsible for the current recordings could only be classified by their biophysical and pharmacological properties. Many of these currents can now be ascribed to particular channels such as those containing Kv1.1. A notable example highlighting the function of Kv1.1 is the low threshold, voltage-gated potassium current (Ikl) found in the auditory system [28]. The medial nucleus of the trapezoid body of the auditory system receives and preserves auditory inputs from the cochlear nucleus. Kv1.1 containing channels are the predominant source of Ikl and reduce the jitter in the action potential firing rate generated by inputs from the cochlear nucleus. This system has exquisite temporal precision and makes it possible to localize audio sources based on the timing of stereo inputs preserved in part by the Ikl of the medial nucleus of the trapezoid body.

We focused our studies on the expression of Kv1.1 in the CA1 region of the hippocampus. The predominant source of Kv1.1 in the hippocampus is in the axons of CA3 where it helps control the action potential frequency in these neurons, exemplified by the hyperexcitability of these neurons in the Kv1.1 knockout mouse [17]. We observed an increase of Kv1.1 expression in dendrites of the CA1 region after suppressing mTOR. Establishing the currents that this increased Kv1.1 influence and the physiological impact of these currents is a pressing goal stemming from this study. There is by now a greater appreciation that dendrites are not electrically passive and there are a variety of voltage gated ion channels with heterogeneous distribution patterns throughout the dendrites. A heavily studied potassium channel current in CA1 dendrites is IA, characterized by rapid activation and deactivation as well as being highly sensitive to 4-AP. Kv4.2 is largely responsible for IA but there are likely many other voltage-gated

potassium channels that contribute to IA. It has already been documented from outside-out dendritic patch recordings of CA1 neurons that approximately 20 percent of potassium channels are sensitive to the Kv1 blocker α-dendrotoxin [29]. Perhaps this fraction of dendrotoxin sensitive channels would increase if the local translation of Kv1.1 were increased.

Based upon previous studies of voltage-gated potassium channels in dendrites, there are a number of possible impacts that locally translated Kv1.1 can have on dendrites [30]. Locally translated Kv1.1 may contribute to the IA of the dendrite. IA limits the excitability of dendrites and attenuates the back propagation of action potentials. Even if Kv1.1 is not a component of IA it could still have a similar impact of reducing the excitability of dendritic branches. The locally translated Kv1.1 may also contribute to a sustained voltage-gated potassium current detected in the dendrites of CA1 neurons. Recordings of untreated neurons reveal this current to be uniform along the length of the dendrite, though single channel recordings from dendritic membranes reveals patchy channel distribution [31]. This apparent uniformity may be altered by local translation of Kv1.1. The effect of an increased density of channels that contribute to sustained voltage-gated potassium currents in certain dendritic regions could lower the excitability of the dendrite in that region.

Unlike the major role of voltage-gated calcium and sodium channels to generate action potentials, voltage-gated potassium channels have a major responsibility to modulate the distance traveled and the frequency of action potentials. Being able to change the voltage-gated potassium channel density in a subset of dendritic regions can change the magnitude of a subset of EPSPs, influence the path that back propagating

action potentials travel, and influence the relative contribution of merging EPSPs heading toward the soma.

We have uncovered a new way for neurons to control dendritic excitability in a spatially restricted manner. There are a number of exciting avenues to explore the implications of this discovery. Further elaboration of the translational regulation of Kv1.1 will detail the conditions that influence the level of Kv1 channels. There may be other channels or proteins that are modified along with Kv1.1. Additionally, more studies into the physiological impact of locally translated Kv1.1 can shed light on how neurons integrate and process inputs and the behavioral manifestations of these computations.

References

1. Kennedy, M. J., M. D. Ehlers (2006). Organelles and trafficking machinery for postsynaptic plasticity. *Annu Rev Neurosci*, 29:325-362.

2. Steward, O. (1983). Polyribosomes at the base of dendritic spines of central nervous system neurons--their possible role in synapse construction and modification. *Cold Spring Harb Symp Quant Biol*, 48 Pt 2:745-759.

3. Steward, O., B. Fass (1983). Polyribosomes associated with dendritic spines in the denervated dentate gyrus: evidence for local regulation of protein synthesis during reinnervation. *Prog Brain Res*, 58:131-136.

4. Steward, O., W. B. Levy (1982). Preferential localization of polyribosomes under the base of dendritic spines in granule cells of the dentate gyrus. *J Neurosci*, 2:284-291.

5. Steward, O., E. M. Schuman (2003). Compartmentalized synthesis and degradation of proteins in neurons. *Neuron*, 40:347-359.

6. Link, W., U. Konietzko, G. Kauselmann, M. Krug, B. Schwanke, U. Frey, D. Kuhl (1995). Somatodendritic expression of an immediate early gene is regulated by synaptic activity. *Proc Natl Acad Sci U S A*, 92:5734-5738.

7. Lyford, G. L., K. Yamagata, W. E. Kaufmann, C. A. Barnes, L. K. Sanders, N. G. Copeland, D. J. Gilbert, N. A. Jenkins, A. A. Lanahan, P. F. Worley (1995). Arc, a growth factor and activity-regulated gene, encodes a novel cytoskeleton-associated protein that is enriched in neuronal dendrites. *Neuron*, 14:433-445.

8. Tiedge, H., F. E. Bloom, D. Richter (1999). RNA, whither goest thou? *Science*, 283:186-187.

9. Steward, O., P. M. Falk, E. R. Torre (1996). Ultrastructural basis for gene expression at the synapse: synapse-associated polyribosome complexes. *J Neurocytol*, 25:717-734.

10. Spacek, J., K. M. Harris (1997). Three-dimensional organization of smooth endoplasmic reticulum in hippocampal CA1 dendrites and dendritic spines of the immature and mature rat. *J Neurosci*, 17:190-203.

11. Pierce, J. P., T. Mayer, J. B. McCarthy (2001). Evidence for a satellite secretory pathway in neuronal dendritic spines. *Curr Biol*, 11:351-355.

12. Ju, W., W. Morishita, J. Tsui, G. Gaietta, T. J. Deerinck, S. R. Adams, C. C. Garner, R. Y. Tsien, M. H. Ellisman, R. C. Malenka (2004). Activity-dependent regulation of dendritic synthesis and trafficking of AMPA receptors. *Nat Neurosci*, 7:244-253.

13. Grigston, J. C., H. M. VanDongen, J. O. McNamara, 3rd, A. M. VanDongen (2005). Translation of an integral membrane protein in distal dendrites of hippocampal neurons. *Eur J Neurosci*, 21:1457-1468.

14. Krichevsky, A. M., K. S. Kosik (2001). Neuronal RNA granules: a link between RNA localization and stimulation-dependent translation. *Neuron*, 32:683-696.

15. Miller, S., M. Yasuda, J. K. Coats, Y. Jones, M. E. Martone, M. Mayford (2002). Disruption of dendritic translation of CaMKIIalpha impairs stabilization of synaptic plasticity and memory consolidation. *Neuron*, 36:507-519.

16. Browne, D. L., S. T. Gancher, J. G. Nutt, E. R. Brunt, E. A. Smith, P. Kramer, M. Litt (1994). Episodic ataxia/myokymia syndrome is associated with point mutations in the human potassium channel gene, KCNA1. *Nat Genet*, 8:136-140.

17. Smart, S. L., V. Lopantsev, C. L. Zhang, C. A. Robbins, H. Wang, S. Y. Chiu, P. A. Schwartzkroin, A. Messing, B. L. Tempel (1998). Deletion of the K(V)1.1 potassium channel causes epilepsy in mice. *Neuron*, 20:809-819.

18. Petersson, S., A. S. Persson, J. E. Johansen, M. Ingvar, J. Nilsson, G. Klement, P. Arhem, M. Schalling, C. Lavebratt (2003). Truncation of the Shaker-like voltage-gated potassium channel, Kv1.1, causes megencephaly. *Eur J Neurosci*, 18:3231-3240.

19. Gao, X., Y. Zhang, P. Arrazola, O. Hino, T. Kobayashi, R. S. Yeung, B. Ru, D. Pan (2002). Tsc tumour suppressor proteins antagonize amino-acid-TOR signalling. *Nat Cell Biol*, 4:699-704.

20. Inoki, K., Y. Li, T. Zhu, J. Wu, K. L. Guan (2002). TSC2 is phosphorylated and inhibited by Akt and suppresses mTOR signalling. *Nat Cell Biol*, 4:648-657.

21. Gingras, A. C., B. Raught, N. Sonenberg (2001). Control of translation by the target of rapamycin proteins. *Prog Mol Subcell Biol*, 27:143-174.

22. Scheetz, A. J., A. C. Nairn, M. Constantine-Paton (2000). NMDA receptor-mediated control of protein synthesis at developing synapses. *Nat Neurosci*, 3:211-216.

23. Gong, R., C. S. Park, N. R. Abbassi, S. J. Tang (2006). Roles of glutamate receptors and the mammalian target of rapamycin (mTOR) signaling pathway in activity-dependent dendritic protein synthesis in hippocampal neurons. *J Biol Chem*, 281:18802-18815.

24. Schratt, G. M., E. A. Nigh, W. G. Chen, L. Hu, M. E. Greenberg (2004). BDNF regulates the translation of a select group of mRNAs by a mammalian target of rapamycin-phosphatidylinositol 3-kinase-dependent pathway during neuronal development. *J Neurosci*, 24:7366-7377.

25. Schuman, E. M., J. L. Dynes, O. Steward (2006). Synaptic regulation of translation of dendritic mRNAs. *J Neurosci*, 26:7143-7146.

26. Hille, B., *Ionic channels of excitable membranes*, 2nd ed. Sinauer Associates. Sunderland, Mass., 1992

27. Pongs, O., T. Leicher, M. Berger, J. Roeper, R. Bahring, D. Wray, K. P. Giese, A. J. Silva, J. F. Storm (1999). Functional and molecular aspects of voltage-gated K+ channel beta subunits. *Ann N Y Acad Sci*, 868:344-355.

28. Gittelman, J. X., B. L. Tempel (2006). Kv1.1 Containing Channels are Critical for Temporal Precision during Spike Initiation. *J Neurophysiol.*

29. Hoffman, D. A., J. C. Magee, C. M. Colbert, D. Johnston (1997). K+ channel regulation of signal propagation in dendrites of hippocampal pyramidal neurons. *Nature*, 387:869-875.

30. Johnston, D., B. R. Christie, A. Frick, R. Gray, D. A. Hoffman, L. K. Schexnayder, S. Watanabe, L. L. Yuan (2003). Active dendrites, potassium channels and synaptic plasticity. *Philos Trans R Soc Lond B Biol Sci*, 358:667-674.

31. Chen, X., D. Johnston (2004). Properties of single voltage-dependent K+ channels in dendrites of CA1 pyramidal neurones of rat hippocampus. *J Physiol*, 559:187-203.

Appendix

Appendix

Common to most people's experiences, the path of pursuing a scientific project is an unpredictable journey and sometimes it does not reach a satisfying conclusion. I have the fortunate opportunity to continue working on some of these projects after graduation. Moreover, I hope others may be inspired to carry on their own investigations that are based upon some of the curious observations made in the lab. I will give a brief chronological description of my scientific pursuits over the past seven years in graduate school and describe a project involving the interaction of GABA-B receptors and 14-3-3 with some promising preliminary data.

After joining the lab, the initial experiment was to apply recent advances in microarray technology to ask the simple question, what mRNA transcripts are present in neuronal processes? The potential of microarrays became readily apparent with information on the abundance of 8,800 transcripts derived from cDNA isolated from total hippocampal preparations as well as synaptosomes isolated from hippocampi (GEO accession: GSE5516). Attention was focused on transcripts with a high synaptosomal mRNA/ total hippocampal mRNA ratio. An interesting pattern emerged that a number of channel and receptor subunits that form multimeric complexes only had a single subunit with an enriched synaptosomal mRNA transcript.

We hypothesized that the local translation of the subunit transcript localized in the neuronal process regulated the assembly and localization of the multimeric channel or receptor. To test this hypothesis, we wanted to verify the presence of the mRNA in neuronal processes using techniques complementary to the microarray data. We measured mRNA concentrations using real time PCR to verify the mircroarray data and

focused on candidates that were enriched in synaptosomes by both microarray and real time PCR methods of measuring RNA. The most fruitful and extensive studies came from characterizing the regulation of Kv1.1 local translation. As detailed in Chapter 2, we found further evidence of Kv1.1 transcripts localized to neuronal dendrites and discovered a signaling pathway that regulated the local translation of Kv1.1 and its surface expression on dendrites.

Another locally translated candidate transcript from the microarray experiment was the GABA-B R2 subunit. GABA-B receptors consist of both a GABA-B R1 (GB1) and a GABA-B R2 (GB2) subunit [1-3]. The GB1 subunit has an ER retention/retrieval motif [4] and we speculated that the local translation of GB2 would provide a means of establishing the assembly of the GB1 and GB2 subunits in neuronal dendrites. The GABA-B receptor would then be trafficked to the surface, near the site of GB2 local translation. However, the real time PCR data did not corroborate the microarray findings of enrichment of GABA-B R2 subunit in synaptosomes.

However, 14-3-3 eta, one of the seven isoforms of the 14-3-3 family was a transcript found in both the microarray and real time PCR experiments to be enriched in the synaptosomal fraction isolated from rat hippocampi. Around the time of doing the microarray experimnents, a paper by Couve et al. [5] showed that 14-3-3 interacts with GB1. However, the functional impact of this interaction between 14-3-3 and GB1 receptors was not reported and we decided to investigate the influence of 14-3-3 on GABA-B receptor function. 14-3-3s are highly abundant, purported to compose nearly 1% of cytosolic protein in the human brain [6]. They interact with hundreds of proteins

and are involved in a wide variety of roles such as regulating cell division, neurotransmitter release, apoptosis, enzyme function, and protein trafficking [7-9].

The seven isoforms are very similar to one another but there is some difference in their subcellular localization in neurons with the epsilon, eta, gamma, beta, and zeta isoforms found in biochemically isolated synaptic membranes [10]. 14-3-3 proteins can dimerize, forming both homomers and heteromers [11]. The potential diversity in functionality from having so many isoforms is not well understood and even the specificity of the isoforms with particular protein binding partners is not well established. Having only the 14-3-3 eta isoform identified in our microarray screen presents the enticing possibility that this isoform is specialized among the 14-3-3 isoforms to be locally translated and regulate the surface expression of GABA-B receptors.

To look at the influence of 14-3-3 eta on GABA-B receptor surface expression, we performed a series of surface assay experiments that were developed in the lab [12]. HA-tagged GB1 was transfected into Cos7 cells and very little trafficked to the surface (mean percent relative to GB1HA + GB2 surface expression: 5.5 +/- 1.8%, $n = 6$, $p < 0.001$ for GB1HA alone; Fig. 1A). When co-transfected with GB2 subunit, there was a dramatic increase in GB-1 HA reaching the surface as described previously [4]. Transfecting 14-3-3 eta with GB1-HA and GB2 leads to GB-1HA surface expression that is around 20% lower than without 14-3-3 eta (mean percent relative to GB1HA + GB2 surface expression: 78.7 +/- 9.3%, $n = 15$, $p < 0.05$ for GB1HA, GB2, and 14-3-3 eta; Fig. 1A).

There are a number of possibilities of how 14-3-3 eta can lead to a reduction of GABA-B surface expression. 14-3-3s have been found to be involved in the forward

transport of proteins retained in the Endoplasmic Reticulum [13] and impact the surface expression of membrane proteins [14]. To get a better handle on the stage of 14-3-3s involvement with GABA-B receptors that causes a reduction in GABA-B receptor surface expression, colocalization studies with organelle markers were performed. Preliminary immunostaining of GB1-HA, 14-3-3, and the Golgi marker GM130 indicates that there are subcellular regions positive for all three in HEK cells (Fig. 1B). More experiments with a panel of organelle markers should narrow the circumstances that lead to 14-3-3 eta interacting with GABA-B receptors.

Another important goal of this project is to look at the impact of 14-3-3 eta on GABA-B receptors in neurons. Initial experiments of staining neurons for endogenous GABA-B receptors and 14-3-3 eta reveal an interesting pattern of some colocalization in major dendritic processes of GB1 and 14-3-3 eta as well as 14-3-3 eta expression being more extensive than GB1 (Fig. 1C).

A major concern dealing with 14-3-3s is that they have so many potential impacts on cellular function. Moreover, all cells have endogenous levels of 14-3-3 that may confound overexpression experiments. We have been working on developing tools to reduce endogenous 14-3-3 levels to examine the impact reducing 14-3-3 has on GABA-B receptor function and surface expression. Two promising strategies to knock down 14-3-3 function are to utilize a cell permeable inhibitor of 14-3-3 we developed and siRNA specific to 14-3-3 eta.

A potent blocker of 14-3-3, named R18, is a 20 amino acid peptide that blocks the ligand binding groove of 14-3-3 with a Kd of around 80 nanomolar [15]. We synthesized this peptide to penetratin, a peptide sequence that can transport itself and its cargo

through cell membranes [16]. Incubating Cos7 cells with R18-Pen increased the surface expression of GABA-B receptors in a dose dependent manner (Fig. 2A). We also created a siRNA construct that dramatically reduces 14-3-3 eta levels (Fig. 2B).

Another strategy to overcome the shortcomings of 14-3-3's ability to interact with so many proteins is to focus on altering GB1 in such a way that it leads to a disruption in its interaction with 14-3-3 eta. A general approach we are considering is to alter the phosphorylation state of GB1 either pharmacologically or genetically removing phosphorylation sites within GB1. We can then look at other effects disrupting 14-3-3's interaction with GB1 has on GABA-B receptor function.

Currently, there are a number of possibilities for future work with this project. One focus can be to further characterize the site and regulation of 14-3-3 eta translation in neurons. We have found some evidence of 14-3-3 eta transcript being localized to neuronal processes and time lapse imaging of Kaede-14-3-3 eta constructs similar to the time lapse experiments described in Chapter 2 could provide insight into the site of 14-3-3 eta translation. These experiments may be more difficult than monitoring Kaede-Kv1.1 translation because 14-3-3 eta is a cytosolic protein and Kaede-14-3-3 eta is likely to be much more mobile than Kaede-Kv1.1.

Instead of focusing on the site of translation, one can look at the determinants within the 14-3-3 eta transcript that are required for being localized to neuronal processes. The potential advantage of this approach is that 14-3-3 eta is very abundant and this may overcome some of the challenges of needing a robust signal to visualize RNA.

Regardless of whether 14-3-3 eta is locally translated, having a better understanding of the conditions that lead it to interact with GB1 and the impact this has on GABA-B receptor function is an open question. Our preliminary data suggests that 14-3-3 eta reduces GABA-B receptors but at what stage in the biosynthetic or degradation pathway the interaction occurs is unknown. Moreover, we do not know the signaling required for the initiation or termination of the interaction between 14-3-3 eta and GB1.

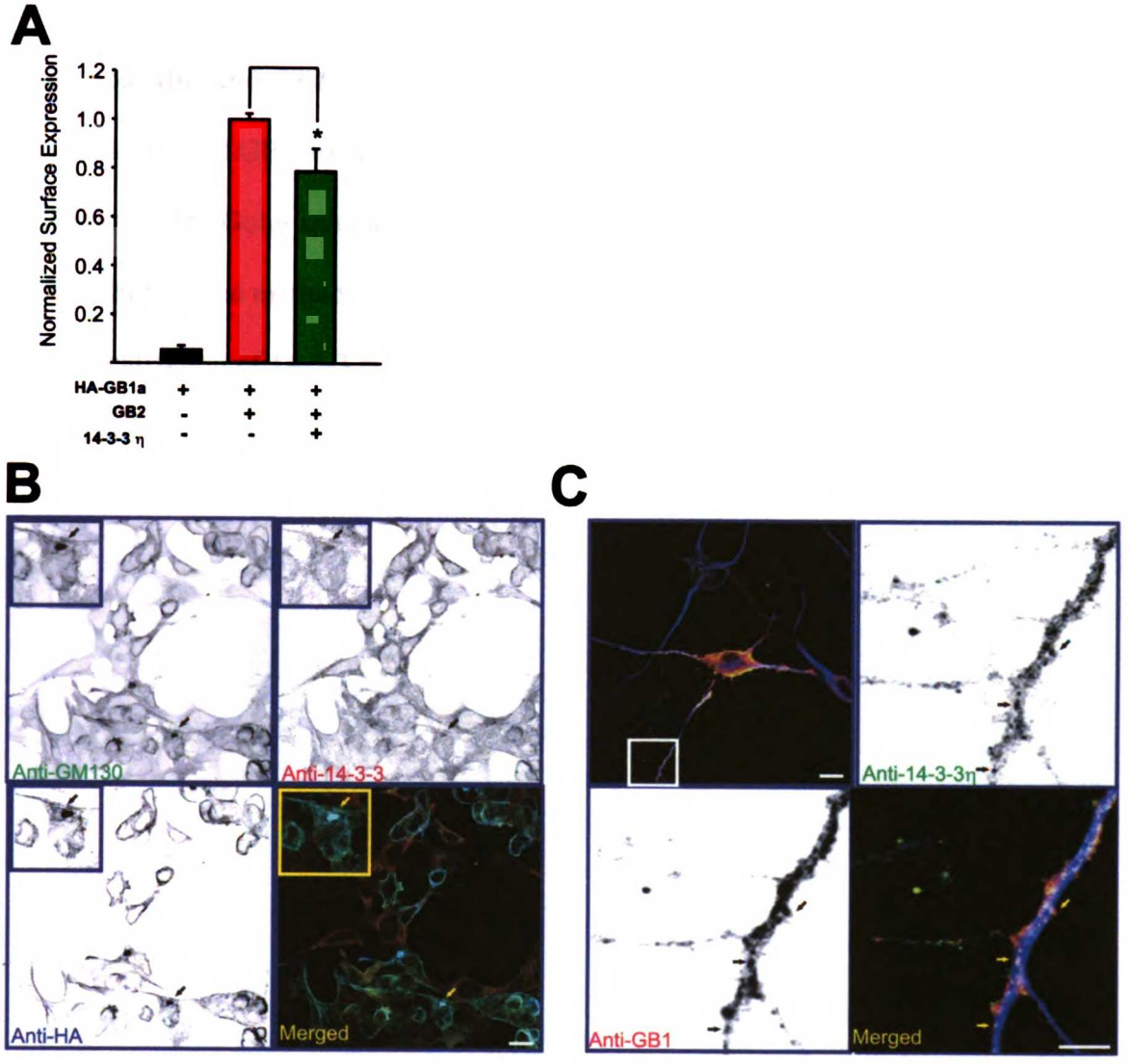
A
Normalized Surface Expression
1.2
1.0
0.8
0.6
0.4
0.2
*
HA-GB1a + + +
GB2 - + +
14-3-3 η - - +
B
Anti-GM130
Anti-14-3-3
Anti-HA
Merged
C
Anti-14-3-3η
Anti-GB1
Merged

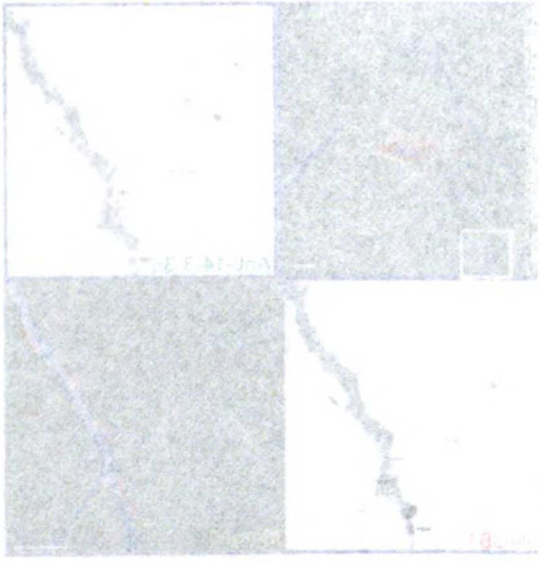

Figure 1. 14-3-3 eta reduces GABA-B receptor surface expression, colocalizes with Golgi apparatus and GB1. (A) Surface expression of GABA-B receptors is reduced when GB1-HA and GB2 are transfected with 14-3-3 eta in Cos7 cells. (B) Co-localization of the Golgi apparatus marker GM130 (upper left box, green merged), 14-3-3 (upper right box, red merged), and GB1-HA (lower left box, blue merged) in HEK cells. (C) Co-localization of 14-3-3 eta (upper right box, green merged) and GB1 (lower left box, red merged) in cultured hippocampal neurons.

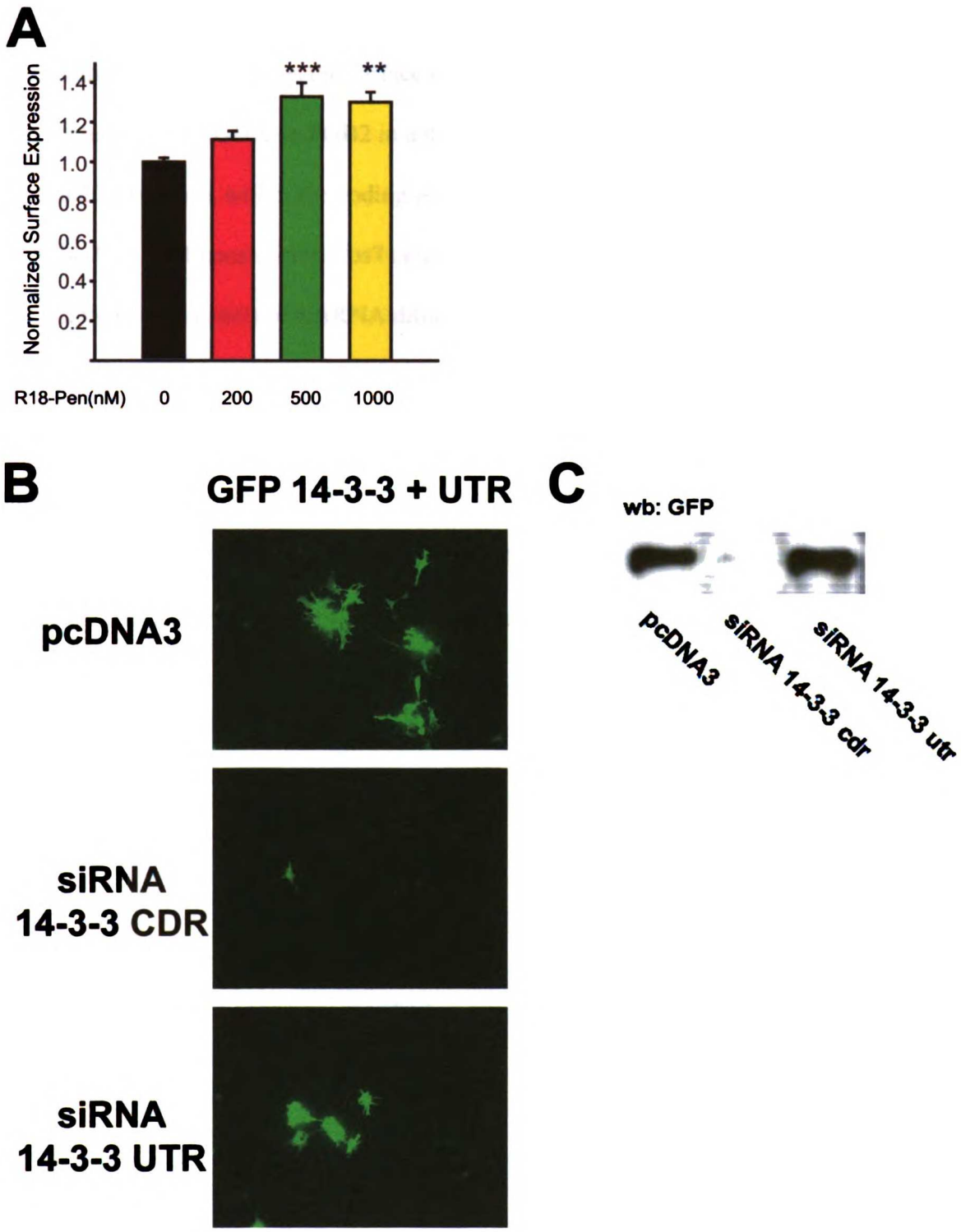
A
Normalized Surface Expression
1.4
1.2
1.0
0.8
0.6
0.4
0.2
***
**
R18-Pen(nM)
0
200
500
1000
B
GFP 14-3-3 + UTR
pcDNA3
siRNA
14-3-3 CDR
siRNA
14-3-3 UTR
C
wb: GFP
pcDNA3
siRNA 14-3-3 cdr
siRNA 14-3-3 utr

Figure 2. R18-Pen or siRNA reduces levels of functional 14-3-3. (A) Incubation for 1 hour with R18-Pen increases the surface expression of GABA-B receptors on Hek cells transfected with GB1-HA and GB2 in a dose-dependent manner. (B) siRNA designed to bind to 20 base pairs within the coding region of 14-3-3 eta reduces the expression of a GFP-14-3-3+UTR construct in Cos7 cells. Cos7 cells transfected with GFP-14-3-3+UTR and pcDNA3 (top panel) or a siRNA directed to a region within the 3'UTR (bottom panel) expressed GFP-14-3-3+UTR (green) whereas transfection with GFP-14-3-3+UTR and siRNA against a portion of the coding region (middle panel) had very little expression of GFP-14-3-3+UTR. (C) Immunoblot of GFP from Cos7 cells transfected with GFP-14-3-3+UTR and pcDNA3, siRNA 14-3-3 cdr, or siRNA 14-3-3. There is a greatly reduced level of GFP-14-3-3+UTR expression in cells transfected with siRNA 14-3-3 cdr compared to those transfected with pcDNA3 or siRNA 14-3-3 utr.

References

1. Jones, K. A., B. Borowsky, J. A. Tamm, D. A. Craig, M. M. Durkin, M. Dai, W. J. Yao, M. Johnson, C. Gunwaldsen, L. Y. Huang, C. Tang, Q. Shen, J. A. Salon, K. Morse, T. Laz, K. E. Smith, D. Nagarathnam, S. A. Noble, T. A. Branchek, C. Gerald (1998). GABA(B) receptors function as a heteromeric assembly of the subunits GABA(B)R1 and GABA(B)R2. *Nature*, 396:674-679.

2. Kaupmann, K., B. Malitschek, V. Schuler, J. Heid, W. Froestl, P. Beck, J. Mosbacher, S. Bischoff, A. Kulik, R. Shigemoto, A. Karschin, B. Bettler (1998). GABA(B)-receptor subtypes assemble into functional heteromeric complexes. *Nature*, 396:683-687.

3. White, J. H., A. Wise, M. J. Main, A. Green, N. J. Fraser, G. H. Disney, A. A. Barnes, P. Emson, S. M. Foord, F. H. Marshall (1998). Heterodimerization is required for the formation of a functional GABA(B) receptor. *Nature*, 396:679-682.

4. Margeta-Mitrovic, M., Y. N. Jan, L. Y. Jan (2000). A trafficking checkpoint controls GABA(B) receptor heterodimerization. *Neuron*, 27:97-106.

5. Couve, A., J. T. Kittler, J. M. Uren, A. R. Calver, M. N. Pangalos, F. S. Walsh, S. J. Moss (2001). Association of GABA(B) receptors and members of the 14-3-3 family of signaling proteins. *Mol Cell Neurosci*, 17:317-328.

6. Boston, P. F., P. Jackson, R. J. Thompson (1982). Human 14-3-3 protein: radioimmunoassay, tissue distribution, and cerebrospinal fluid levels in patients with neurological disorders. *J Neurochem*, 38:1475-1482.

7. Aitken, A. (2006). 14-3-3 proteins: a historic overview. *Semin Cancer Biol*, 16:162-172.

8. Fu, H., R. R. Subramanian, S. C. Masters (2000). 14-3-3 proteins: structure, function, and regulation. *Annu Rev Pharmacol Toxicol*, 40:617-647.

9. Jin, J., F. D. Smith, C. Stark, C. D. Wells, J. P. Fawcett, S. Kulkarni, P. Metalnikov, P. O'Donnell, P. Taylor, L. Taylor, A. Zougman, J. R. Woodgett, L. K. Langeberg, J. D. Scott, T. Pawson (2004). Proteomic, functional, and domain-based analysis of in vivo 14-3-3 binding proteins involved in cytoskeletal regulation and cellular organization. *Curr Biol*, 14:1436-1450.

10. Martin, H., J. Rostas, Y. Patel, A. Aitken (1994). Subcellular localisation of 14-3-3 isoforms in rat brain using specific antibodies. *J Neurochem*, 63:2259-2265.

11. Jones, D. H., S. Ley, A. Aitken (1995). Isoforms of 14-3-3 protein can form homo- and heterodimers in vivo and in vitro: implications for function as adapter proteins. *FEBS Lett*, 368:55-58.

12. Zerangue, N., B. Schwappach, Y. N. Jan, L. Y. Jan (1999). A new ER trafficking signal regulates the subunit stoichiometry of plasma membrane K(ATP) channels. *Neuron*, 22:537-548.

13. O'Kelly, I., M. H. Butler, N. Zilberberg, S. A. Goldstein (2002). Forward transport. 14-3-3 binding overcomes retention in endoplasmic reticulum by dibasic signals. *Cell*, 111:577-588.

14. Shikano, S., B. Coblitz, M. Wu, M. Li (2006). 14-3-3 proteins: regulation of endoplasmic reticulum localization and surface expression of membrane proteins. *Trends Cell Biol.*

15. Wang, B., H. Yang, Y. C. Liu, T. Jelinek, L. Zhang, E. Ruoslahti, H. Fu (1999). Isolation of high-affinity peptide antagonists of 14-3-3 proteins by phage display. *Biochemistry*, 38:12499-12504.

16. Derossi, D., G. Chassaing, A. Prochiantz (1998). Trojan peptides: the penetratin system for intracellular delivery. *Trends Cell Biol*, 8:84-87.